PB-229 432

THE PHOTOCHEMISTRY OF POLLUTED ATMOSPHERES

E. A. Schuck, et al

Stanford Research Institute
South Pasadena, California

December 1960

DISTRIBUTED BY:

NTIS

National Technical Information Service
U. S. DEPARTMENT OF COMMERCE
5285 Port Royal Road, Springfield Va. 22151

PB 229 432

A PROGRESS REPORT ON THE PHOTOCHEMISTRY OF POLLUTED ATMOSPHERES

By

E. A. Schuck
George J. Doyle
Noboru Endow

Southern California Laboratories
Stanford Research Institute

Prepared for

Air Pollution Foundation
2556 Mission Street
San Marino, California

and

United States Public Health Service
Washington, D. C.

December 1960

FOREWORD

This is the fourth Air Pollution Foundation report of work done by Stanford Research Institute in the smog chamber at its Southern California Laboratories.

Students of the report series will realize we have come a long way since construction of the smog chamber was pioneered in 1955. We have gained a great deal of basic knowledge concerning the chemical reactions of hydrocarbons, nitrogen oxides, and sulfur dioxide in the atmosphere. We have sorted out the major reactions taking place and have related some of the products to the undesirable effects of smog. Much more remains to be done, particularly with regard to the formation, growth, and disappearance of aerosols. These mechanisms will have to be elucidated before the problem of long-term chronic health effects of smog on people can be evaluated. The aerosol studies presented in this report are a start in this direction.

The work reported herein has been sponsored not only by the Foundation, but also by the National Institutes of Health, U.S. Public Health Service. Inasmuch as the Foundation will shortly be dissolved, it is hoped that Stanford Research Institute will continue to receive support from NIH and will secure needed additional aid from other donors to allow these most important atmospheric photochemical studies to be continued.

W. L. Faith

Preceding page blank

SUMMARY

During the photooxidation of olefins, three reactions appear important: the reaction of olefins with oxygen atoms, with ozone, and with active intermediates. The active intermediates may be free radicals or zwitterions. The rate of disappearance of olefin, over and above that accountable by reaction with oxygen atoms and ozone, has been termed the "excess rate." The importance of active intermediates in the mechanism of olefin photooxidation is suggested by these observations:

1. Some products cannot be accounted for by simple rupture of the double bond.

2. The excess rate is proportional to the square root of the light intensity and to the square root of the initial nitrogen dioxide concentration.

The major products of the photooxidation are produced by rupture of the double bond, leading to various carbonyl compounds. However, significant amounts of formaldehyde and acetaldehyde are formed from olefins in certain cases in which these compounds could not be formed by simple bond rupture. Secondary photooxidation of the initial products can also contribute to the products.

Alkyl nitrites were identified among the minor products of olefin photooxidation. These nitrites are probably contributing to olefin oxidation since, as was shown previously(1), alkyl nitrites promote destruction of olefins as well as does nitric oxide or nitrogen dioxide. Other minor products identified were alkyl nitrates and epoxides.

Medium to severe eye irritation was obtained with photooxidation of mixtures containing 0.5 ppm each of certain olefins and nitrogen dioxide. These concentrations are comparable to those existing in the Los Angeles atmosphere. These irritation levels can be largely accounted for by the presence of two irritants, formaldehyde and compound X*, formed during photooxidation. The only other eye irritant found to date is acrolein, which is a major product of the photooxidation of 1, 3-butadiene.

---

* Most probable structure is that of a peroxyacylnitrate.

Preceding page blank

The amount of eye irritation caused by photooxidation of auto exhaust probably may be reduced most efficiently by control of olefins rather than by control of oxides of nitrogen. This statement is based on our studies of olefin mixtures of the type found in auto exhaust; these studies show that, under certain circumstances, reduction of the oxides of nitrogen can lead to an increase rather than a decrease in eye irritation.

The predicted effect on irritation of control of either olefins or oxides of nitrogen depends on the following factors:

1. The concentrations of and concentration ratio of olefins and oxides of nitrogen

2. The type of olefins involved

3. The length of irradiation time

Thus, 1 part of an oxide of nitrogen can promote the destruction of 3 parts of most olefins. The presence of excess oxides of nitrogen causes the rates of secondary photooxidations of products to increase. The type of olefin involved will determine whether the irritants result from the initial olefin photooxidation or from secondary photooxidations. Therefore, the presence of excess oxides of nitrogen during olefin photooxidation can lead to either an increase or a decrease in irritation. The length of irradiation time is important because of its relation to the rates of photooxidation of olefins and of their products.

Approximately 50 percent of the eye irritation measured in auto exhaust mixtures results from the photooxidation of ethylene and propylene. This statement is based on the eye-irritating potential of these olefins and their measured disappearance from irradiated exhaust mixtures.

The sensitivity and the precision of the present method of measuring eye irritation and of the analytical methods available for measuring products must be improved if the results from synthetic experiments are to be correlated with conditions in the Los Angeles atmosphere.

Aerosols capable of reducing visibility to less than 10 miles are formed when 0.1 ppm of sulfur dioxide is photooxidized in the presence of an olefin-nitrogen dioxide mixture. In this reaction the photooxidation of the sulfur dioxide, presumably to sulfuric acid, proceeds rapidly. Even with sulfuric acid concentrations of less than 0.01 ppm, supersaturation can occur, causing the formation of sulfuric acid nuclei which grow by absorption of water vapor and products of the olefin oxidation.

At normal ambient temperatures and humidities, the greatest visibility reduction probably stems from the formation of these acid-water aerosols, with variations in humidity playing a secondary role.

Of the tested nuclei thought to be present in the Los Angeles atmosphere, only the acidic product resulting from photooxidation of sulfur dioxide was effective in producing visibility-reducing aerosols. Thus, the presence of sodium chloride, sodium carbonate, and lead chloride during the olefin-nitrogen dioxide reactions does not result in aerosol formation. However, certain of these materials are capable of depressing the amount of light scattering produced from the olefin-nitrogen dioxide-sulfur dioxide reaction. Thus, alkaline materials such as particulate sodium carbonate or gaseous ammonia reduce the amount of light scattering, presumably as a result of neutralization of the acidic aerosols. Formaldehyde also exhibits this ability to reduce the light scattering, while lead chloride nuclei tend to increase light scattering.

CONTENTS

		Page
FOREWORD		iii
SUMMARY		v
I	INTRODUCTION	1
II	RESULTS AND DISCUSSION	2
	A. Products Produced by Photooxidation	2
	1. Products from Selected Olefins	2
	2. Effect of Varying Initial Olefin and Nitrogen Dioxide Concentrations	4
	3. Sources and Fates of Products Produced by Photooxidation of Isobutene	5
	B. Reactions Occurring during Photooxidation	17
	1. Rate of Reaction of Isobutene	17
	2. Effect of Including Additional Compounds	19
	3. Photolysis of Alkyl Nitrites	22
	4. Reaction Kinetics	25
	C. Eye Irritants Produced by Photooxidation	34
	1. Methods of Exposure	34
	2. Irritation from Photooxidized Mixtures	36
	D. Aerosols Produced by Photooxidation	50
	1. Equilibria and Formation of Sulfuric Acid Mists	51
	2. Effect of Relative Humidity	52
	3. Effect of Added Materials	65
	4. Nuclei Concentrations	67
	5. Other Nuclei Sources	71
	6. Discussion	74
III	FUTURE RESEARCH	76
IV	ACKNOWLEDGMENTS	77
REFERENCES		78

Preceding page blank

		Page
Appendix A -	EXPERIMENTAL CONDITIONS	A-3
Appendix B -	ADDITIONAL DATA ON PRODUCTS OF PHOTOOXIDATION	B-3
Appendix C -	ADDITIONAL INFORMATION ON SULFURIC ACID MISTS	C-3

TABLES

Table		Page
I	Major Products Formed during Photooxidation	3
II	Minor Products Formed during Photooxidation	3
III	Dependence of Excess Rate of Isobutene Disappearance on Initial Nitrogen Dioxide Concentration	19
IV	Results of Linear Correlation of Oxygen-Atom and Ozone Reactions with Isobutene with Appearance and Disappearance of Products and Reactants	30
V	Comparison of Eye Irritation Values Obtained with Two Methods of Exposure	35
VI	Eye Irritation Values from Photooxidized Isobutene-Nitrogen Dioxide Mixtures	37
VII	Effect of Ethylene on Light-Scattering Properties of Aerosols	66
VIII	Effect of Acetylene on Light-Scattering Properties of Aerosols	66
IX	Comparative Effects of Isobutylene and 2-Methyl-2-Butene on the Light-Scattering Properties of Aerosols	68

Tables (Cont.)

Table		Page
X	Effect of Formaldehyde on the Light-Scattering Properties of Aerosols	68
XI	Pertinent Data on Nuclei Concentration	70
XII	Effect of Sodium Chloride Nuclei on the Light-Scattering Properties of Aerosols	73
XIII	Effect of Alkaline Nuclei on the Light-Scattering Properties of Aerosols	73
XIV	Effect of Lead-Bearing Nuclei on the Light-Scattering Properties of Aerosols	75
B-I	Products of the Isobutene-Nitrogen Dioxide Reaction	B-5
B-II	Products of the Ethylene-Nitrogen Dioxide Reaction	B-7
B-III	Products of the Propylene-Nitrogen Dioxide Reaction	B-8

FIGURES

Figure		
1	Average Time-Concentration Curves of Reactants and Major Products during Photooxidation of Isobutene-Nitrogen Dioxide Mixtures	6
2	Average Time-Concentration Curves of Minor Products during Photooxidation of Isobutene-Nitrogen Dioxide Mixtures	7
3	Isobutene Oxide Concentration as a Function of Reacted Isobutene Concentration	8

Figures (Cont.)

Figure		Page
4	Total Product Concentration as a Function of Reacted Isobutene Concentration	9
5	Product Concentration as a Function of Reacted Isobutene Concentration	10
6	Product Concentration as a Function of Reacted Isobutene Concentration	11
7	Calculated Concentration of Formaldehyde Reacting to Form Carbon Monoxide	13
8	Formaldehyde Concentration as a Function of Reacted Isobutene Concentration	14
9	Compound X Concentration as a Function of Reacted Isobutene Concentration	15
10	Acetone Concentration as a Function of Reacted Isobutene Concentration	16
11	Dependence of Excess Rate of Isobutene Disappearance on Initial Nitrogen Dioxide Concentration	20
12	Rates of Reaction during Photooxidation of Nitrogen Dioxide and Isobutene	28
13	Eye Irritation Index as a Function of Time to Irritation	38
14	Observed Time to Irritation as a Function of Predicted Time to Irritation	40
15	Eye Irritation from Photooxidation of 2-Methyl-2-Butene	42
16	Eye Irritation from Photooxidation of Isobutene	43
17	Eye Irritation from Photooxidation of Ethylene	44

Figures (Cont.)

Figure		Page
18	Eye Irritation from Photooxidation of Propylene	45
19	Eye Irritation from Photooxidation of 1, 3-Butadiene	46
20	Eye Irritation from Photooxidation of Certain Olefins	47
21	Expected Eye Irritation as a Function of Olefin and Nitrogen Dioxide Concentration	49
22	Effect of Humidity on Light Scattering of Photooxidized Mixtures of Sulfur Dioxide with 2-Methyl-2-Butene and Nitric Oxide	53
23	Effect of Humidity on Cross Section of 0.2μ Diameter Droplet of Sulfuric Acid	53
24	Count Data at Various Humidities for Aerosols Produced by Photooxidation of 0.1 ppm of Sulfur Dioxide	55
25	Frequency Distribution to be Expected if Diffusion is the Only Factor Affecting Aerosol Growth in a Stirred-Flow Reactor	56
26	Reciprocals of the Terminating Slopes at Small Diameters of the Curves of Figure 24 Plotted Against Relative Humidity	57
27	Intercepts of the Curves of Figure 24 Plotted Against Relative Humidity	58
28	Light Scattering of Effluents Conditioned at 10 Percent Relative Humidity	60
29	Light Scattering of Effluents Conditioned at 85 Percent Relative Humidity	61

Figures (Cont.)

Figure		Page
30	Particle Count Distribution for Effluents Conditioned at 10 Percent Relative Humidity after 110 Minutes of Irradiation	62
31	Particle Count Distribution for Effluents Conditioned at 85 Percent Relative Humidity after 110 Minutes of Irradiation	63
32	Typical Temporal Behavior of Particle Count Distribution of Aerosols Formed at 10 Percent Relative Humidity and Conditioned at 85 Percent Relative Humidity	64
33	Typical Transient in Nuclei Concentration Observed during Experiments on the Effect of Relative Humidity	69
34	Semiquantitative Interpretation of the Decay of the Nuclei Concentration Transient at Three Relative Humidities	72
A-1	Irradiation Facility	A-4
B-1	Formaldehyde Formed in the Ethylene-Nitrogen Dioxide Reaction	B-6
C-1	Volume of Pure Sulfuric Acid per Volume of Solution in Water as a Function of Weight Fraction of Sulfuric Acid in the Solution at 25°C	C-6
C-2	Interpolated Values of the Surface Tension of Sulfuric Acid Solutions in Water at 25°C As a Function of Weight Fraction of Sulfuric Acid	C-7
C-3	Partial Molal Volumes of Water and Sulfuric Acid in Aqueous Solutions of Sulfuric Acid at 25°C	C-8
C-4	Limiting Size of Sulfuric Acid Droplets at 100 Percent Relative Humidity and 25°C as a Function of Sulfuric Acid Content and of Droplet Size at 0 Percent Relative Humidity	C-9

Figures (Cont.)

Figure		Page
C-5	Growth of Sulfuric Acid Droplets of Various Sizes Due to Acquisition of Water at Various Humidities at 25°C	C-10
C-6	Intercept of Plane of Critical Composition with Free Energy Barrier Surface for Nucleation of a Two-Component System	C-15

A PROGRESS REPORT ON THE PHOTOCHEMISTRY OF POLLUTED ATMOSPHERES

I Introduction

The deleterious effects of photochemical interaction of atmospheric pollutants are now recognized as a growing problem in most urban areas in the United States and throughout the world.

Although photochemical smog has been the subject of twelve years of research, little of a basic nature is understood about the reactions producing the symptoms of eye irritation, visibility reduction, and plant damage. We know that hydrocarbons, oxides of nitrogen and sulfur, and light lead to these smog symptoms, and we can describe the gross kinetics. However, important questions remain unanswered. Primarily we need to know the details of the chemical reactions involved, so that adequate control measures may be devised and their effect on human health and welfare can be estimated.

The major portion of the pollutants responsible for this problem is emitted to the atmosphere in the exhausts from the 70 million automobiles in these United States. Assuming that proposed remedial devices reduce the olefin content of the exhaust to almost zero, one can envision conditions wherein eye irritation would be reduced more than 50 percent, visibility increased only slightly, and ozone values reduced not at all, although the rate to reach the maximum ozone value would be reduced markedly. Thus we would have reduced the incidence of eye irritation and smog damage to vegetation but not markedly affected visibility or ozone damage to vegetation. In addition, we have no idea of the chemistry of the effluent from automobiles with attached control devices. Therefore, our over-all objective is understanding the reactions involved in photochemical smog. Specifically, the research reported here is concerned with:

1. The formation and identification of the reaction products of the photooxidation of certain olefin-nitrogen dioxide mixtures

2. The reaction mechanism of photooxidation

3. The identification of eye irritants among reaction products at olefin-nitrogen dioxide levels comparable to those in the Los Angeles Basin

4. The effect of relative humidity and nuclei sources on the formation of aerosol particles in photooxidized olefin-nitrogen dioxide-sulfur dioxide mixtures

This investigation was supported by the Air Pollution Foundation, San Marino, California and by Public Health Service Research Grant RG 6828 from the Division of General Medical Science, United States Public Health Service.

II Results and Discussion

A. Products Produced by Photooxidation

The work reported here is a continuation of the program to investigate the chemistry of the photooxidation of certain unsaturated hydrocarbons considered to be representative of the type of compound emitted to the atmosphere. Among the aims of the program are the identification of the eye irritants and the elucidation of the mechanism of the rapid disappearance of the olefins. In this regard it is necessary to have a detailed knowledge of the products formed during photooxidation.

In a previous report[1] it was shown that the major products resulting from photooxidation of olefins were carbonyl compounds of the type expected from rupture of the double bond. In this report we have extended our analysis of products to include the identification of the so-called minor products which are present at one-tenth or less the concentration of the major products. In addition, we have initiated a series of experiments which will indicate the effect of variations in the initial olefin and nitrogen dioxide concentrations on the rate of reaction of the olefin and the rates of formation and the concentrations of the various products. The experimental conditions under which these studies were conducted are described in Appendix A.

1. Products from Selected Olefins

The olefins selected for study were chosen on the basis of (a) their contribution in atmospheres polluted with auto exhaust and (b) their importance as precursors of eye irritants. The olefins selected were ethylene, propylene, isobutene, 1,3-butadiene, and 2-methyl-2-butene. The various identified major and minor products are listed in Tables I and II (see also Appendix B).

Most of the major products listed in Table I are expected from rupture of the double bond. An exception occurs in the photooxidation of 2-methyl-2-butene in that substantial amounts of formaldehyde are detected. This occurrence has at least two possible explanations: (1) a mechanism involving active intermediates and (2) secondary photooxidation of the

Table I

MAJOR PRODUCTS FORMED DURING PHOTOOXIDATION

Major Products Formed	From Ethylene	From Propylene	From Isobutene	From 1, 3-Butadiene	From 2-Methyl-2-Butene
Formaldehyde	X	X	X	X	X
Acetaldehyde		X			X
Acetone			X		X
Acrolein				X	
Ozone	X	X	X	X	X
Carbon monoxide	X	X	X	X	X
Compound X			X		X

Table II

MINOR PRODUCTS FORMED DURING PHOTOOXIDATION

Minor Products Formed	From Ethylene	From Propylene	From Isobutene	From 1, 3-Butadiene	From 2-Methyl-2-Butene
Methyl nitrate	X				
Ethyl nitrate	X	X	X	X	
Methyl nitrite			X		
Propylene oxide		X		X	
Isobutene oxide			X		
Ethylene oxide					X
Isobutyraldehyde			X		
Propionaldehyde		X		X	
Acetone		X		X	
Acetyl nitrate		X			
Acetaldehyde	X		X		
Methanol	X		X		
Compound X				X	
Isopentene oxide					X

major products. Probably both processes are occurring, although other data presented in the rate section of this report favor an intermediate mechanism rather than secondary photooxidation. That secondary photooxidations do occur is evidenced by the appearance of carbon monoxide as a secondary product in isobutene photooxidations. However, the amount of formaldehyde formed from 2-methyl-2-butene is somewhat larger than can be accounted for by secondary photooxidations.

Among the minor products identified and listed in Table II are some compounds which cannot be accounted for on the basis of bond rupture. For example, the formation of propionaldehyde from propylene and from 1, 3-butadiene suggests an intermediate mechanism, as does the formation of isobutyraldehyde from isobutene. The formation of acetaldehyde from isobutene can be due to either an intermediate mechanism or secondary photooxidation.

2. Effect of Varying Initial Olefin and Nitrogen Dioxide Concentrations

The effect of varying the initial nitrogen dioxide concentration was studied in a series of experiments in which the initial hydrocarbon level was maintained at 3 ppm and the initial nitrogen dioxide concentration was 0.1 ppm, 0.3 ppm, 1.0 ppm, and 3 ppm. The light intensity was equivalent to full sunlight. All of the samples were taken after 60 min of irradiation and generally over a period of 30 min. In general it is noted that the concentrations of products formed are direct functions of the amount of nitrogen dioxide available when the initial nitrogen dioxide concentration is less than 1 ppm. This follows from the fact that 1 ppm of nitrogen dioxide can promote the destruction of approximately 3 ppm of an olefin. Thus, below an initial nitrogen dioxide concentration of 1 ppm, the nitrogen dioxide is the limiting factor in the photooxidation. When the initial nitrogen dioxide concentration is above 1 ppm, some of the products appear to enter into reaction with the excess nitrogen dioxide present and to be destroyed. Thus, the amount of formaldehyde observed relative to isobutene reacted is lower when using 3 ppm of nitrogen dioxide than when using 1 ppm of nitrogen dioxide.

Analysis of the data obtained using fixed nitrogen dioxide concentrations and variable olefin concentrations indicates the importance of the rate of the reaction to the amount of products formed in a given time period. As shown in previous reports[1, 2], this in turn indicates the importance of the concentration ratio of hydrocarbon to oxides of nitrogen.

3. Sources and Fates of Products Produced by Photooxidation of Isobutene

The photooxidation of isobutene in the presence of an oxide of nitrogen leads to the major products of formaldehyde, acetone, carbon monoxide, and compound X. The presence of formaldehyde and acetone indicates a splitting of the isobutene molecule at the double bond. We will examine here the various products and postulate their sources and fates. Definite information on the breakup of the isobutene molecule will aid in the mechanism studies, since this information will eliminate consideration of many possible reactions.

Data suitable for the analysis were obtained from several experiments involving isobutene. Thus, Figure 1 shows the average time-concentration curves of reactants and products for five experiments in which the initial isobutene concentration was approximately 3 ppm and the initial nitrogen dioxide concentration was 1 ppm. These data were obtained from infrared spectra. Figure 2 shows the average time-concentration curves of minor products obtained in a set of three similar experiments. These data were obtained using gas chromatography.

Among the products shown in Figures 1 and 2, it is noted that only isobutene oxide and isobutyraldehyde can be assigned as having originated from the entire isobutene molecule. Figure 3, in which the amount of isobutene oxide formed is plotted against the amount of isobutene reacted, indicates that a small constant amount of the isobutene is converted to this oxide.

In a previous report[1] it was shown that approximately all of the carbon atoms in the reacted isobutene could be accounted for in terms of the products shown in Figures 1 and 2. Figure 4, in which the total concentration of products is plotted against the total concentration of isobutene reacted in parts per million, supports the postulate that the isobutene molecule is primarily split at the double bond--that is, 1.9 ppm of products per 1 ppm of reacted isobutene.

Further information may be gained by examining the individual products as functions of the isobutene reacted. The concentrations of these products as functions of the concentration of reacted isobutene are shown in Figures 5 and 6. It is noted that the curves of formaldehyde, acetone, and compound X are approximately linear over a major portion of the 100-min reaction time and that the carbon monoxide curve is rapidly increasing over most of this period. The shape of these curves indicates that formaldehyde, acetone, and compound X are primary products of the isobutene reaction, while carbon monoxide is a secondary product.

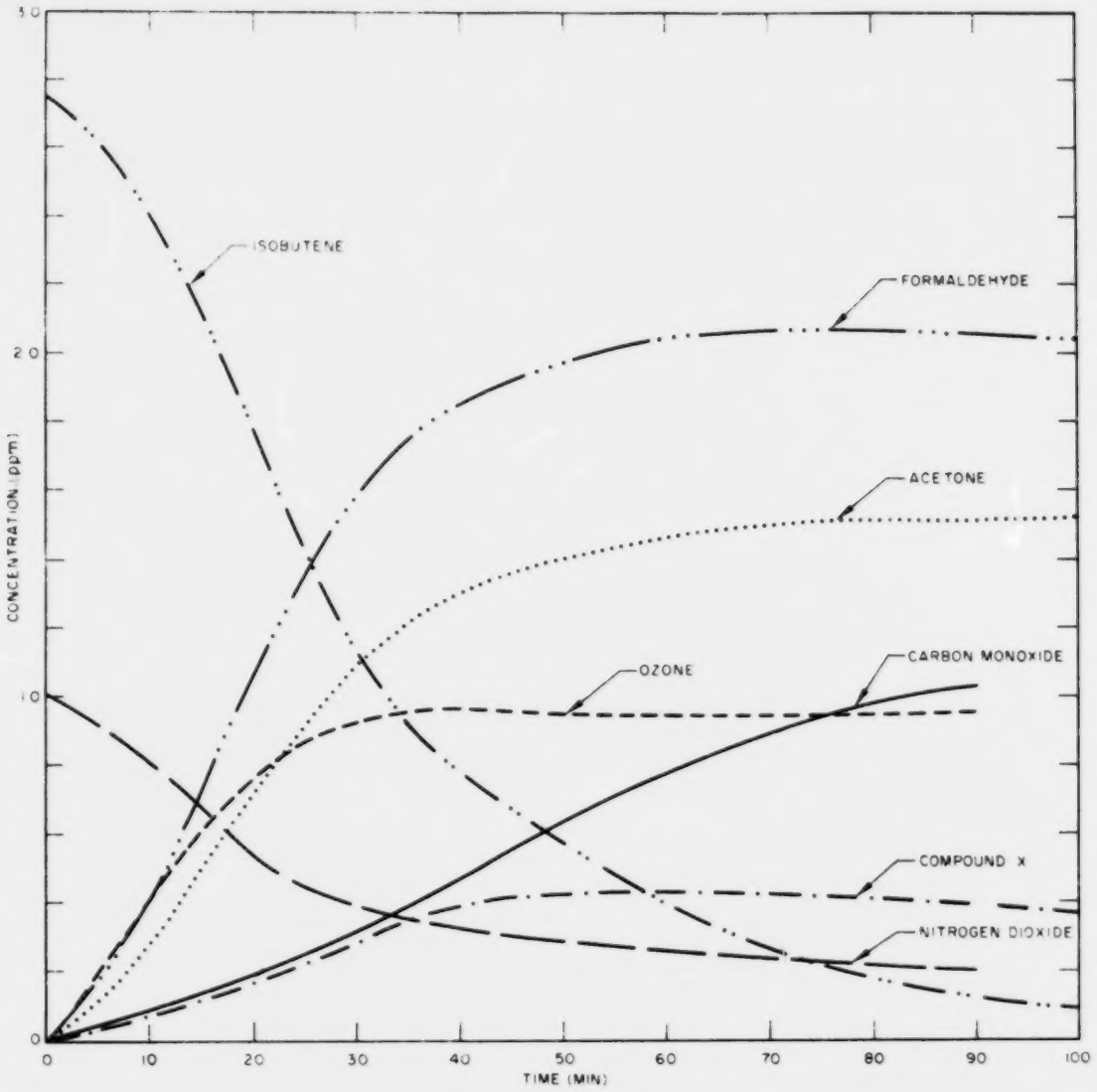

Fig. 1

AVERAGE TIME-CONCENTRATION CURVES OF REACTANTS AND MAJOR PRODUCTS DURING PHOTOOXIDATION OF ISOBUTENE-NITROGEN DIOXIDE MIXTURES

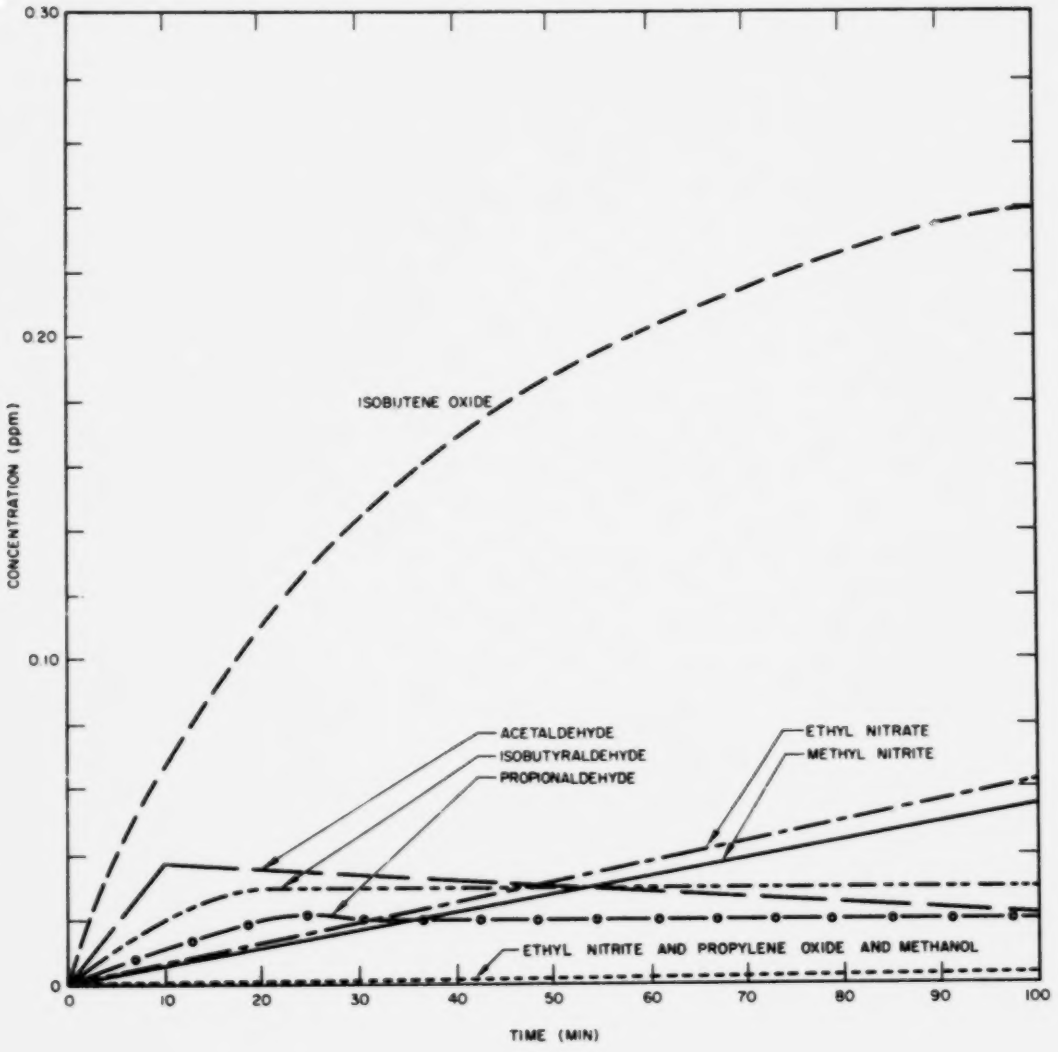

Fig. 2

AVERAGE TIME-CONCENTRATION CURVES OF MINOR PRODUCTS DURINC PHOTOOXIDATION OF ISOBUTENE-NITROGEN DIOXIDE MIXTURES

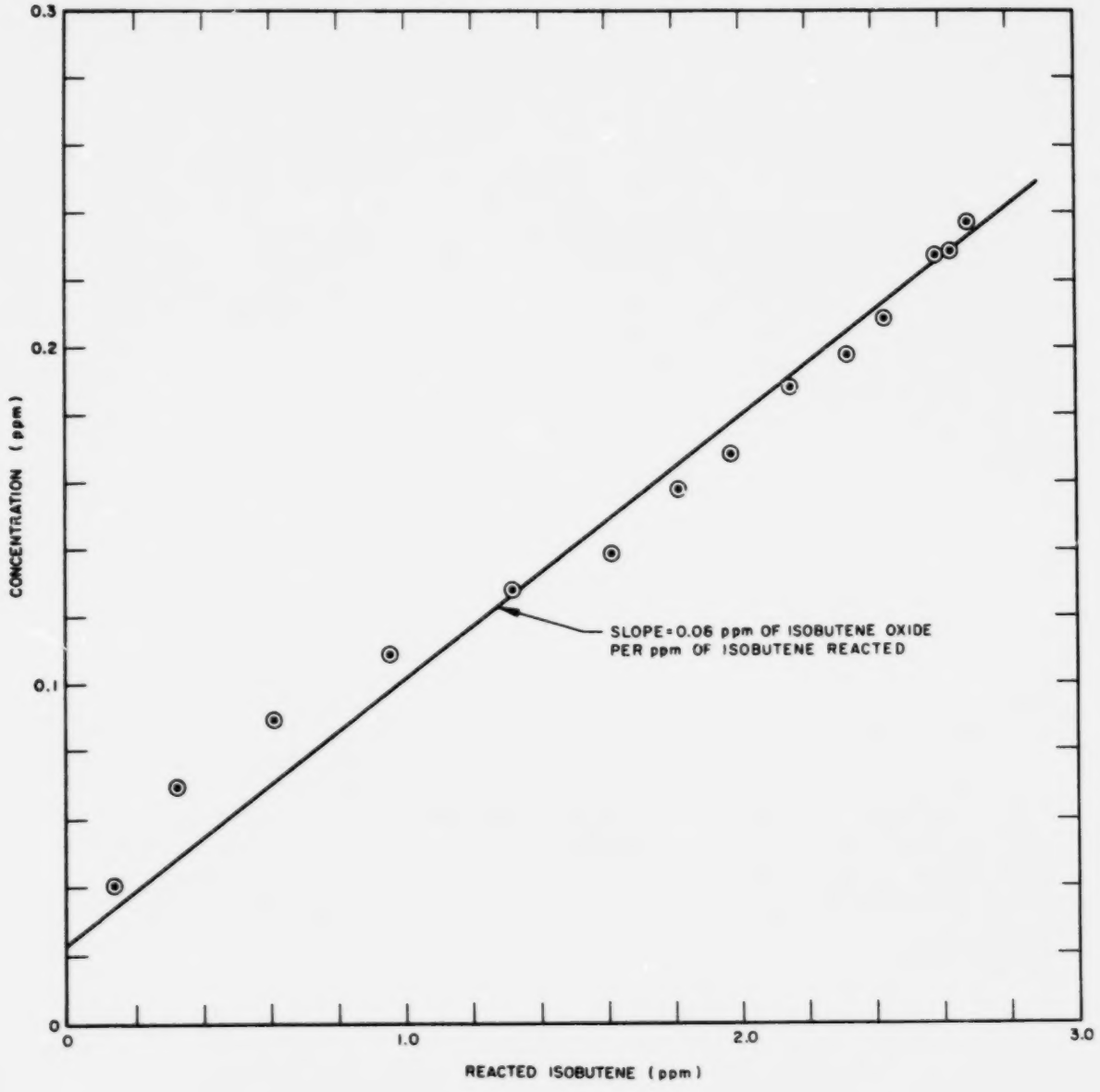

Fig. 3

ISOBUTENE OXIDE CONCENTRATION AS A FUNCTION
OF REACTED ISOBUTENE CONCENTRATION

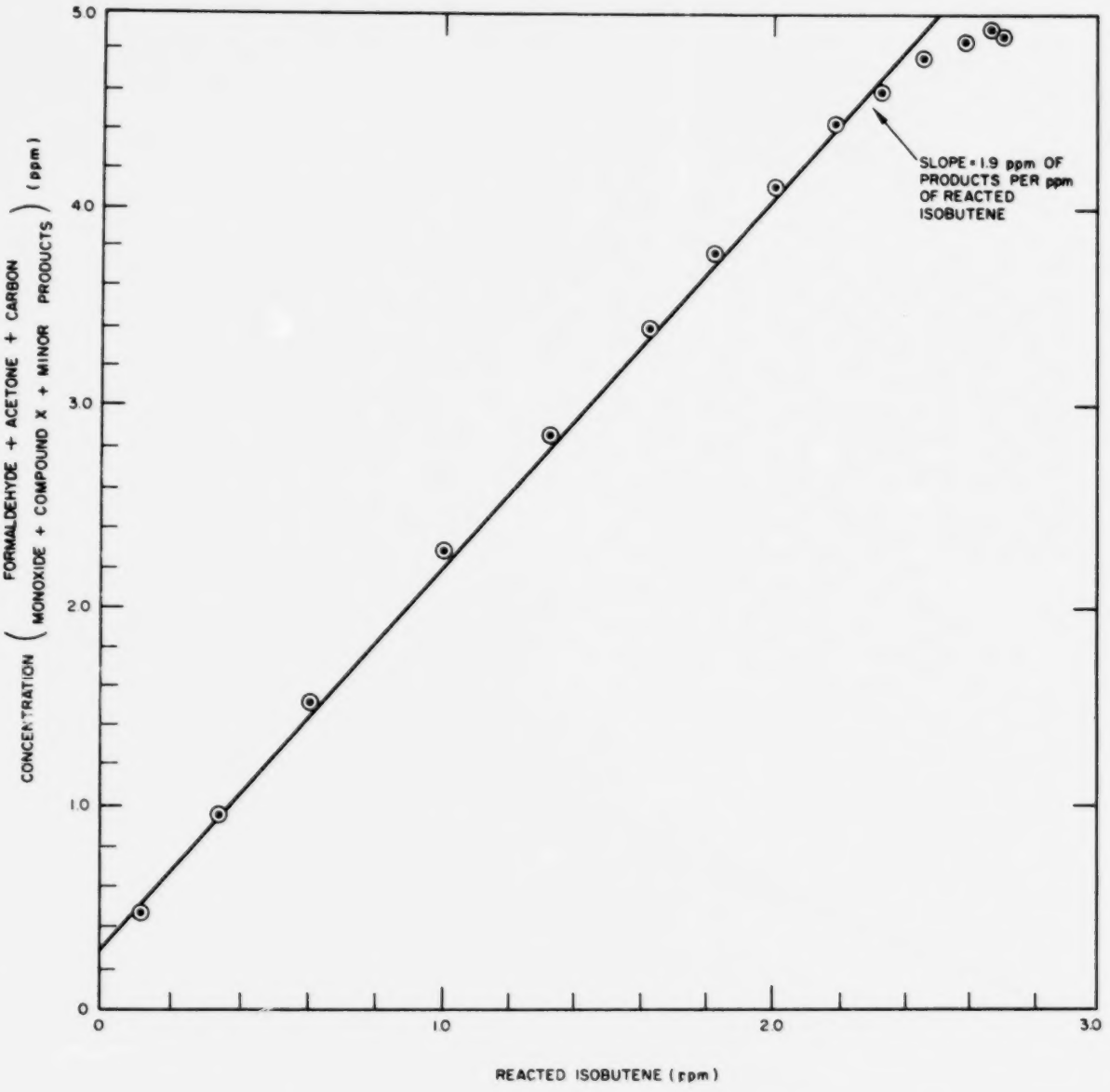

Fig. 4

TOTAL PRODUCT CONCENTRATION AS A FUNCTION OF REACTED ISOBUTENE CONCENTRATION

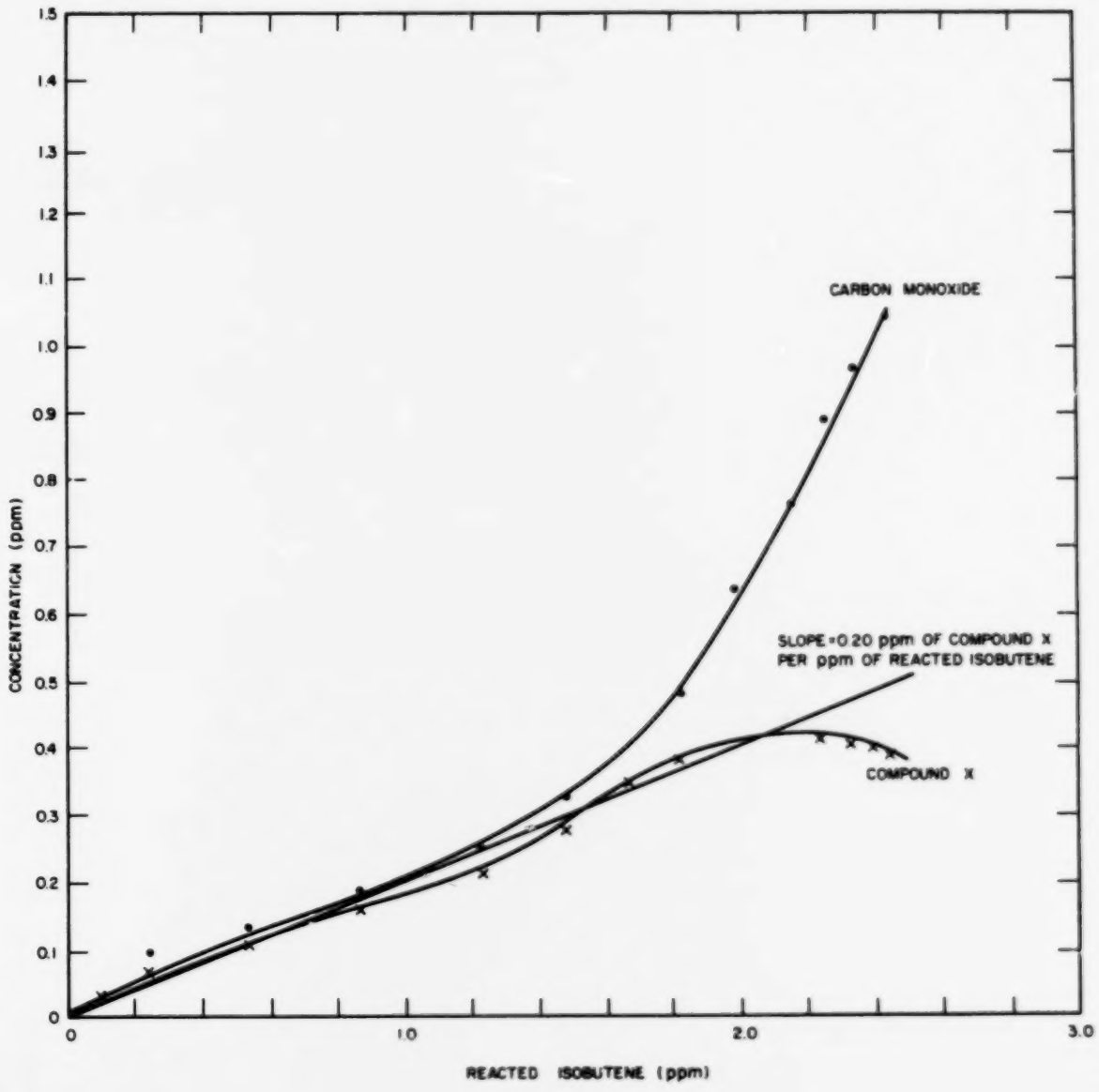

Fig. 5

PRODUCT CONCENTRATION AS A FUNCTION OF
REACTED ISOBUTENE CONCENTRATION
(Carbon Monoxide and Compound X)

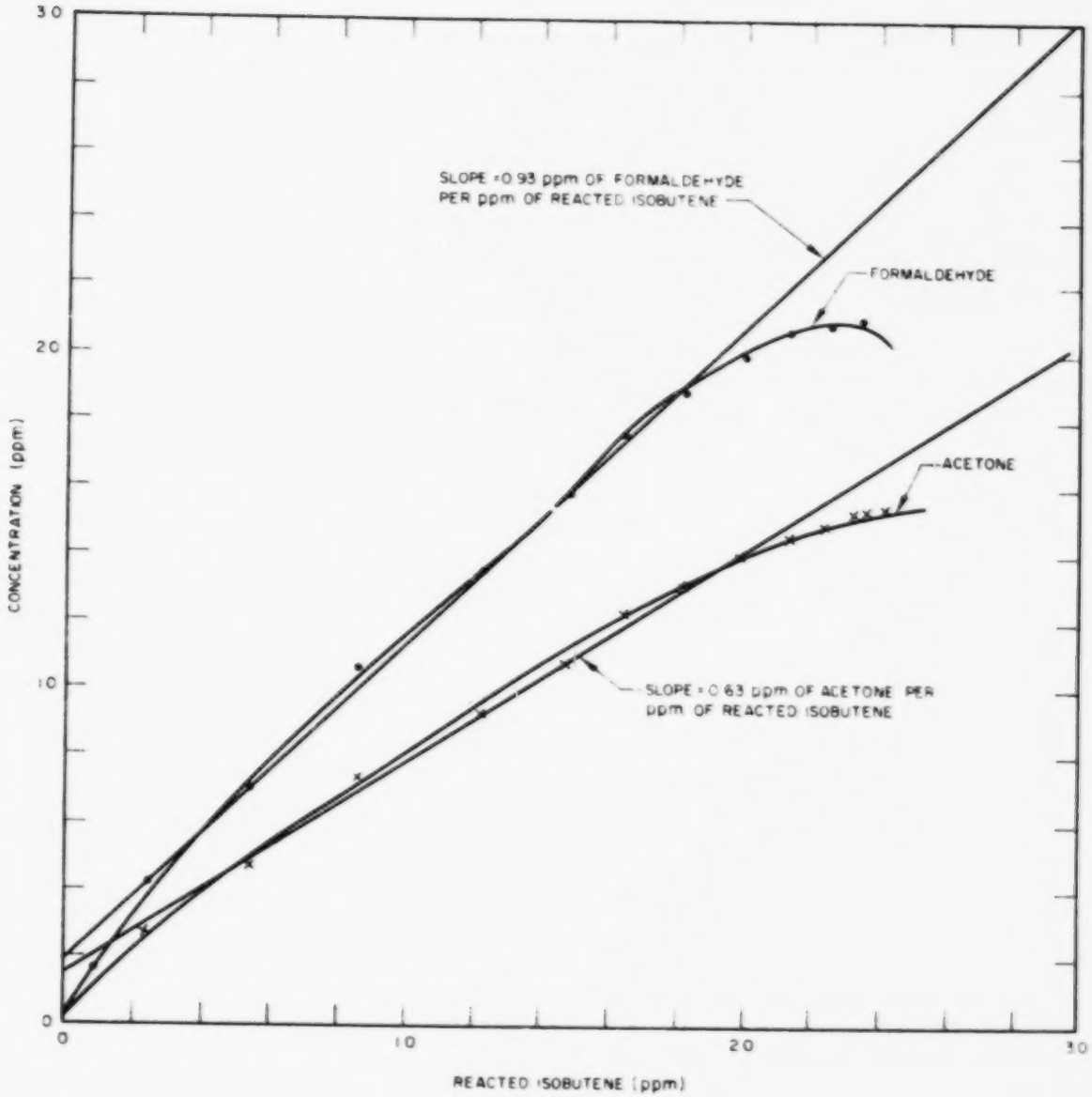

Fig. 6

PRODUCT CONCENTRATION AS A FUNCTION
OF REACTED ISOBUTENE CONCENTRATION
(Formaldehyde and Acetone)

The slope of the formaldehyde curve, disregarding the values beyond 70 min, is 0.93 ppm of formaldehyde per 1 ppm of reacted isobutene. Again, this indicates a splitting of the isobutene molecule at the double bond. It also indicates that formaldehyde is the only product obtained from the methylene carbon of the isobutene molecule. The slope for acetone is 0.63 ppm of acetone per 1 ppm of reacted isobutene. For compound X it is 0.20 ppm per 1 ppm of reacted isobutene. Thus, these data indicate that the three-carbon portion of the isobutene molecule forms primarily acetone and compound X. The sum of the acetone plus the compound X plus the other minor products (excluding isobutene oxide) will be approximately equal to 1 ppm of products per 1 ppm of reacted isobutene. This sum can be calculated by subtracting the slope of the formaldehyde curve (0.93) from the slope of the sum of all products (1.9) shown in Figure 4.

The next question to be considered was the source of the carbon monoxide. Since carbon monoxide is a secondary product, it is reasonable to assume that it could arise from reaction of the formaldehyde, acetone, and compound X. This assumption appears more reasonable when one notes the "tailing off" of the curves at longer reaction times as shown in Figures 5 and 6. Among these products, formaldehyde is the most susceptible to analysis, since we can assume the formation of 1 molecule of carbon monoxide per molecule of reacted formaldehyde. In addition, we have determined a value for the normalized rate constant of formaldehyde in the presence of nitrogen dioxide and irradiation (0.35×10^{-2} min^{-1}). Using this rate constant value and the observed formaldehyde values, we calculated the amount of formaldehyde converted to carbon monoxide during each 10 min of the reaction. The sum of these amounts at any given time represents the amount of formaldehyde reacting to form carbon monoxide. These are shown in Figure 7 as a function of the amount of isobutene reacted. Adding this calculated amount of reacted formaldehyde to the observed formaldehyde values gives a value for the total formaldehyde formed. This sum is shown in Figure 8, plotted against the amount of isobutene reacted. For purposes of comparison, the observed formaldehyde values are also plotted. The resulting sum curve is close to a straight line and has a slope of 1 ppm of formaldehyde per 1 ppm of isobutene reacted.

This same treatment was applied to peroxyacetylnitrate and acetone, as shown in Figures 9 and 10. However, since no values were available for the normalized rates of reaction of these compounds, three more assumptions had to be made. It was assumed that, whatever the values of the normalized rate constants, the sum curve of the amounts reacting as a function of the amount of isobutene reacted would have the same general shape as that shown for formaldehyde in Figure 7. It was

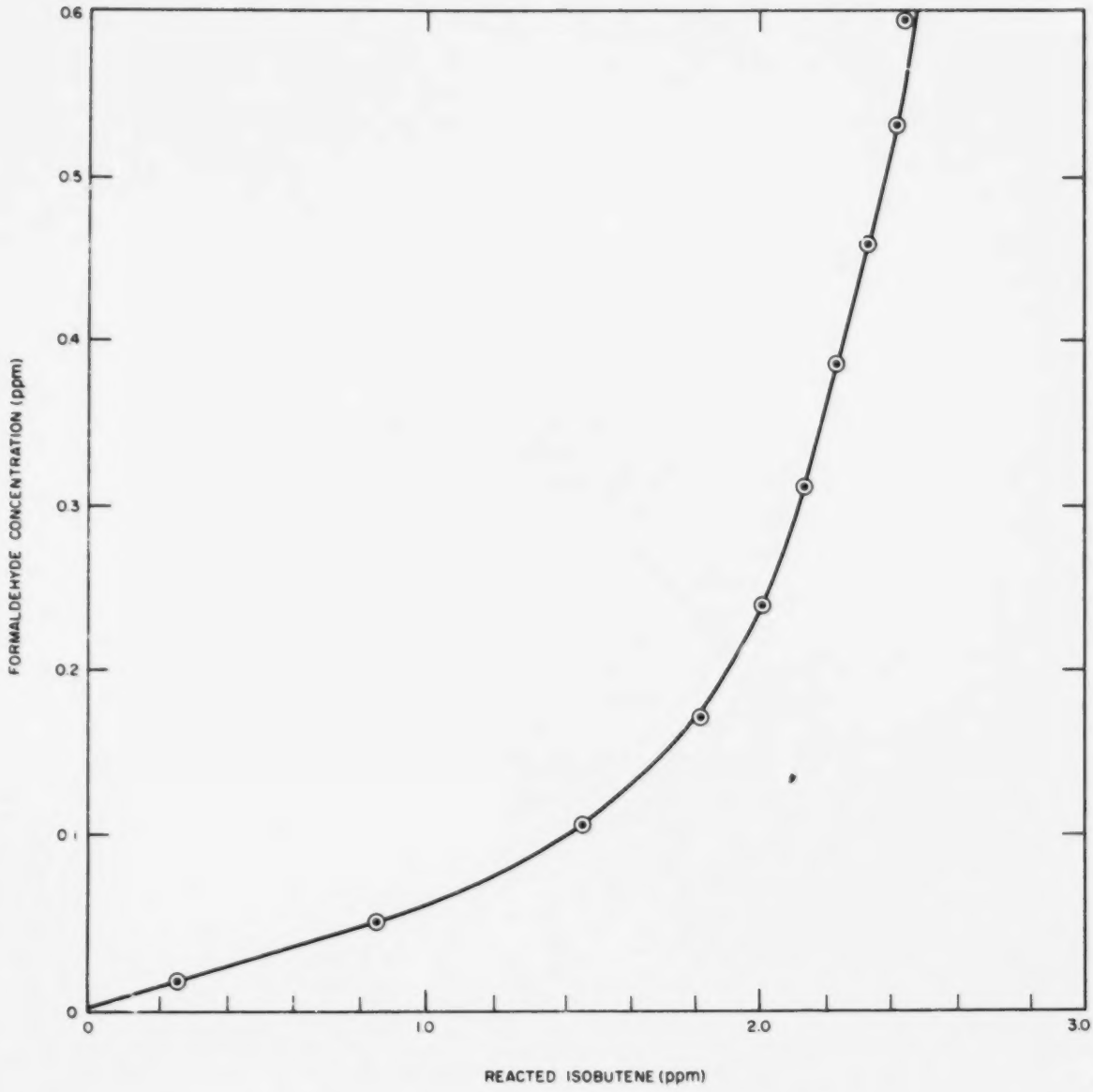

Fig. 7

CALCULATED CONCENTRATION OF FORMALDEHYDE
REACTING TO FORM CARBON MONOXIDE

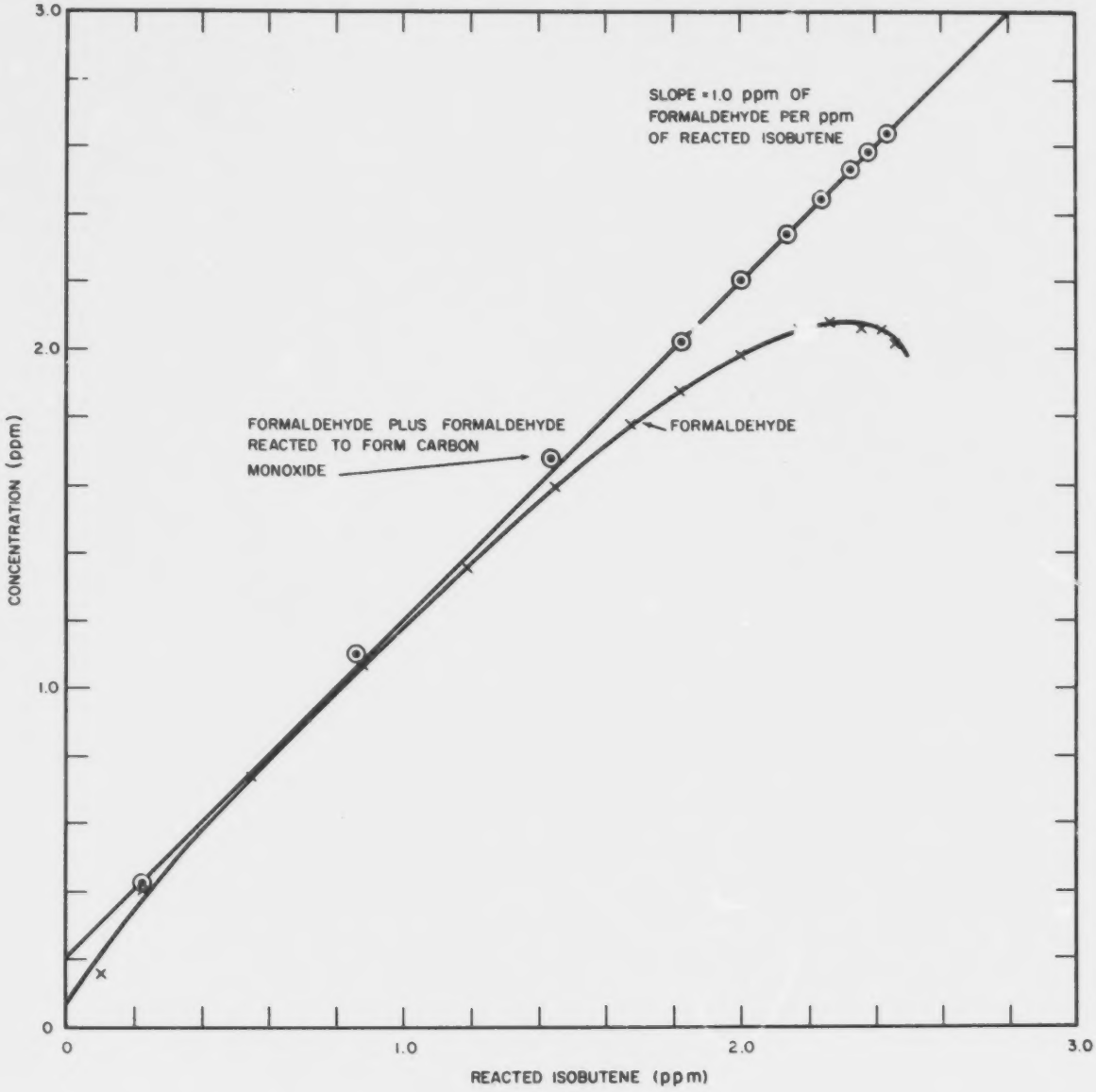

Fig. 8

FORMALDEHYDE CONCENTRATION AS A FUNCTION OF REACTED ISOBUTENE CONCENTRATION

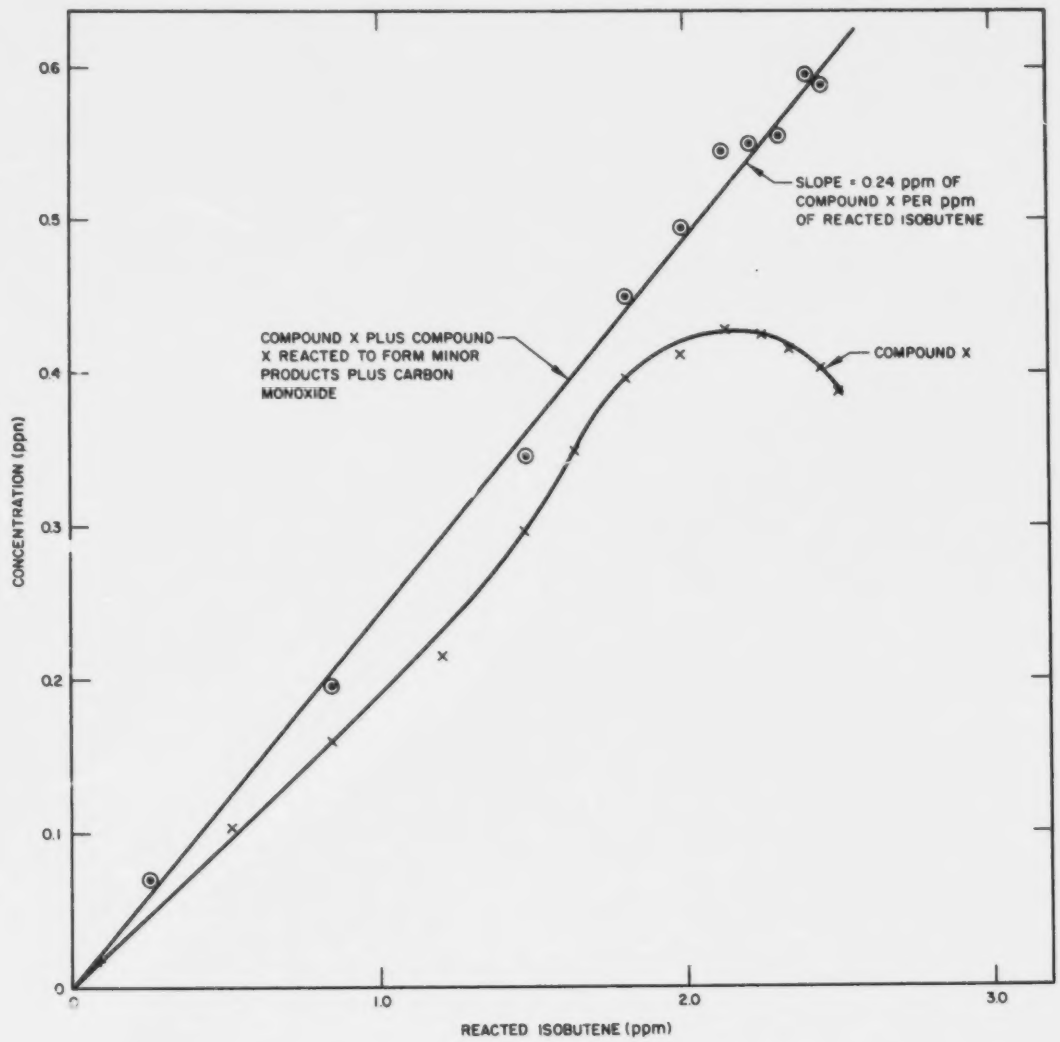

Fig. 9

COMPOUND X CONCENTRATION AS A FUNCTION OF REACTED ISOBUTENE CONCENTRATION

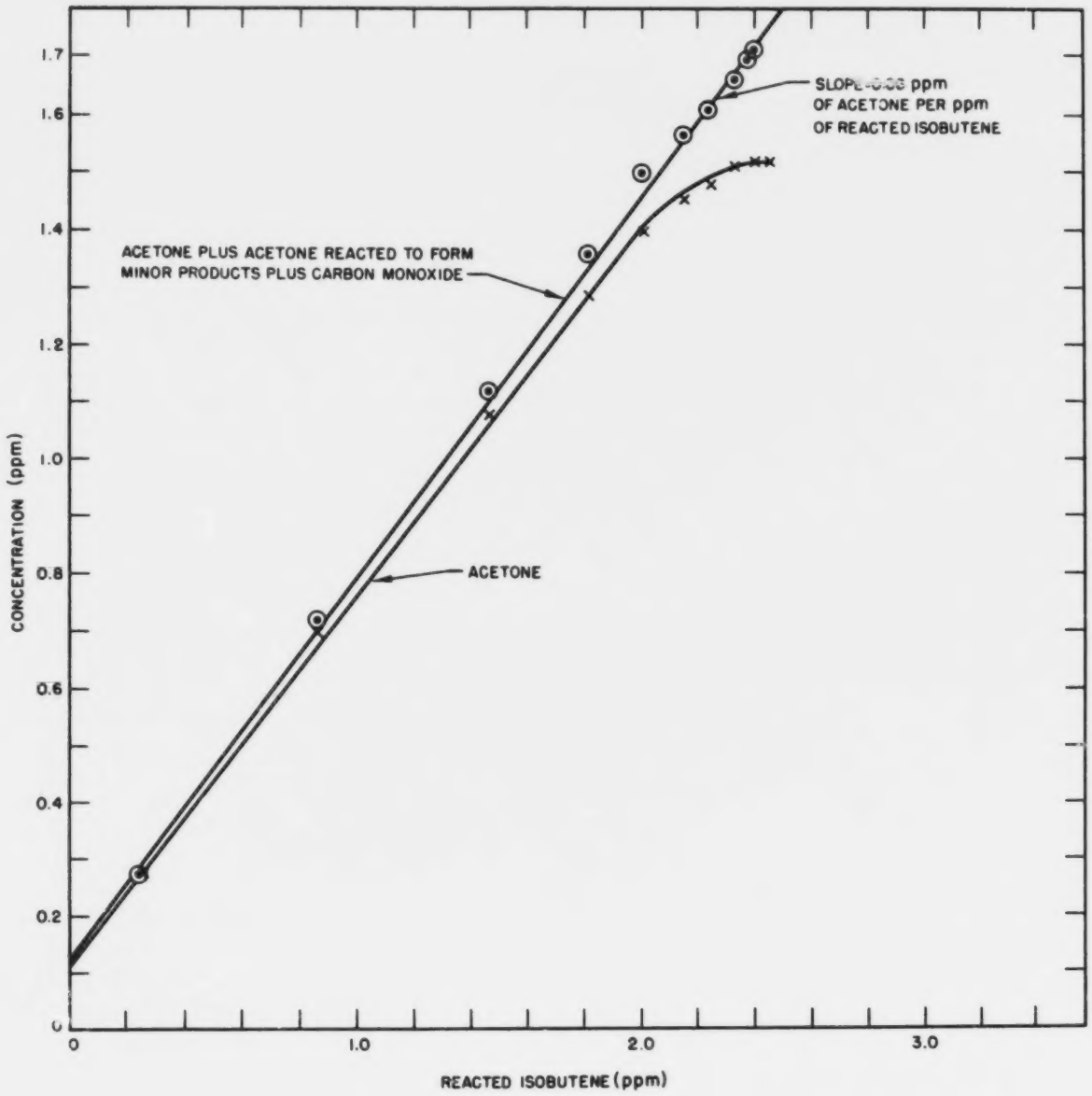

Fig. 10

ACETONE CONCENTRATION AS A FUNCTION
OF REACTED ISOBUTENE CONCENTRATION

also assumed that only 1 molecule of carbon monoxide would arise from each acetone or compound X molecule reacted. It was further assumed that the maximum amount reacted at 100 min would be equal to the difference between the straight line through the points and the observed curves shown in Figures 5 and 6. It was then possible to read from Figure 7 the amounts of acetone and compound X that had reacted to form carbon monoxide; the corrected curves are shown in Figures 9 and 10. Taking into account the calculated amounts of carbon monoxide arising from the photooxidation of formaldehyde, acetone, and compound X, we find a total of 0.25 ppm of carbon monoxide which is not accounted for but which could be due to further photolysis of the minor products.

Thus, the data indicate that 90 percent of the isobutene is split at the double bond. Most of the remaining 10 percent appears as isobutene oxide, which is a stable end product. The split at the double bond results in the formation of formaldehyde from the methylene carbon of the isobutene molecule. Sixty-six percent of the isobutene three-carbon fragment ultimately appears as acetone and 24 percent as compound X. These two products therefore account for 90 percent of the three-carbon fragment. The remaining 10 percent appears as minor end products. The formaldehyde, acetone, and compound X all can undergo secondary photooxidation to form carbon monoxide and minor end products. Eighty percent of the carbon monoxide can be accounted for on the basis of photooxidation of formaldehyde, acetone, and compound X. The remaining carbon monoxide probably arises from photooxidation of the minor products.

B. Reactions Occurring during Photooxidation

1. Rate of Reaction of Isobutene

Analyses of the rate of photooxidation of isobutene by nitrogen dioxide in air for a series of 32 experiments were presented in a previous report.[1] In that work the effect of light intensity and of initial hydrocarbon concentration was studied and the following conclusions were drawn:

1. The rate of isobutene disappearance due to oxygen atom and ozone attack is proportional to the light intensity and independent of the initial isobutene concentration.

2. Initially, the rate of isobutene disappearance is accounted for by oxygen atom attack.

3. The final ozone concentration varies directly with the square root of the light intensity and is independent of the initial isobutene concentration.

4. The rate of isobutene disappearance in excess of that due to atomic oxygen and ozone attack is also proportional to the square root of the light intensity but varies linearly with initial isobutene concentration.

The initial hydrocarbon-to-nitrogen dioxide concentration ratios for which the above results were found to be true were from 1 to 6 at an initial nitrogen dioxide concentration of 1 ppm. The region below a ratio of 1 is currently under investigation. Finding (4) seems to indicate that there is little, if any, excess rate when this ratio is much less than 1. This appears to be confirmed in the current investigation. For values of the ratio somewhat above 6, the excess rate also disappears. This apparent peaking of the excess rate at certain initial hydrocarbon-to-nitrogen dioxide ratios indicates the occurrence of two other types of reactions involving the hydrocarbon in addition to the atomic oxygen and ozone reactions.

One of the purposes of the present set of experiments has been to determine the nature of the dependence of the rate of disappearance of the hydrocarbon on the initial nitrogen dioxide concentration. The data from a portion of this series of 16 experiments have been analyzed; in this work the initial hydrocarbon concentrations and the light intensity values were fixed and the initial nitrogen dioxide concentrations were varied. The hydrocarbon studied was isobutene with its initial concentration fixed at 3 ppm while the initial nitrogen dioxide level was varied between 0.1 ppm and 3 ppm. The light intensity was fixed at 1.15×10^{16} quanta cm^{-2} sec^{-1}.

The isobutene, nitrogen dioxide, and ozone time-concentration data were used to compute the total rate of isobutene disappearance. From this total rate of disappearance we subtracted the rates of disappearance due to ozone and oxygen atom attack to give us what has been designated as the excess rate.

The results of the analysis of the dependence of this excess rate at its maximum value on the initial nitrogen dioxide concentration are presented in Table III. When these excess rates at maximum value are plotted against the one-half power of the initial nitrogen dioxide concentration, we obtain the direct dependence shown in Figure 11. The result is consistent with the finding that the excess rate of hydrocarbon disappearance is proportional to the square root of the light intensity. The results indicate

Table III

DEPENDENCE OF EXCESS RATE OF ISOBUTENE D'SAPPEARANCE ON INITIAL NITROGEN DIOXIDE CONCENTRATION (AT FULL LIGHT INTENSITY)

Initial Hydrocarbon Concentration (ppm)	Initial Nitrogen Dioxide Concentration (ppm)	Maximum Excess Rate (min^{-1})
2.86	0.11	0.0057
3.06	0.32	0.0120
2.80	1.00	0.0452
3.16	1.02	0.0297
2.52	3.02	0.0457

Note: It was implicitly assumed in the regression calculations that the excess rate was zero for no initial nitrogen dioxide.

that the reactions involved in the excess rate process are chain reactions initiated by oxygen atoms produced by the photolysis of nitrogen dioxide, and that the species attacking the hydrocarbon disappear principally by a recombination process.

2. Effect of Including Additional Compounds

One method of obtaining additional information on the rates of reaction and products of photooxidation reactions is to add compounds to the reacting olefin-oxide of nitrogen mixture and thus attempt to alter this reaction. The data taken from these experiments may then be compared with data taken from photooxidation experiments in which no compounds have been added.

Our previous results have shown that the formation of aerosol in reactions requires the presence of sulfur dioxide in addition to olefins and an oxide of nitrogen. The role of sulfur dioxide in the photooxidation experiments is being extensively studied, using separate experimental equipment. However, it is of interest to examine the sulfur dioxide-olefin-oxide of nitrogen mixture in the 520-cubic-foot reaction chamber,

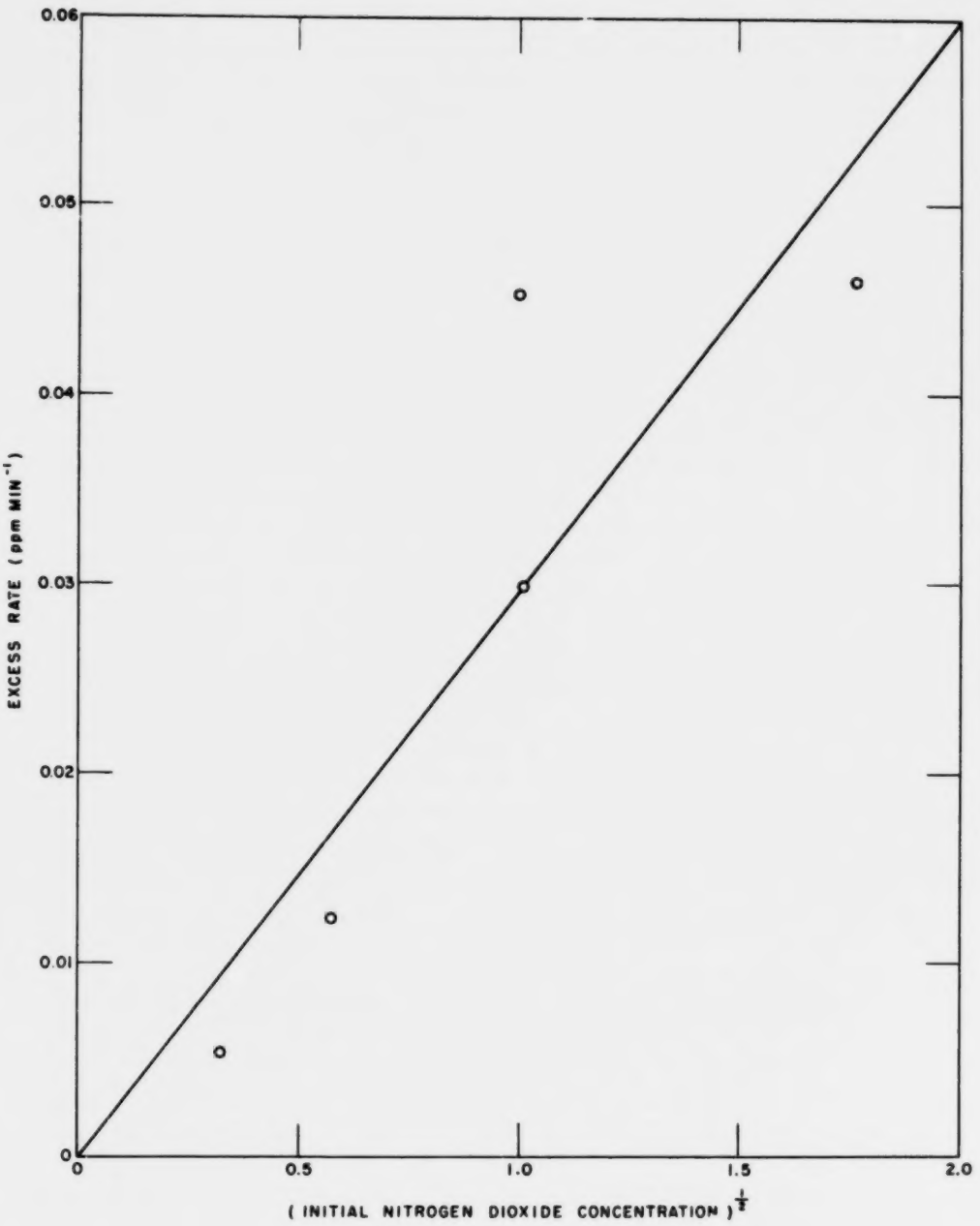

Fig. 11

DEPENDENCE OF EXCESS RATE OF ISOBUTENE DISAPPEARANCE ON INITIAL NITROGEN DIOXIDE CONCENTRATION

using 3 ppm of isobutene, 1 ppm of nitrogen dioxide, and 3 ppm of sulfur dioxide. In this experiment the normalized rate of reaction for the isobutene was found to be 4.08×10^{-2} min^{-1}, which is somewhat higher than the 3.36×10^{-2} min^{-1} value found in the absence of sulfur dioxide. The amounts of products formed were plotted against the amount of isobutene reacted. The resulting curves are very nearly straight lines. The slope of the compound X line represents 0.19 ppm per 1 ppm of reacted isobutene. This is close to the 0.24 value obtained in the absence of sulfur dioxide. The slope of the acetone curve represents 0.53 ppm of acetone per 1 ppm of reacted isobutene, which is similar to the value of 0.66 in the absence of sulfur dioxide. However, the formaldehyde slope is 0.40 compared to 0.93 in the absence of sulfur dioxide.

These results suggest that sulfur dioxide interferes with the course of the reaction caused by the reactive intermediates. It has been suggested that reactions such as

$$HO_2^{\bullet} + SO_2 \longrightarrow HO^{\bullet} + SO_3$$

are very fast. Thus, sulfur dioxide would tend to suppress hydroperoxyl in favor of hydroxyl radicals, and we may be seeing the results of this type of reaction in the suppression of formaldehyde.

This experiment also indicates the possibility that 50 percent of the formaldehyde formed is included in the aerosol particles, thus providing our first indication of the presence of a specific organic in the aerosol particles. Previous analysis of aerosol particles had indicated the presence of organic materials, but had not provided information on their nature. This new indication is interesting in that it supports some preliminary findings of H. Stevenson of the United States Public Health Service. Mr Stevenson found that aerosol particles in the Los Angeles Basin did contain formaldehyde which could be released for analysis in a particle centrifuge.

Addition of propylene oxide also caused a decrease in the normalized rate of reaction of isobutene. Thus, a value of 1.90×10^{-2} min^{-1} was obtained in the presence of propylene oxide compared to 3.36×10^{-2} min^{-1} in the absence of the oxide.

In one photooxidation reaction 0.5 ppm of ozone was added to a mixture of 3 ppm of isobutene and 3 ppm of nitrogen dioxide. The products obtained under these conditions differ from those obtained without added initial ozone in the following respects:

1. No alkyl nitrites were observed when initial ozone was added whereas methyl nitrite was present at low concentrations without added ozone.

2. Propionaldehyde and propylene oxide were present with added ozone whereas little or none appeared without added ozone.

3. On the other hand, isobutene oxide and acetaldehyde, which appeared without added ozone, were absent.

4. The isobutyraldehyde concentration was approximately the same in both cases.

These results indicate that there is less fragmentation of the intermediates to form low-carbon compounds at lower nitric oxide levels. The lower yield of isobutene oxide may be explained in part by the fact that fewer isobutene molecules are being attacked by atomic oxygen.

3. Photolysis of Alkyl Nitrites

a. Ethyl Nitrite

The photolysis of ethyl nitrite was studied to learn in greater detail the nature of the products formed and the reactions by which these products are formed. This study was started when it appeared that this alkyl nitrite was present in low concentrations along with methyl nitrite in the photooxidations of olefin-nitrogen dioxide mixtures. The high absorption coefficients of alkyl nitrites would prevent their forming in high concentrations, but they could act as reaction intermediates.

In this work 3 ppm of ethyl nitrite were photolyzed in the 520-cubic-foot chamber in purified air and with the same light sources as have been described previously for the olefin-nitrogen dioxide mixtures. The nitrite was also photolyzed in nitrogen. The course of the reaction was followed by use of infrared spectrophotometry, gas chromatography, and liquid scrubbers. This photolysis was also studied in the 2-cubic-foot sample cell of the infrared spectrophotometer, and the results were similar to those reported here.

During photolysis in air, the concentration of ethyl nitrite dropped quite rapidly so that approximately 80 percent of the original compound disappeared in 20 min. The principal reaction products at this time were acetaldehyde, compound X, carbon monoxide, nitrogen

dioxide, and ozone. Possible reactions by which these products were formed are outlined below:

$$CH_3CH_2ONO + h\nu \longrightarrow CH_3CH_2O^{\ast}\cdot + NO \quad (1)$$

$$CH_3CH_2O^{\ast}\cdot + O_2 \longrightarrow CH_3CHO^{\ast} + HO_2\cdot \quad (2)$$

$$CH_3H_2O^{\ast}\cdot + O_2 \longrightarrow CH_3CHO + HO_2\cdot \quad (2a)$$

(acetaldehyde)

$$CH_3CHO^{\ast} + O_2 \longrightarrow CH_3\dot{C}O + HO_2\cdot \quad (3)$$

$$CH_3CHO + HO_2\cdot \longrightarrow CH_2\dot{C}O + H_2O_2 \quad (4)$$

$$CH_3\dot{C}O + O_2 \longrightarrow CH_3C(O)OO\cdot \quad (5)$$

$$CH_3C(O)OO\cdot + NO \longrightarrow CH_3C(O)O\cdot + NO_2 \quad (6)$$

(nitrogen dioxide)

$$CH_3C(O)OO\cdot + NO_2 \longrightarrow CH_3C(O)OONO_2 \quad (7)$$

(compound X)

$$CH_3\dot{C}O + M \longrightarrow CH_3\cdot + CO \quad (8)$$

(carbon monoxide)

$$NO_2 + h\nu \longrightarrow NO + O \quad (9)$$

$$O + O_2 + M \longrightarrow O_3 + M \quad (10).$$

After 120 min, the principal products of the reaction were ethyl nitrate, compound X, formaldehyde, carbon monoxide, nitrogen dioxide, and ozone. It is noted that the acetaldehyde present at 20 min had disappeared and that ethyl nitrate and formaldehyde had appeared. In addition, the concentrations of the other products seen earlier had gradually increased. The manner in which these changes probably occur is outlined below. The peaking of acetaldehyde is due to the fact that the rates of reactions (3), (4), and (11) exceed those of (1), (2), and (2a) during this period.

$$CH_3CHO + h\nu \longrightarrow CH_3\cdot + \cdot CHO \quad (11)$$

Ethyl nitrate may appear via reaction (12) and formaldehyde via (13), (14), and (16).

$$CH_3CH_2O\cdot + NO_2 \longrightarrow CH_3CH_2ONO_2 \quad (12)$$
(ethyl nitrate)

$$CH_3\cdot + O_2 \longrightarrow CH_3OO\cdot \quad (13)$$

$$CH_3OO\cdot + NO \longrightarrow CH_3O\cdot + NO_2 \quad (14)$$

$$HO_2\cdot + NO \longrightarrow HO\cdot + NO_2 \quad (15)$$

$$CH_3O\cdot + O_2 \longrightarrow CH_2O + HO_2\cdot \quad (16)$$
(formaldehyde)

The photolysis of ethyl nitrite in nitrogen was found to give principally ethyl nitrate. The oxidation is believed to have been due to the oxygen impurity in the nitrogen, following the reaction sequence (1), (2), (15), and (12).

The fact that the principal product in the photolysis of ethyl nitrite in nitrogen was ethyl nitrate indicates that a portion of the ethoxyl radicals formed in the primary process recombines with nitric oxide to form the original compound. Another portion reacts with molecular oxygen to form hydroperoxyl radicals which oxidize nitric oxide to nitrogen dioxide. In this manner it is possible for nitrogen dioxide to react with the ethoxyl radicals formed in the subsequent photolysis of ethyl nitrite. The absence of peroxyacetylnitrate indicates a low concentration of peroxyacetyl radicals or a low yield for (7) compared with (6). A low concentration of peroxyacetyl radicals would be expected with the rates of (3) and (5) being low due to the low oxygen concentration.

Neither of these experiments included analyses for nitrosomethane (CH_3NO), hyponitrous acid ($H_2N_2O_2$), or formaldoxime (CH_2NOH). Of these three, only nitrosomethane is likely to be eluted from the polyethylene glycol gas chromatographic column under the present operating conditions.

b. Butyl Nitrite

n-Butyl nitrite was photolyzed in the same manner as ethyl nitrite except that minor products were analyzed after approximately 60 min of irradiation. n-Butyraldehyde was observed as the principal

product. No compound X was observed, indicating that reactions corresponding to (4) are not important in this case.

4. Reaction Kinetics

a. Olefin Reactions and Reaction Rates

The need for a better understanding of the complex reaction proceeding in the photooxidation of the unsaturated hydrocarbons prompted study of the dark reactions of ozone with an olefin in air and of ozone and nitrogen dioxide with an olefin in air. Isobutene was used as the representative unsaturated hydrocarbon in both instances. The products of the straight ozonation were principally formaldehyde, acetone, and two unidentified compounds, one tentatively considered to be isobutyraldehyde. A small amount of ethylene oxide appeared to be present after 60 min. More formaldehyde than acetone was formed on a molar basis.

When nitrogen dioxide was added to the initial mixture in the dark, the principal products were found to include compound X in place of isobutyraldehyde. In this case, the acetone and formaldehyde were formed in nearly equimolar quantities. Also, numerous minor products were formed, including acetaldehyde, isobutene oxide, propionaldehyde, and several unidentified compounds.

The results of these preliminary experiments indicate that some intramolecular transfer of hydrogen takes place in the ozonation, as is the case with atomic oxygen attack, and that the nitrogen dioxide reacts with the intermediates formed by the ozonation. The formation of the compound X may proceed according to the following:

$$(CH_3)_2\,C = CH_2 + O_3 \longrightarrow (CH_3)_2\,\overset{+}{C}\overset{-}{O}O + H_2CO \qquad (17)$$

$$NO_2 + O_3 \longrightarrow NO_3 + O_2 \qquad (18)$$

$$NO_3 + NO_2 \longrightarrow N_2O_5 \qquad (19)$$

$$N_2O_5 + H_2O \longrightarrow 2HONO_2 \qquad (20)$$

$$CH_3\!-\!\overset{+}{C}\overset{-}{O}O\!-\!CH_3 \rightleftharpoons CH_3\!-\!C(=O)\!-\!CH_3 \qquad (21)$$

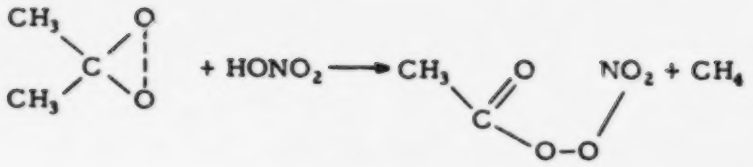

(22).

As indicated in previous reports, the rate of photooxidation of an olefin in the presence of an oxide of nitrogen is much faster than can be accounted for by reaction of the olefin with oxygen atoms and ozone. Interpreting the experimental results which led to this statement depends on knowing the value of the second-order rate constants for the reaction between the olefin and ozone or oxygen atoms. Given values for these constants, it is possible to calculate the rate of olefin reaction due to reaction with ozone and oxygen. These values can then be subtracted from the observed rate of olefin reaction, and the difference will represent the rate of olefin reaction which is not accounted for by reaction with ozone and oxygen atoms. Since these calculated rates are determined from rate constants, it was thought advisable to use our experimental equipment to redetermine the value of some of them. Thus, we investigated the rate constants of ozone with 1-hexene and ozone with isobutene.

The value for 1-hexene had been established by two other research teams, with good agreement between their results. Therefore, determining this constant in our system was a test of our experimental equipment and methods. The 520-cubic-foot chamber was used for three experiments in which 3 ppm of 1-hexene were mixed with 1 ppm of ozone in air. The ozone and 1-hexene concentrations were determined once each minute for various time periods up to 200 min. The rate constant (k) was determined by two methods. In the first method k was determined from a knowledge of the time-concentration curve of the olefin and the initial ozone value. In addition, a small correction was used to account for the known rate of destruction of ozone alone in the chamber. The equation used for calculation of the rate constant was:

$$k = - \frac{\ln \frac{[H]}{[H]_f} + \alpha \int_0^t \ln \frac{[H]_0}{[H]} \, dt}{\int_0^t \left([H]_0 - [H] - [0_3]_0 \right) dt}$$

where $[H]$ = concentration of 1-hexene
$[H]_0$ = concentration of 1-hexene at zero time
$[H]_f$ = concentration of 1-hexene at final time
α = the decay rate of ozone in our system.

This method provided a calculated rate constant of $1.66 + 0.45 \times 10^{-2}$ ppm^{-1} min^{-1} for the 1-hexene reaction with ozone.

The second method involves the observed values of olefin and ozone during the experiment. The equation used for this calculation was:

$$k = \frac{1}{t - t_0} \int_0^t \frac{d \ln \frac{[H]_0}{[H]}}{[O_3]}$$

With this method the calculated value was $1.74 \pm 0.43 \times 10^{-2}$ ppm^{-1} min^{-1}.

The average value for these two methods is $1.70 \pm 0.44 \times 10^{-2}$ ppm^{-1} min^{-1}, which is within experimental error of the values determined by other investigators. The ratio of olefin reacted to ozone reacted is 1.3 for the three experiments.

Since this determination appeared satisfactory, we next studied the ozone-isobutene reaction. Six experiments were conducted with the rate constant determined by the two methods described above. The average value is $2.15 \pm 0.54 \times 10^{-2}$ ppm^{-1} min^{-1}. The 99 percent confidence interval is 1.85 to 2.45. The average value is twice as large as that found by the Franklin Institute[2]. Furthermore, the ratio of reacted olefin to reacted ozone is 2.4. Evidently we are not dealing with a simple second-order reaction, the basis on which these calculations were carried out. Other evidence which supports this postulate shows that the rate constant decreases with time. The value reported above holds approximately for the first 60 min of the reaction. At the end of 100 min, the rate drops to approximately 1.0×10^{-2} ppm^{-1} min^{-1}.

More detailed work is needed to determine the nature of the olefin-ozone reactions. In lieu of this information, we accepted the 2.15×10^{-2} ppm^{-1} min^{-1} value as being our best estimate of the rate constant representing the reaction of isobutene with ozone, plus reaction of isobutene with products of the ozone-isobutene reaction, during the first 60 min of the reaction. Using this value, we estimated the contribution of these reactions to the loss of isobutene during photooxidation of nitrogen dioxide and isobutene mixtures. The results of these calculations are shown in Figure 12, which provides a comparison with the observed rate of isobutene reaction. It can be seen that the rate of reaction of isobutene during photooxidation is still twice as great as can be accounted for by the oxygen atom reaction and the ozone-complex reaction.

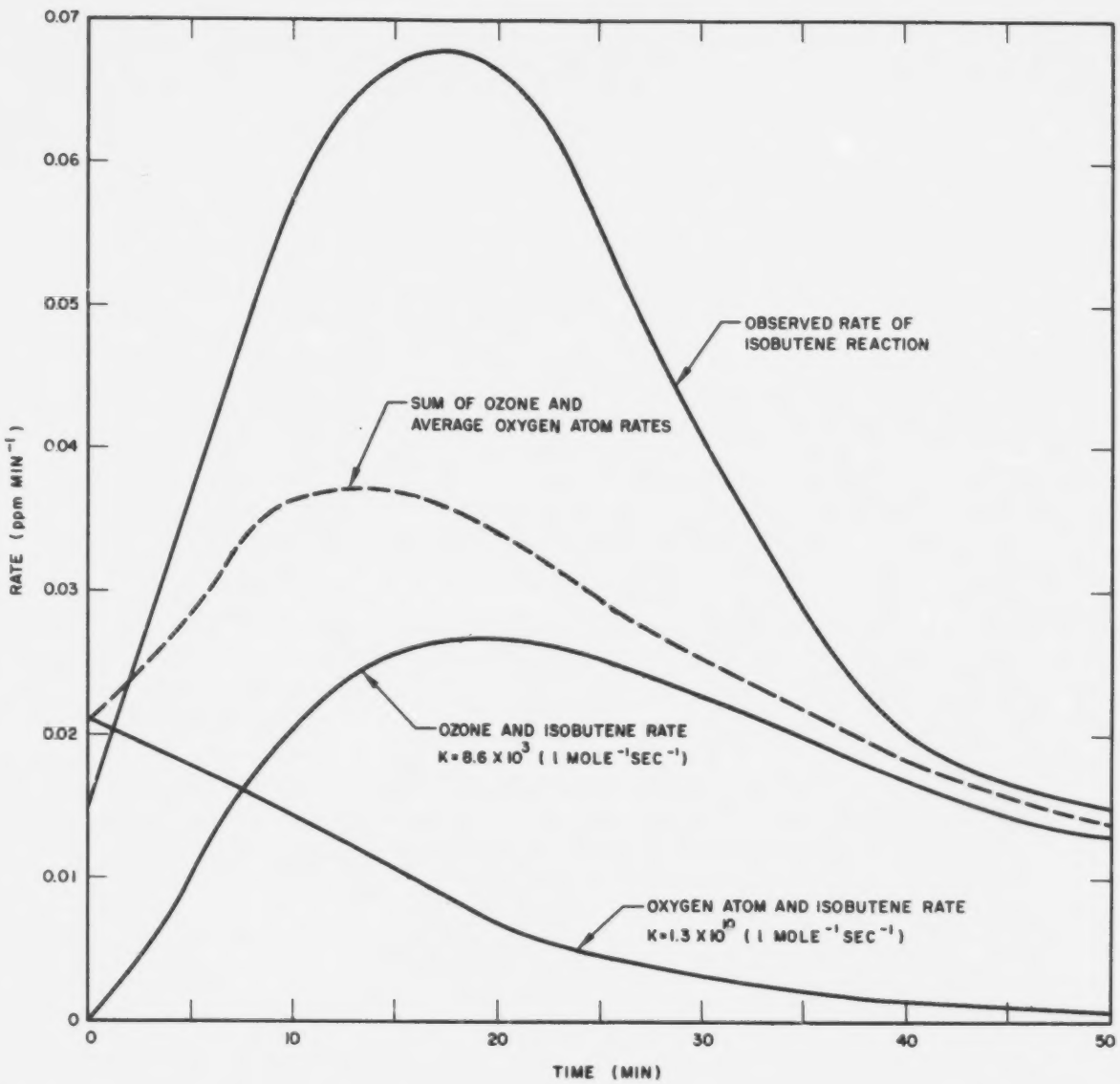

Fig. 12

RATES OF REACTION DURING PHOTOOXIDATION OF NITROGEN DIOXIDE AND ISOBUTENE

Uncertainty as to the reaction constants of the oxygen atom and ozone with isobutylene has led to the suggestion that the excess rate may be fictitious. One necessary but not sufficient condition that this be true is that there be a good linear correlation of disappearance and appearance of major reactants and products with the integrals

$$I_1 = \int_0^t (O_3)\,(HC)dt$$

$$I_2 = \int_0^t (NO_2)\,(HC)\,dt$$

during an appreciable fraction of the reaction.

The insufficiency of this relationship to prove the absence of an excess rate lies in the possible approximate linear dependence of reactive intermediate concentration on ozone and nitrogen dioxide during the first stages of the reaction, combined with the smoothing effects of using integrals for correlation. However, the use of such a correlation will lead to suggestions on (1) the relative importance of the two reactions, (2) the tenability of the hypothesis of excess rate, and (3) more sophisticated treatment of the data, using the same general approach. This correlation was tested by use of the experimental data of Figure 1 (3 ppm of isobutylene, 1 ppm of nitrogen dioxide). The correlation was tested by plotting I_1 and I_2, both divided by the quantity in question against each other, noting the fit to a straight line and the slope and intercept of the best fit. It was found that a good fit was obtained by a straight line for all quantities tested for the first 25-30 min of the reaction. After this period, significant deviations became apparent. The results are summarized in Table IV. The coefficients for both I_1 and I_2 would be about 10-20 if only the bimolecular reactions between oxygen atom and isobutene and between ozone and isobutene governed the disappearance of reactants and the appearance of products. It is interesting to note that some of the coefficients lie in or near this range. The accuracy of the coefficients is not very great.

It is possible to use these numbers to obtain a great many suggested relationships, especially when one takes full advantage of the large probable errors. Of interest is the strong correlation with the ozone-hydrocarbon reaction, which suggests that, although the oxygen-atom reaction may start the chain, the reactions following the ozone-hydrocarbon reaction are very important in sustaining the reaction. In this connection one notes that the ozone and the oxygen-atom reactions are equally important in producing more ozone.

Table IV

RESULTS OF LINEAR CORRELATION OF OXYGEN-ATOM AND OZONE REACTIONS WITH ISOBUTENE WITH APPEARANCE AND DISAPPEARANCE OF PRODUCTS AND REACTANTS

Quantity (ppm x 10^3)	Coefficient of $I_1 = \int_0^t (O_3)\,(HC)dt$ (ppm^2 min)	Coefficient of $I_2 = \int_0^t (NO_2)\,(HC)dt$ (ppm^2 min)	Remarks
$(HC)_0$-(HC)	44.5	4.85	Slight excess in consumption appeared at 25-35 min
$(NO_2)_0$-(NO_2)	25.8	2.82	Deficiency in consumption appeared at 20 min
(HCHO)	39.6	9.4	Deficiency in formation appeared at 35 min
(CO)	6.9	1.6	Excess in formation appeared at 25 min
$\left(\begin{matrix}CH_3\\ \diagdown\\ \quad C{=}O\\ \diagup\\ CH_3\end{matrix}\right)$	30.2	4.7	Deficiency in formation appeared at 35 min
$(CH_3\text{-}\overset{\overset{O}{\|}}{C}\text{-}O\text{-}ONO_2)$	7.0	1.5	Slight excess in formation appeared at 35 min but returned to line at 60 min
(O_3)	11.7	14.2	Deficiency in formation appeared at 30 min

One approximate, partial over-all reaction suggested by these numbers is

$$10\ NO_2 + 10\ \begin{matrix} CH_3 \\ \diagdown \\ \quad C{=}CH_2 \\ \diagup \\ CH_3 \end{matrix} + 10\ O_3 \xrightarrow[NO_2]{h\nu,\ O_3} 10\ HCHO$$

$$+\ 10\ CH_3\overset{\overset{O}{\|}}{C}\text{-}O\text{-}ONO_2 + 10\ CO + \text{reactive intermediates.} \qquad (23)$$

The precursor of the carbon monoxide apparently includes a methyl radical from the branched half of the hydrocarbon. The reactive intermediates must produce the over-all approximate reaction

$$15\ NO_2 + 30\ \begin{matrix} CH_3 \\ \diagdown \\ \quad C{=}CH_2 \\ \diagup \\ CH_3 \end{matrix} + 30\ O_2 \longrightarrow 30\ HCHO$$

$$+\ 30\ \begin{matrix} H_3C \\ \diagdown \\ \quad C = O \\ \diagup \\ H_3C \end{matrix} + \text{other products} \qquad (24)$$

to account for the other coefficients. One possible oversimplified partial mechanism may be as follows:

$$10\ \begin{matrix} CH_3 \\ \diagdown \\ \quad C{=}CH_2 \\ \diagup \\ CH_3 \end{matrix} + 10\ O_3 \longrightarrow 10\left[\begin{matrix} CH_3 \\ \diagdown \\ \quad C\text{-}O\text{-}O \\ \diagup \\ CH_3 \end{matrix}\right] + 10\ H_2CO \qquad (25)$$

$$10\left[\begin{matrix} CH_3 \\ \diagdown \\ \quad C\text{-}O\text{-}O \\ \diagup \\ CH_3 \end{matrix}\right] + 10\ NO_2 \xrightarrow{O_2,\ O_3,} 10\ CH_3^{\bullet} + 10\ CH_3\text{-}\overset{\overset{O}{\|}}{C}\text{-}O\text{-}O\text{-}NO_2,$$

which is suggested by the results of a dark reaction between isobutylene, nitrogen dioxide, and ozone. One can then devise several plausible mechanisms which will convert the methyl radical to carbon monoxide, consume nitrogen oxides, and produce both hydroxyl and perhydroxyl radicals, using one or more photolytic steps. Hydroxyl and perhydroxyl would then be interconvertible by, for example,

$$HO_2^{\bullet} + NO \longrightarrow HO^{\bullet} + NO_2 \qquad (26)$$

$$NO_2 + h\nu \longrightarrow NO + O \quad (27)$$

$$O + O_2 + M \longrightarrow O_3 + M \quad (28)$$

$$O_3 + HO^{\bullet} \longrightarrow O_2 + HO_2^{\bullet} \quad (29).$$

The hypothesized production of perhydroxyl radicals is important because in experiments in which atomic hydrogen was reacted with molecular oxygen to produce, presumably, perhydroxyl radicals, added olefins were oxygenated at the double bond to produce carbonyl compounds, presumably by[3, 4]

$$C_2H_4 + HO_2^{\bullet} \xrightarrow{O_2} 2H_2CO + HO_2^{\bullet} \quad (30)$$

$$H_2C{=}CH_2{-}CH{=}CH_2 + HO_2^{\bullet} \xrightarrow{O_2} H_2CO + H_2C{=}CH{-}CHO + HO_2^{\bullet} \quad (31)$$

$$H_3C{-}CH_2{-}CH{=}CH_2 + HO_2^{\bullet} \xrightarrow{O_2} H_3C{-}CH_2{-}\overset{\overset{O}{\|}}{\underset{H}{C}} + H_2CO + HO_2^{\bullet} \quad (32).$$

Some ethylene oxide was also produced in the first case, presumably by

$$C_2H_4 + HO_2^{\bullet} \longrightarrow C_2H_4O^{\bullet} + {}^{\bullet}OH \quad (33).$$

This indicates that a large part of our reaction may be due to very short chains of the sort

$$\begin{matrix} CH_3 \\ \diagdown \\ \quad C{=}CH_2 \\ \diagup \\ CH_3 \end{matrix} + HO_2^{\bullet} \xrightarrow{O_2} \begin{matrix} CH_3 \\ \diagdown \\ \quad C{=}O \\ \diagup \\ CH_3 \end{matrix} + H_2CO + HO_2^{\bullet} \quad (34)$$

with a length of 1 to 3 units. There is a host of possible terminating reactions--for example, hydrogen-abstraction,

$${}^{\bullet}OH \text{ or } {}^{\bullet}O_2H + RH \longrightarrow H_2O \text{ or } H_2O_2 + R^{\bullet} \text{ (inactive)} \quad (35)$$

$$2HO_2^{\bullet} \longrightarrow H_2O_2 + O_2 \quad (36)$$

$$^{\bullet}OH + NO_2 + M = HNO_3 + M \qquad (37)$$

$$HO_2^{\bullet} \text{ or } {}^{\bullet}OH + \text{wall} \longrightarrow \text{inactive products} \qquad (38),$$

which would explain the shortness of the chains. It might be mentioned in passing that our two experiments with added hydrogen have been contradictory, one indicating inhibition and the other indicating no effect. The above partial mechanism would be amenable to the second result. We will rerun this experiment.

Thermodynamically, any peroxy radical of the form $XO_2^{\bullet}$ can produce the reaction

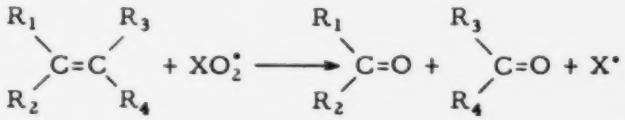

(39),

provided that the OO-X bond energy is less than about 140 kcal. If the reaction is a two-step process,

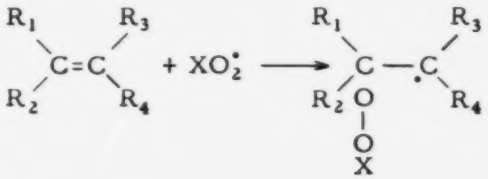

(40)

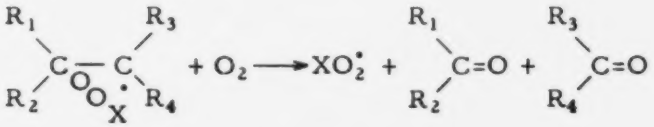

(41),

there is no requirement on the bond energy.

b. Effect of Molecular Oxygen

An important question is the effect of molecular oxygen on the products of oxygen atom attack. One possible sequence of reactions was discussed in our last report[1]; subsequent discussion has resulted in the suggestion of other reactions. Written for isobutylene, the suggested reactions are

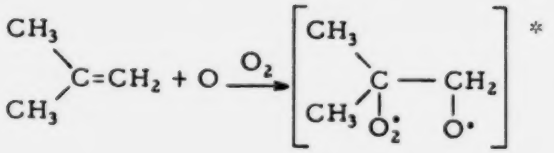

(42)

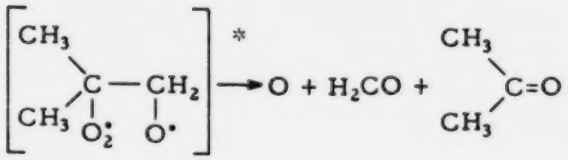

(43)

followed by

$$O + O_2 + M \rightarrow O_3 + M \qquad (44)$$

Reactions (42) and (43) are exothermic and result in no net loss of active intermediates--that is, chain carrying intermediates. This would also explain the strong suppression by molecular oxygen of the yield of epoxide and aldehyde from atomic oxygen attack. It is suspected that the importance of this scheme varies strongly with the molecular weight and type of olefin. The alternate to reaction (43) would be zwitterion formation, and, indeed, the over-all reaction (43) could go through such an intermediate. The lifetime of the zwitterion would strongly depend on the particular olefin under consideration.

It is possible that reaction (43) is also playing a part in dark ozonization, although the energy change would be somewhat less favorable. Such short non-branching chains could provide an explanation for the findings of our kinetic study of the dark reaction of ozone with isobutylene.

C. Eye Irritants Produced by Photooxidation

1. Methods of Exposure

To date our eye irritation studies have employed measurements of human responses. Reliable and consistent measures of irritation are attainable if certain procedures are followed. Although we have found that an individual response is not a reliable measure, the average response from a panel of ten subjects exposed for five-minute intervals does lead to statistically reliable results. Our method of exposure as described in previous reports[1, 5, 6] involves piping air to subjects seated in booths. More recently we have adopted an exposure procedure in which the subjects' eyes are exposed directly to the irradiated mixtures via openings or eye ports in the reaction chamber. For reasons not clearly understood,

this latter procedure has doubled the sensitivity of our eye irritation measurement. Thus, as shown in Table V, the irritation values of various mixtures measured are twice as great at the eye ports as at the booths. We have eliminated as possible explanations light, heat, and loss of materials during passage of the gases to the booths. We have not investigated the psychological factors; however, it has been suggested that we are dealing with an attention factor. Regardless of the cause, we have found the eye port measurements to be as reliable as the booth measurements and have therefore adopted the eye port method because of the greater sensitivity registered.

Table V

COMPARISON OF EYE IRRITATION VALUES
OBTAINED WITH TWO METHODS OF EXPOSURE

Compound and Concentration	Nitrogen Dioxide Concentration (ppm)	Eye Irritation Index (Arbitrary Units)	
		At Booths	At Eye Ports
Formaldehyde 3 ppm	none	11.0	20.0
Formaldehyde 3.4 ppm	none	12.5	21.2
Formaldehyde[(a)] 3 ppm	none	--	18.2
Formaldehyde[(a)] 3 ppm	none	--	20.0
Isobutene 3 ppm	1	11.2	20.0
Isobutene 3 ppm	1	10.4	21.4

-- Not determined.

(a) No irradiation.

2. Irritation from Photooxidized Mixtures

a. Isobutene-Nitrogen Dioxide Mixtures

Our past reports have shown that a major portion of the irritation arising from photooxidation of mixtures of olefin and oxide of nitrogen is due to the presence of formaldehyde and acrolein among the reaction products. Because of the gain in sensitivity with use of the port exposure method, we were able to examine less concentrated mixtures than had been possible previously. Thus, a series of experiments was designed in which the olefin content was varied from 0.25 ppm to 3 ppm and the nitrogen dioxide concentration was varied from 0.1 ppm to 3 ppm. On the basis of their predicted importance in the Los Angeles atmosphere and their contribution to eye irritation, five olefins were chosen for study: isobutene, 1,3-butadiene, ethylene, propylene, and 2-methyl-2-butene.

The eye irritation results from the two-hour photooxidations of isobutene-nitrogen dioxide mixtures are shown in Table VI. It will be noted that two columns are listed as measures of eye irritation. The first is the eye irritation index, or the average maximum irritation during the 5-min exposure time. The second column, which is based on a method currently used by the Los Angeles County Air Pollution Control District, is the averaged time for the first appearance of irritation. It is shown in Figure 13 that these two methods of calculating eye irritation are measures of the same parameter. These two measures can be related mathematically by the equation

$$25 - (\text{eye irritation index}) = 0.1t$$

where t = time in seconds to detection of irritation. When the results in Figure 13 are thus related, we find that the standard deviation between the two measures is ± 15 seconds or ± 1.5 eye irritation index units. These deviations are less than the known experimental deviation in eye irritation and are thus comparable. An average of the measured time to irritation and the calculated time to irritation derived from the eye irritation index may provide a more precise measure of irritation since, while being measures of the same parameter, the two values are calculated from distinctly different responses of the subjects.

Since our past experiments indicated that formaldehyde is the principal irritant arising from photooxidation of isobutene, we applied this postulate to these current data. Additional data from other sources were used to modify the method of analysis prior to application. Dr. E.R. Stephens of William Scott & Associates has shown that compound X is an irritant comparable to formaldehyde. Our previous experiments had not

Table VI

EYE IRRITATION VALUES FROM PHOTOOXIDIZED ISOBUTENE-NITROGEN DIOXIDE MIXTURES

Initial Concentrations (ppm)		Measured Irritation After Two Hours of Reaction	
Isobutene	Nitrogen Dioxide	Eye Irritation Index (Arbitrary Units)	Time to Irritation (sec)
3.0	3.0	16.8	87
3.0	1.0	21.4	55
3.0	0.3	16.7	110
3.0	0.1	13.2	132
2.0	3.0	16.7	90
2.0	1.0	20.0	68
2.0	0.3	17.4	63
2.0	0.1	12.0	115
1.0	3.0	8.0	192
1.0	1.0	1.60	98
1.0	0.3	14.6	85
1.0	0.1	12.8	114
0.5	3.0	6.0	200
0.5	1.0	8.0	159
0.5	0.3	12.6	123
0.25	0.3	10.9	115

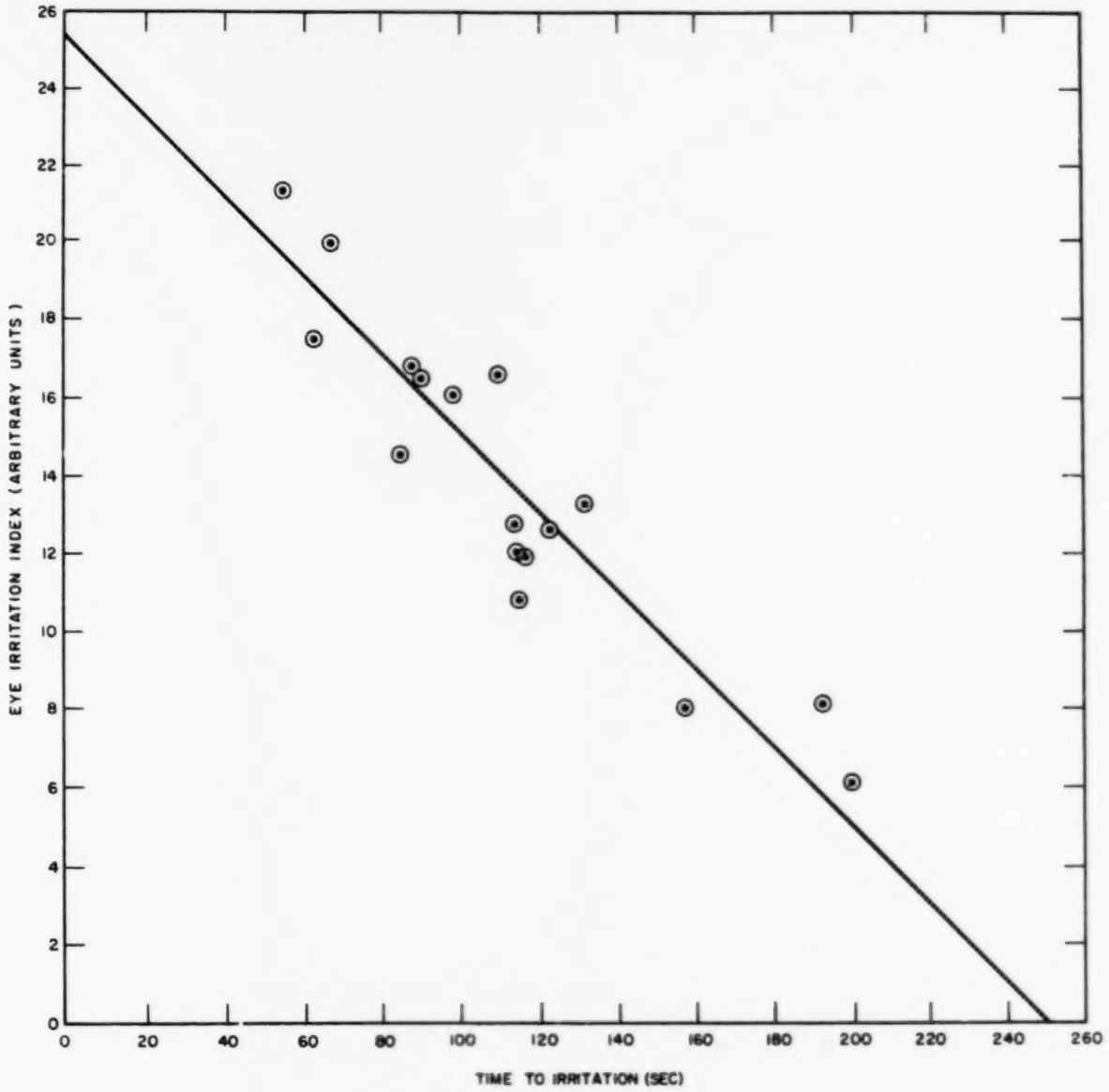

Fig. 13

EYE IRRITATION INDEX AS A FUNCTION
OF TIME TO IRRITATION

taken this factor into consideration because compound X has a concentration only one-fifth as great as formaldehyde. In our current studies we have taken the effect of compound X into account by assuming that it has the same irritation quality as formaldehyde.

The Los Angeles Air Pollution Control District has conducted an extensive series of formaldehyde irritation tests. From these data it was possible to predict that the relationship between formaldehyde concentration and eye irritation would approximately follow the equation

$$\sqrt{C} \times t = 100$$

where C is the formaldehyde concentration in parts per million and t is the time to irritation in seconds. How closely the predicted time to irritation corresponds to the observed irritation is shown in Figure 14. The slope of the straight line through the data is very close to 1, which indicates that most of the irritation is accounted for by the concentrations of formaldehyde and compound X. The correlation between predicted and observed time to irritation is 0.820, which is essentially the same as that reported earlier[1] for isobutene concentrations of 3 ppm or greater. Thus, even at olefin concentrations of less than 0.5 ppm, the formaldehyde formed in the photochemical reaction appears to be the major irritant. The contribution of compound X to this irritation is approximately the same as that found at higher olefin concentrations--that is, 20 percent of the irritation is contributed by the compound X.

b. Effect of Variations in Olefin and Nitrogen Dioxide Concentrations

The amount of irritants formed by photooxidation from a given quantity of olefin is a function of the oxide of nitrogen concentration. Olefins irradiated with near ultraviolet light in the absence of an oxide of nitrogen do not photooxidize. Inclusion of nitric oxide or nitrogen dioxide in the mixture initiates and accelerates both the oxidation of the olefin to form irritants and the reaction leading to destruction of the irritants. However, the olefin photooxidation reaction leading to products which are irritants is accelerated by several orders of magnitude while the reaction leading to destruction of the irritants is accelerated by a factor of only 2 or 3. Thus, relatively stable concentrations of eye irritants can be formed.

Experimentally, we have shown[1] that 1 part of nitrogen dioxide can accelerate the destruction of up to 3 parts of an olefin. Thus, with less than 1 part of nitrogen dioxide available for 3 parts of an olefin, we would expect less olefin destruction and, therefore, the formation of

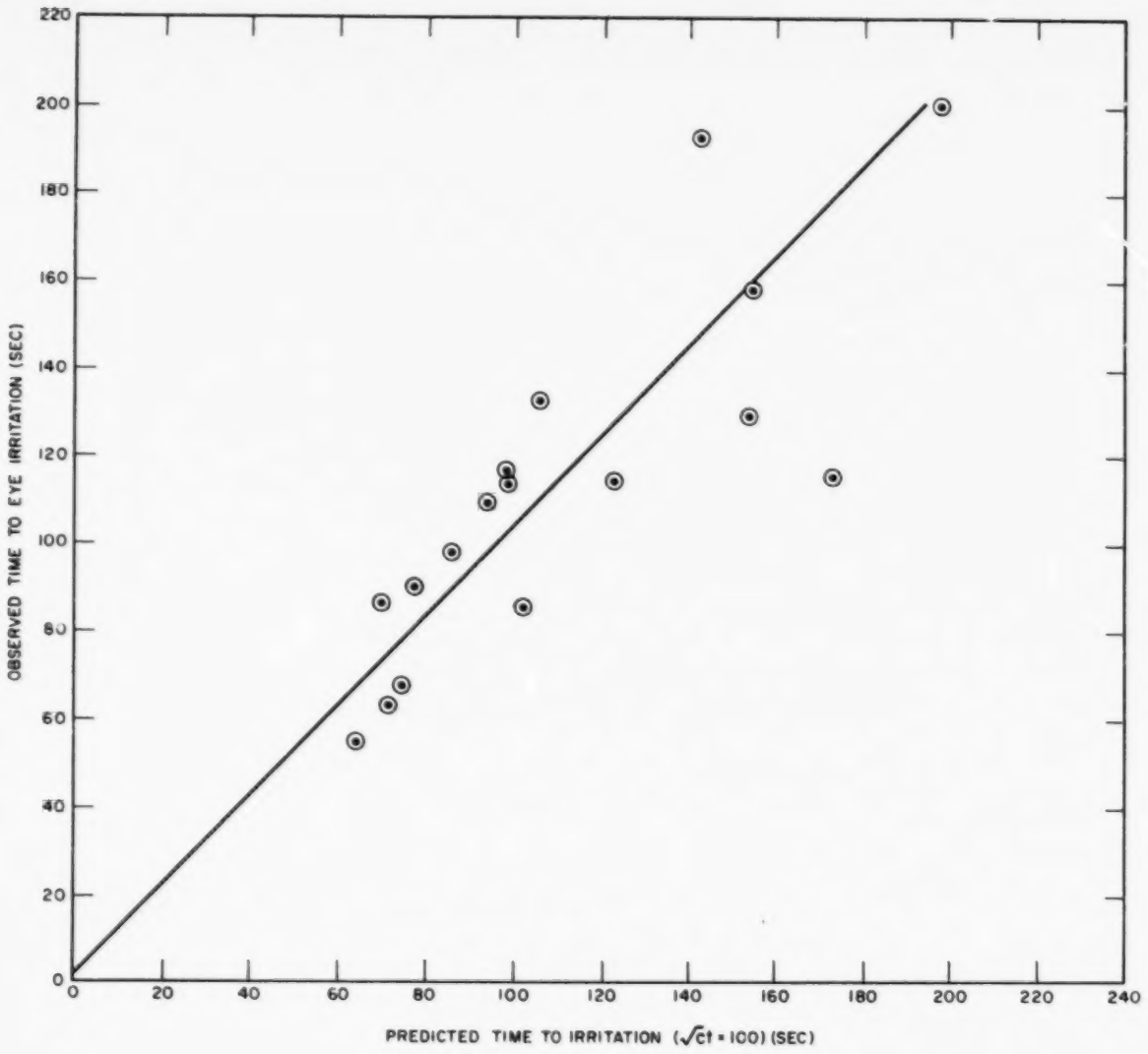

Fig. 14

OBSERVED TIME TO IRRITATION AS A FUNCTION
OF PREDICTED TIME TO IRRITATION

less eye irritants. We would also predict that the presence of more than 1 part of nitrogen dioxide per 3 parts of olefin would lead to destruction of the already formed irritants. These predictions are experimentally supported by our investigation of auto exhaust[1], which showed that eye irritation has a maximum which is a function of the hydrocarbon-to-oxides of nitrogen concentration ratio.

To determine the effect on eye irritation of variations in oxide of nitrogen concentration, the five olefins selected previously as being of particular importance in their contribution to eye irritation in auto exhaust were studied at various olefin and nitrogen dioxide concentrations. The results of this study are shown graphically in Figures 15 through 19. At first glance it is apparent that eye irritants were formed under many of the conditions studied. However, not all irritation values are in line with the prior prediction that the amount of irritation decreases when excess nitrogen dioxide is present: increasing the nitrogen dioxide value above a 3 to 1 olefin-to-nitrogen dioxide ratio does not lead to a definite decrease in eye irritation for mixtures containing propylene or ethylene and in fact leads to an increase in irritation for 2-methyl-2-butene mixtures. These data are shown in a single graph in Figure 20. Of the olefins tested, only isobutene follows the prior prediction.

Explaining the irritation values obtained requires an examination of each individual case in terms of rate of reaction and products formed. Thus, with 2-methyl-2-butene we find that the initial products are acetone and acetaldehyde, neither of which is an eye irritant. Excess nitrogen dioxide speeds up the destruction of acetaldehyde to form formaldehyde, an irritant; thus, excess nitrogen dioxide leads to an increase in eye irritation, as shown in Figure 20.

The initial products of the propylene reaction are formaldehyde and acetaldehyde. In this case excess nitrogen dioxide, while promoting the destruction of the formaldehyde, also leads to the formation of an approximately equal amount of formaldehyde via photooxidation of the acetaldehyde. Thus, we would expect no change in irritation, as shown in Figure 20.

With ethylene as the olefin, we have a relatively slow rate of reaction and the available ethylene is not consumed at the end of the 2 hours or irradiation. Thus, excess nitrogen dioxide promotes further ethylene destruction as well as further formaldehyde destruction. The net result is no change in eye irritation, as shown in Figure 20.

The isobutene irritation level drops as expected, due to destruction of the formaldehyde by excess nitrogen dioxide, again as shown in Figure 20.

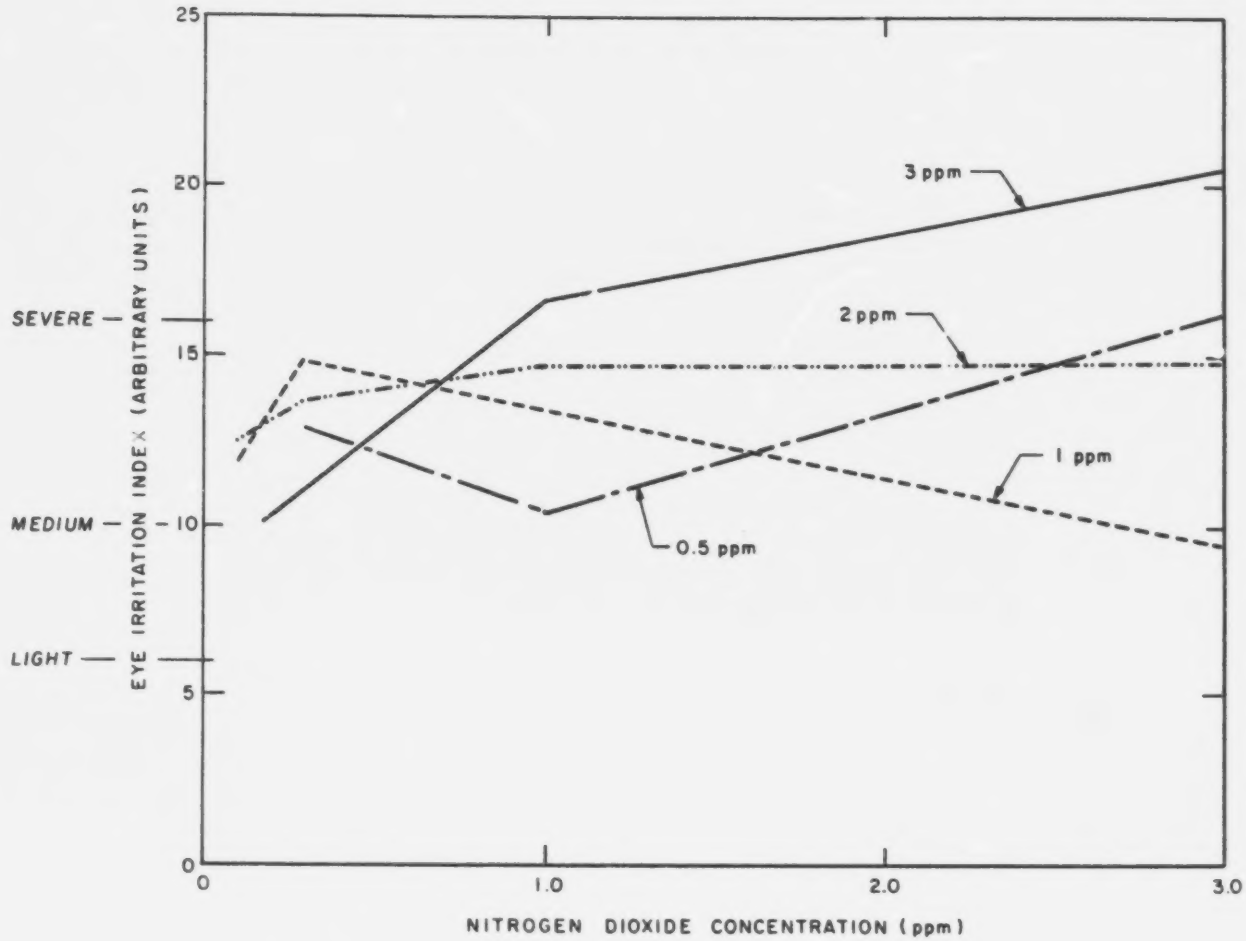

Fig. 15

EYE IRRITATION FROM PHOTOOXIDATION
OF 2-METHYL-2-BUTENE

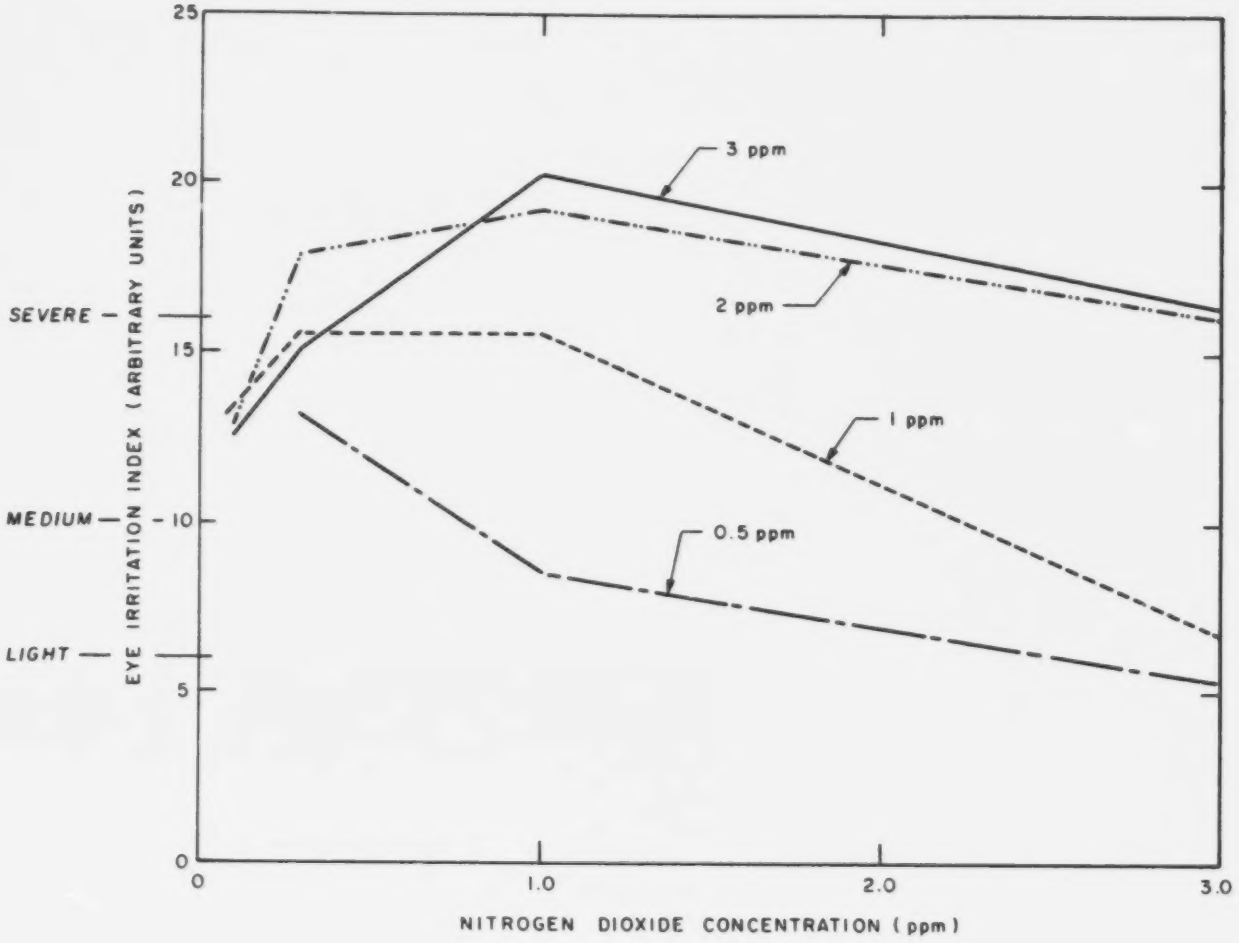

Fig. 16

EYE IRRITATION FROM PHOTOOXIDATION
OF ISOBUTENE

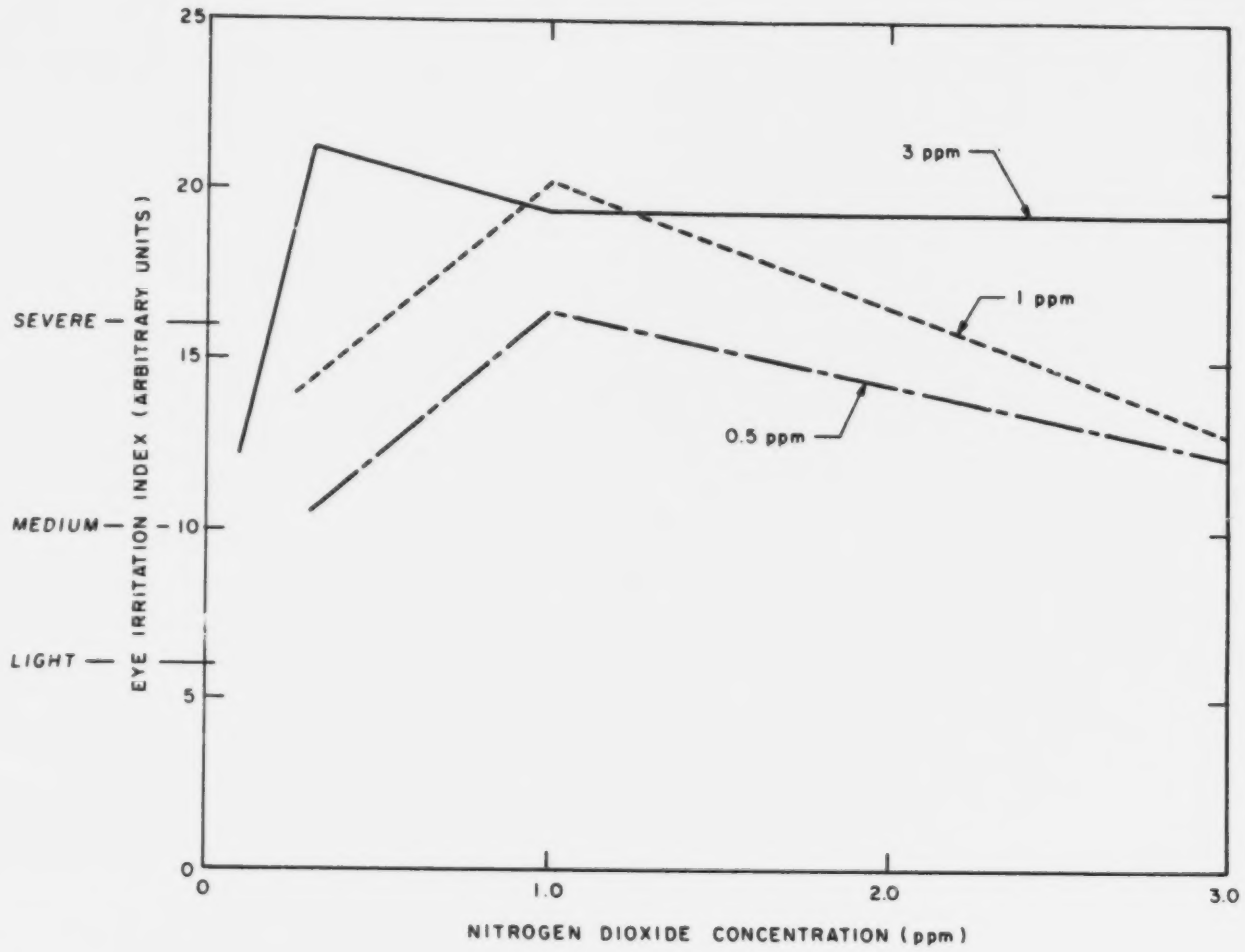

Fig. 17

EYE IRRITATION FROM PHOTOOXIDATION
OF ETHYLENE

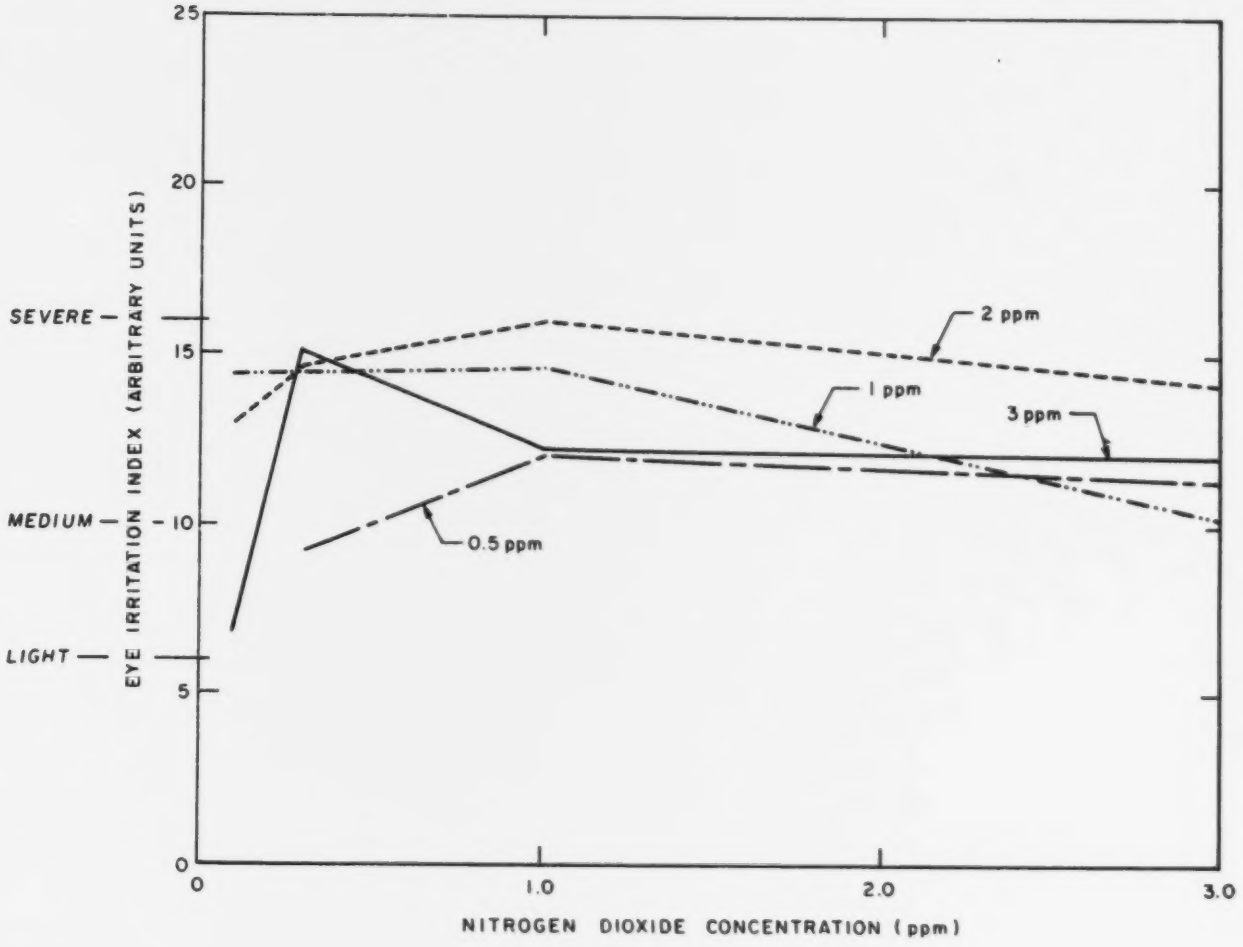

Fig. 18

EYE IRRITATION FROM PHOTOOXIDATION
OF PROPYLENE

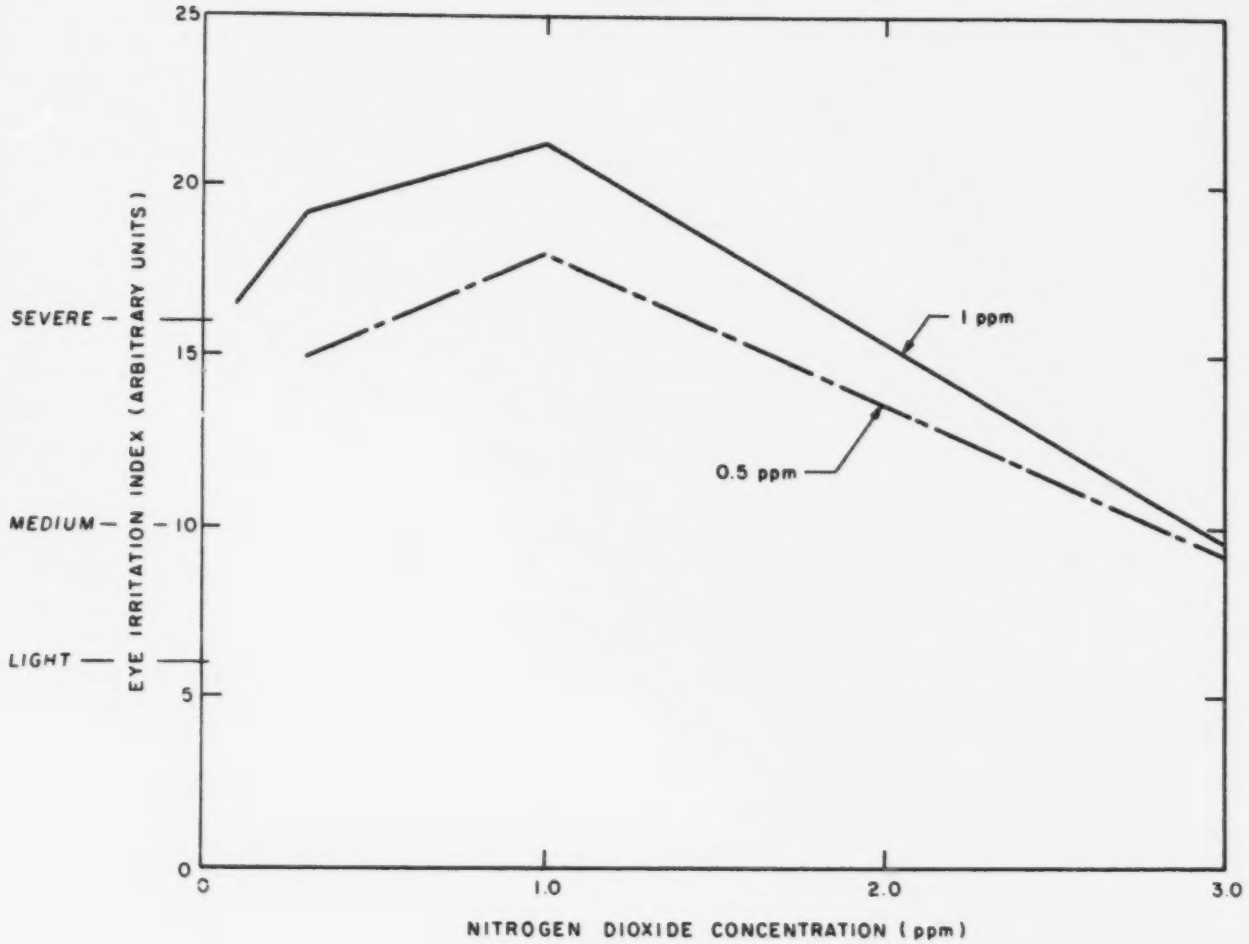

Fig. 19

EYE IRRITATION FROM PHOTOOXIDATION
OF 1,3-BUTADIENE

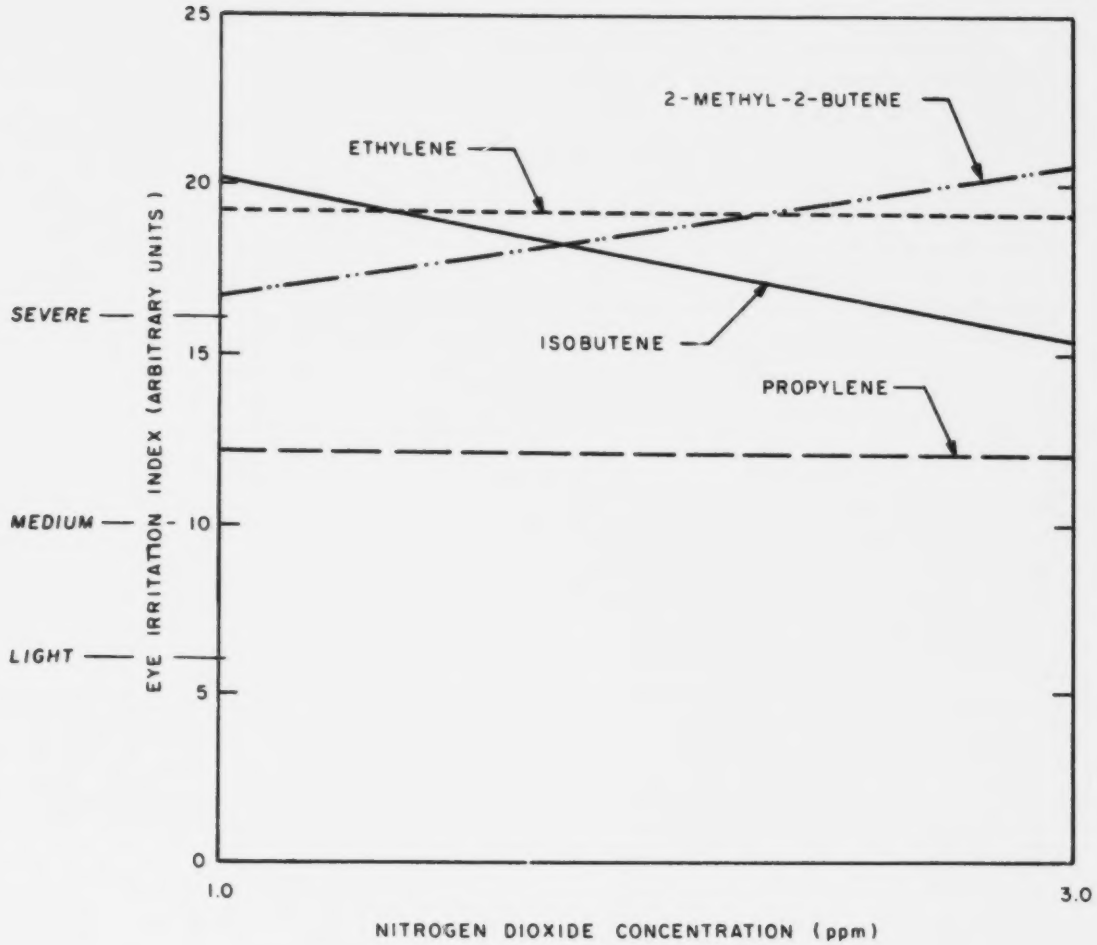

Fig. 20

EYE IRRITATION FROM PHOTOOXIDATION
OF CERTAIN OLEFINS

c. Extrapolations to the Atmosphere

At certain olefin-to-oxide of nitrogen concentration ratios a reduction in the oxide of nitrogen concentration could lead to an increase in eye irritation. This is illustrated in Figure 21 in which the severity of irritation is shown as a function of the olefin and nitrogen dioxide concentrations. The olefin irritation data used in Figure 21 were obtained by averaging the data in Figures 15 through 19 after applying factors designed to approximate the contribution of each olefin to irritation arising from auto exhaust mixtures. Previous data[6] indicate that the irritation from an auto exhaust mixture is contributed approximately as follows: 32 percent from ethylene, 23 percent from propylene, 16 percent from normal butene-1 and isobutene, 18 percent from internal olefins such as cis- and trans-butene-2 and 2-methyl-2-butene, and 11 percent from diolefins of the butadiene type.

The data in Figure 21 indicate that the most logical method of reducing eye irritation would be to reduce olefins. In any event reduction in eye irritation will be strongly influenced by the olefin-to-oxide of nitrogen ratio. Thus, if this ratio is 6 to 1, a 50 percent reduction in olefin concentration may not lead to as marked a reduction in eye irritation, since the amount of oxide of nitrogen present could promote the photooxidation of only one-half of the original olefin. Nevertheless, olefin reduction beyond the 3 to 1 ratio should lead to a reduction in eye irritation.

d. Correlation with Irritation Observed in Los Angeles Basin

During the past year, from September 1, 1959 to August 31, 1960, eye irritation in the East Los Angeles Basin has been severe on 11 days. Definite irritation was reported on a total of 75 days of the year. This information was generated from daily reports of our eye irritation subjects on samples taken each day at 2 P.M.

Assuming a relationship between our pure compound experiments and the atmosphere samples, we postulate that the concentration of formaldehyde was between 0.1 ppm and 0.2 ppm on most of the 75 days of irritation. Measuring the correlation between the observed atmospheric irritation and the postulated formaldehyde values awaits improvement of both the eye irritation measure and the analytical procedure for measuring formaldehyde. Our present test panel is composed of a mixture of individuals with varying sensitivity to eye irritation. At low irritation values, the number of individuals reporting zero irritation increases; this leads to a drastic increase in error of measurement since, in effect,

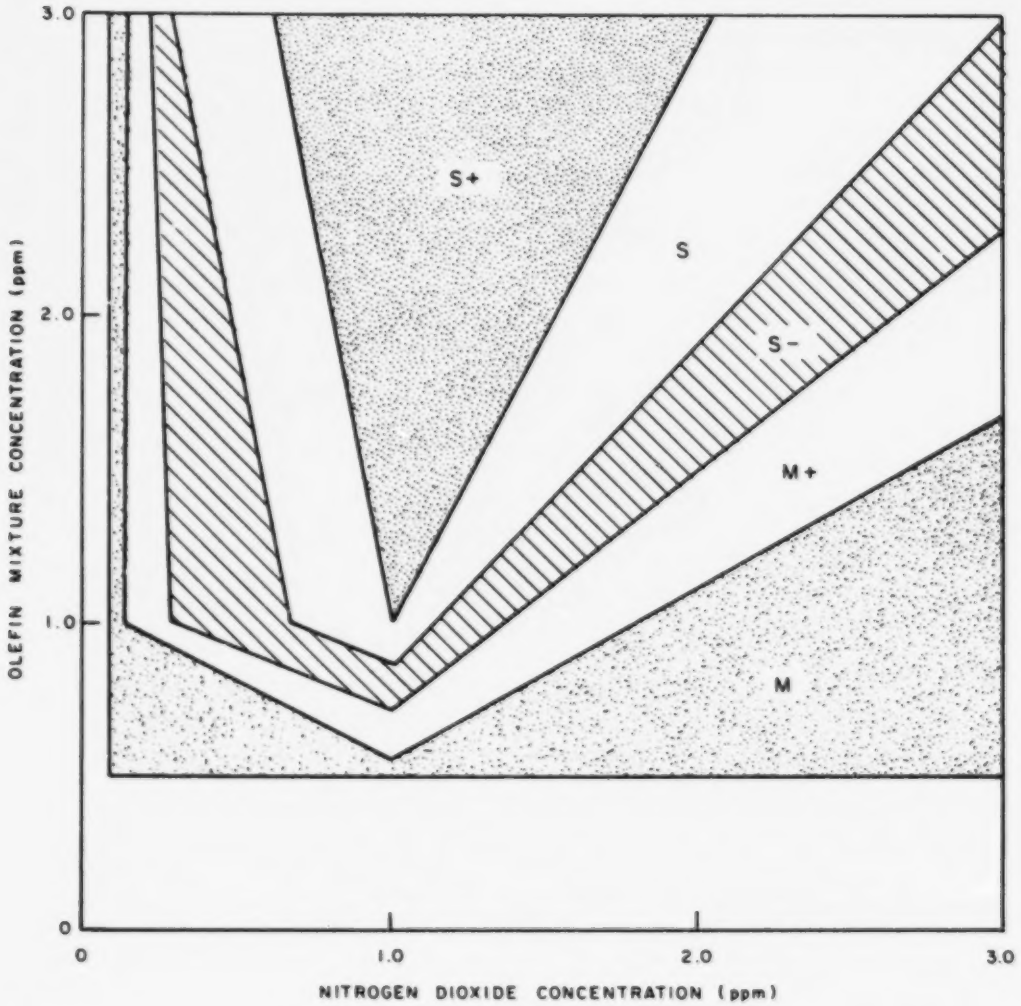

Fig. 21

EXPECTED EYE IRRITATION AS A FUNCTION OF OLEFIN AND NITROGEN DIOXIDE CONCENTRATION (TWO-HOUR IRRADIATION OF AN OLEFIN MIXTURE)

our panel is becoming smaller. Also, at these low concentrations we must rely on the chromotropic acid method* to measure formaldehyde. Present indications are that, at 0.5 ppm of formaldehyde, the standard deviation of this method is ±40 percent. Thus, in present form, neither the eye irritation value nor the formaldehyde analysis is a good quantitative tool for use in studying mixtures comparable to those predicted to exist in the outside atmosphere.

D. Aerosols Produced by Photooxidation

To date, the known or likely products of photooxidation of olefins in polluted atmospheres of the type found in Los Angeles all have vapor pressures sufficiently high to forestall supersaturation relative to a pure liquid or solid phase at parts per million concentrations and ambient temperatures. Yet the formation of aerosols can be demonstrated in systems simulating polluted atmospheres[6, 7], and strong presumptive evidence indicates that they are photochemically formed in urban atmospheres[8, 9]. This evidence has stimulated a number of suggestions:

1. Supersaturation may be achieved relative to a multicomponent liquid phase, with one of the components always present at high concentration--for example, water or carbon dioxide.

2. A minor product of photooxidation having a very low vapor pressure may be responsible for aerosol formation.

3. Naturally present nuclei may act as condensation centers for polymer formation by either thermal or photochemical reaction[10].

4. Catalytically or chemically active nuclei may be formed by any of the above processes, possibly number (1); they then act as a polymerization center for one or more of the major photooxidation products, possibly the aldehydes.

It is possible that several of these processes are contributing to aerosol formation.

---

* See Appendix A.

Previous work in this[1] and other laboratories[11] has demonstrated that the presence of trace amounts of sulfur dioxide can cause the formation of aerosol in photooxidizing mixtures of olefin and nitrogen oxides in air at parts per million concentrations.

1. Equilibria and Formation of Sulfuric Acid Mists

One suggested explanation of these results is a combination of suggestions (1) and (4) above, with aqueous sulfuric acid playing the part of the active nuclei. Although this hypothesis may not be true in detail, it certainly suggests that nucleation and growth of multicomponent aerosols are probably important in air pollution. This has stimulated some continuing calculation on two-component aerosol nucleation and growth, with the sulfuric acid-water system employed as an example.*

In humid air a sulfuric acid aerosol is essentially a two-component system, sulfuric acid-water. Treatment of this system* is complicated by the non-ideality of aqueous sulfuric acid solutions. However, the treatment of multicomponent systems outlined by Volmer[12] was applied to nuclei and droplets of aqueous sulfuric acid with the aid of some approximations which fail for very small nuclei.

The equilibrium size of droplets was calculated from published data on the density, surface tension, and activity of water in aqueous sulfuric acid. The results showed that the greatest size change will be caused by humidity changes from 0 percent to 10 percent and from 85 percent to 100 percent. Intermediate humidities will cause less marked, but moderate, changes in size. At saturation, the droplets reach a terminal size and droplets grown from submicron sizes at lower humidities will contain only a few percent or less of sulfuric acid.

A preliminary attack on the problem of rate of nucleation was hampered by lack of adequate data on the partial pressures of sulfuric acid above its aqueous solutions (that is, activity referred to a hypothetical state of sulfuric acid gas at 1 atm and 25°C). The objective of this calculation was to obtain an estimate of the lowest gaseous concentration of sulfur dioxide (when converted to sulfuric acid) which would nucleate aerosol formation at an appreciable rate at atmospheric humidities. The results to date consist of a qualitative description of the shape of the free

---

* See Appendix C.

energy barrier for nucleation and some preliminary estimates of supersaturations caused by low (~1 pphm) sulfuric acid concentration. These calculations indicate that very low concentrations (much less than 1 pphm) can initiate the nucleation of a haze at atmospheric humidities.

2. Effect of Relative Humidity

Experimental work* performed during the period covered by this report included light-scattering studies of photochemical aerosols formed at various humidities from 0.1 ppm of sulfur dioxide, 3 ppm of 2-methyl-2-butene, and 1 ppm of nitric oxide. It was found that increasing the humidity increased the light scattering somewhat, as was expected for hygroscopic droplets. However, a simple interpretation of the particle size distribution suggests that increasing the humidity causes an increase in the particle generation rate and a decrease in the rate of growth of individual particles. This finding accords with the anticipated effect of the increased availability of one aerosol material (water) and the limited availability of the second (compounds derived from sulfur dioxide). This suggests that at higher humidities we are dealing with a more highly dispersed aerosol which, if the non-water aerosol material were apportioned among the same number of particles at all humidities, would tend to suppress the effect on the observed light scattering.

In all experiments sulfur dioxide was completely consumed by the reaction. Light scattering of the effluent is shown in Figure 22. It is apparent that the major changes in light scattering occur from 0 percent to 10 percent relative humidity and from 70 percent to 85 percent relative humidity. A suggestive comparison is given by Figure 23, which shows how the geometrical cross section of a 0.2 μ diameter sulfuric acid droplet changes with increasing humidity. Although it is obvious that water vapor will have effects other than hygroscopic swelling of the particles, it is also highly probable that the general similarity of the two curves shown in Figures 22 and 23 has its origin in a major contribution by hygroscopic swelling of the particle. The usual range of humidity during smog attacks would restrict this increase in particle size to a maximum of about 30 percent (when going from 10 percent to 85 percent relative humidity). Hygroscopic swelling of the particles, therefore, does not contribute to visibility reduction under the usual conditions for formation of aerosols during photooxidation.

---

* For a description of equipment used, see Appendix C.

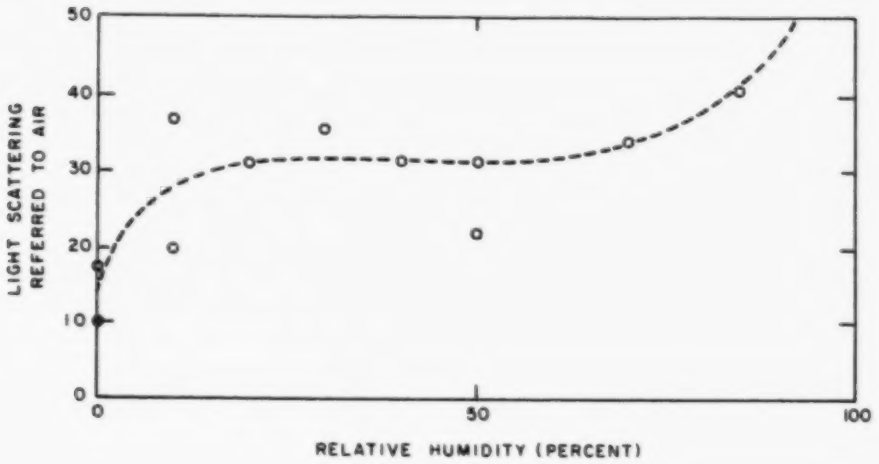

Fig. 22

EFFECT OF HUMIDITY ON LIGHT SCATTERING OF PHOTOOXIDIZED MIXTURES OF SULFUR DIOXIDE WITH 2-METHYL-2-BUTENE AND NITRIC OXIDE

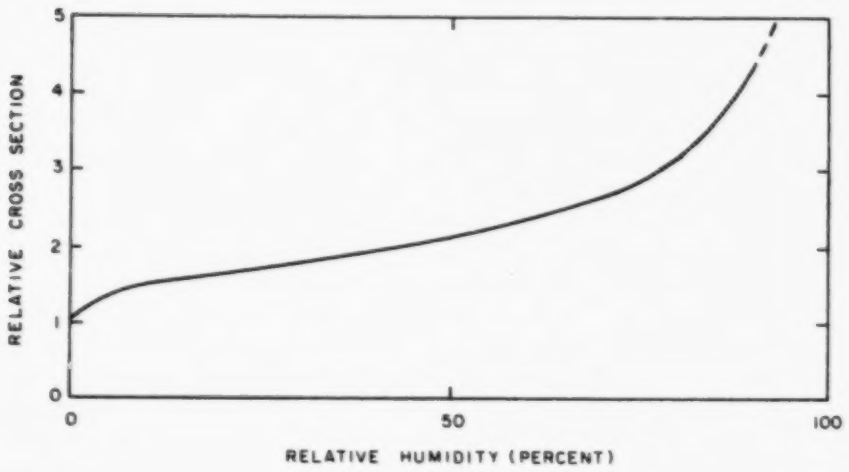

Fig. 23

EFFECT OF HUMIDITY ON CROSS SECTION OF 0.2μ DIAMETER DROPLET OF SULFURIC ACID
(Diameter at 10 Percent Relative Humidity)

Particle count data for these experiments are shown in Figure 24, plotted as cumulative count above a diameter against that diameter squared. This method of data presentation is used because of its connection with a simple theory of particle growth in the reactor. If it is assumed that coagulation and wall deposition are negligible and that the particles grow by diffusion according to $dr^2/dt = k$, a constant, (13) it is also assumed that the square of the initial radius of the particles is negligible when compared with the radius of any countable particle. This rate of growth, combined with the distribution of lifetimes of particles in a stirred flow reactor, yields as the frequency distribution of radii $f(r)dr = (1/k\tau) \exp(-r^2/k\tau)\, d(r^2)$, where τ = residence time; the cumulative number per unit volume is then

$$N \int_r^\infty = \tau G e^{-\frac{r^2}{k\tau}} \text{ or } \ln\left(N \int_r^\infty\right) = \ln \tau G - \frac{r^2}{k\tau}$$

where G = particle generation rate per unit volume of the reactor. This frequency distribution is shown in Figure 25 with the radii plotted as ratios to a characteristic length, $\sqrt{k\tau}$, $\rho = r\sqrt{k\tau}$. Also shown are the mode of the distribution and two moments of interest.

It is obvious that this simple theory cannot closely describe the data given in Figure 24. The deviations from the theory are most marked at low humidities and for the larger particles. For the smaller particles there is a tendency toward slopes and intercepts which show some dependence on humidity. Estimates were made of these slopes and intercepts from the two lower diameters and were plotted against relative humidity, as shown in Figures 26 and 27. The values at 0 percent relative humidity are exceptional, as might be expected. Apparently, according to this simple theory, there is an increase in particle generation rate and a decrease in growth rate, with both rates approaching constant values as humidity increases. The generation rate increases from 8 particles/sec cm^3 to 300 particles/sec cm^3 as humidity goes from 10 percent to 80 percent. The limiting value of k is about 3×10^{-14} cm^2 sec^{-1} at high humidity. Obviously, these limits represent the sum of a number of processes--for example, coagulation of particles combined with nucleation and growth--complicated by the variation in the response of the counter-photometer to particles of varying refractive index as well as size. There will also be an interrelationship between an increase in generation rate and a decrease in growth rate because of the limited amount of aerosol material available

The hygroscopicity of aerosols formed by the mode involving sulfur dioxide is of interest because it provides (1) some knowledge of the chemical nature and probable mode of nucleation of aerosols and

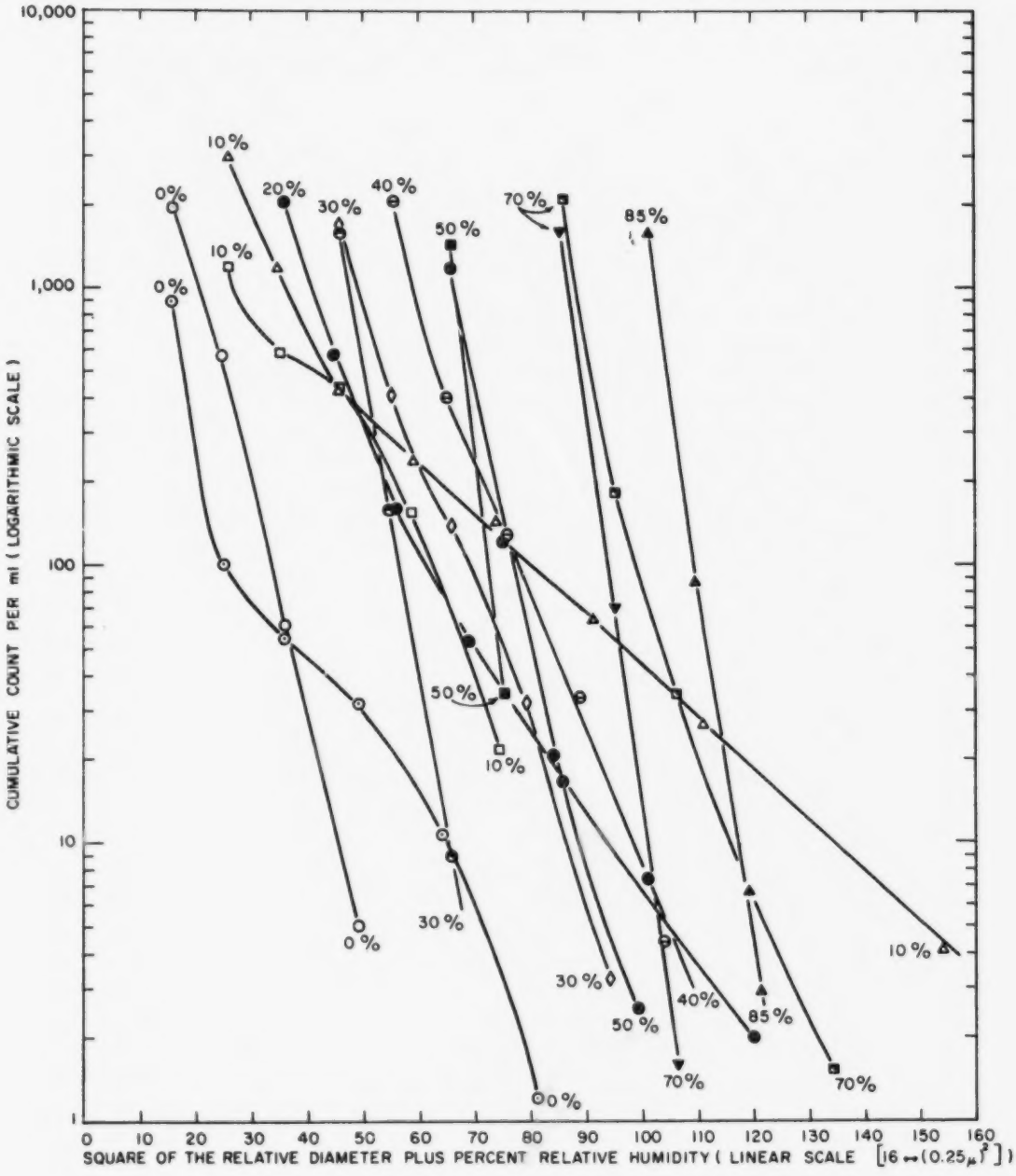

Fig. 24

COUNT DATA AT VARIOUS HUMIDITIES FOR AEROSOLS
PRODUCED BY PHOTOOXIDATION OF
0.1 PPM OF SULFUR DIOXIDE

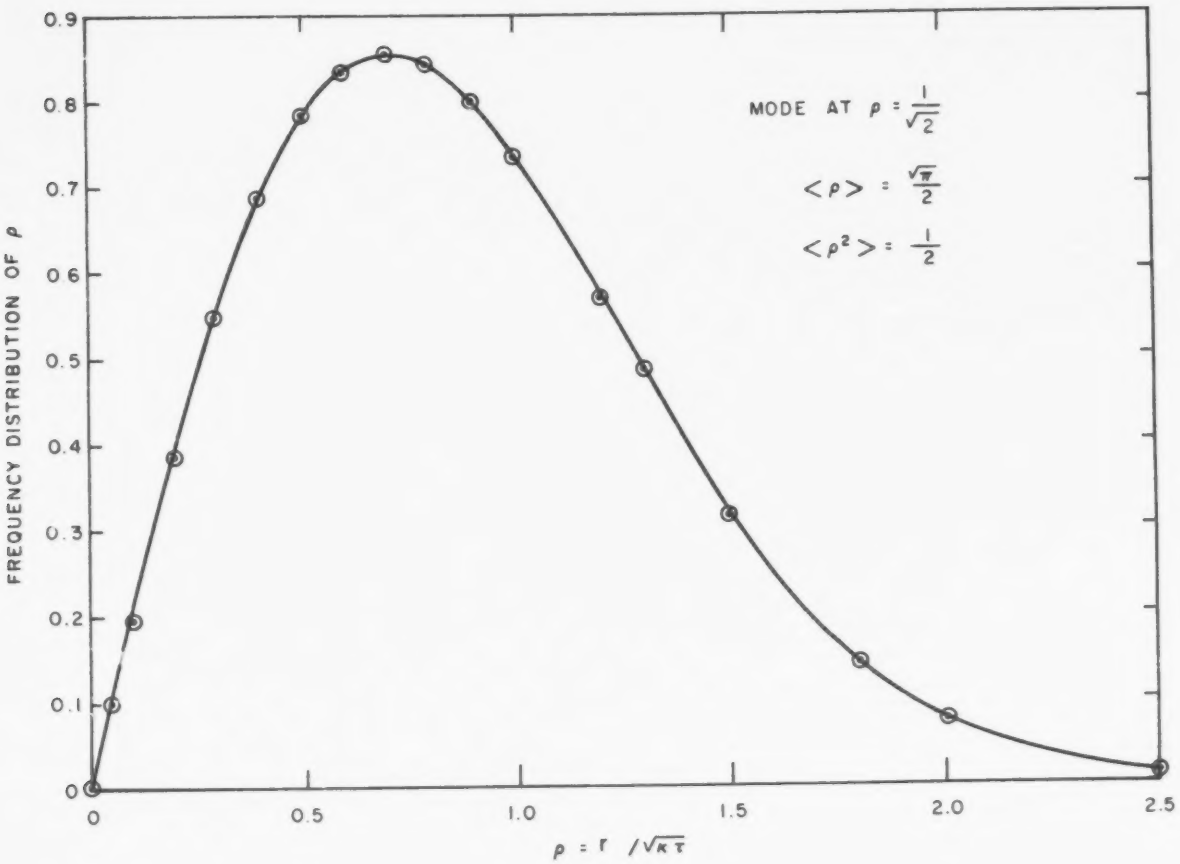

Fig. 25

FREQUENCY DISTRIBUTION TO BE EXPECTED IF DIFFUSION IS THE ONLY FACTOR AFFECTING AEROSOL GROWTH IN A STIRRED-FLOW REACTOR

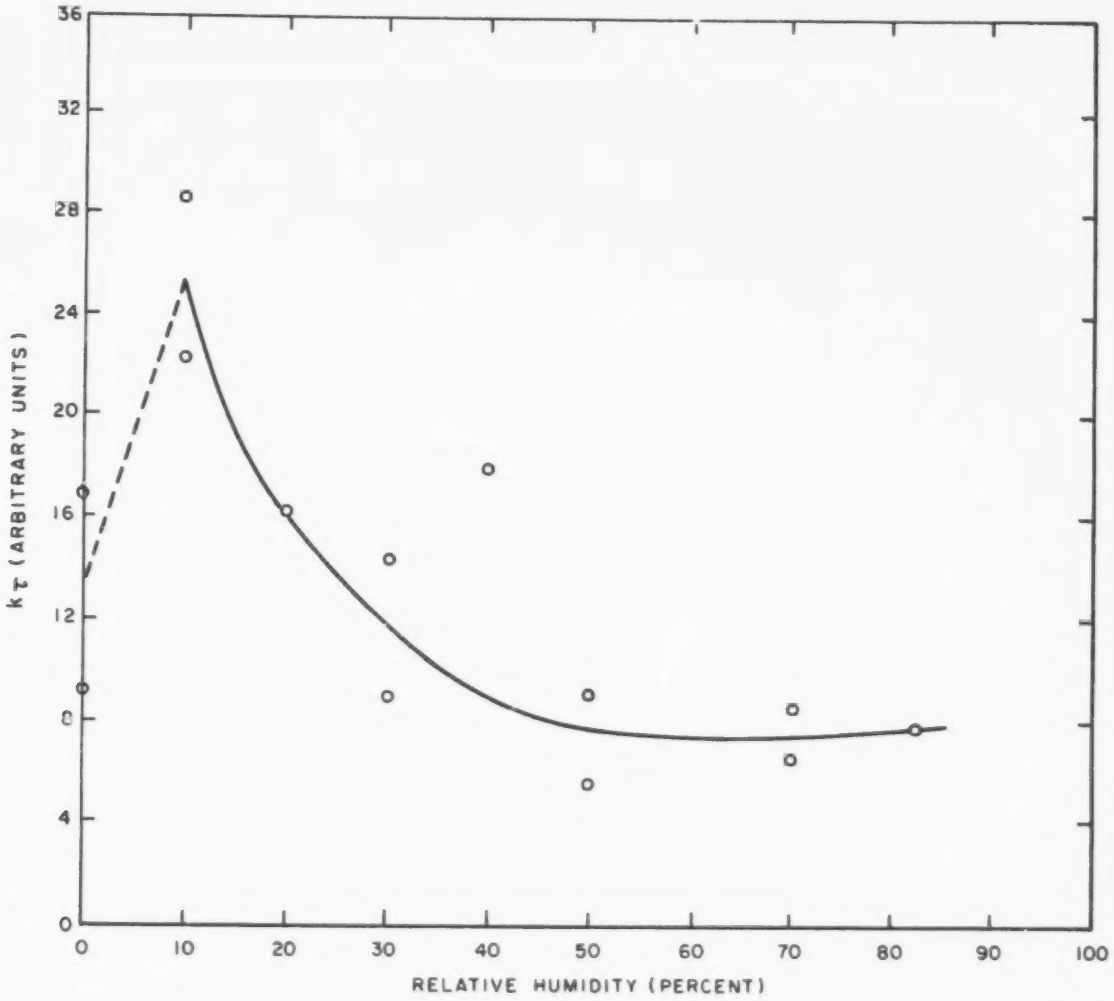

Fig. 26

RECIPROCALS OF THE TERMINATING SLOPES AT SMALL DIAMETERS OF THE CURVES OF FIGURE 24 PLOTTED AGAINST RELATIVE HUMIDITY

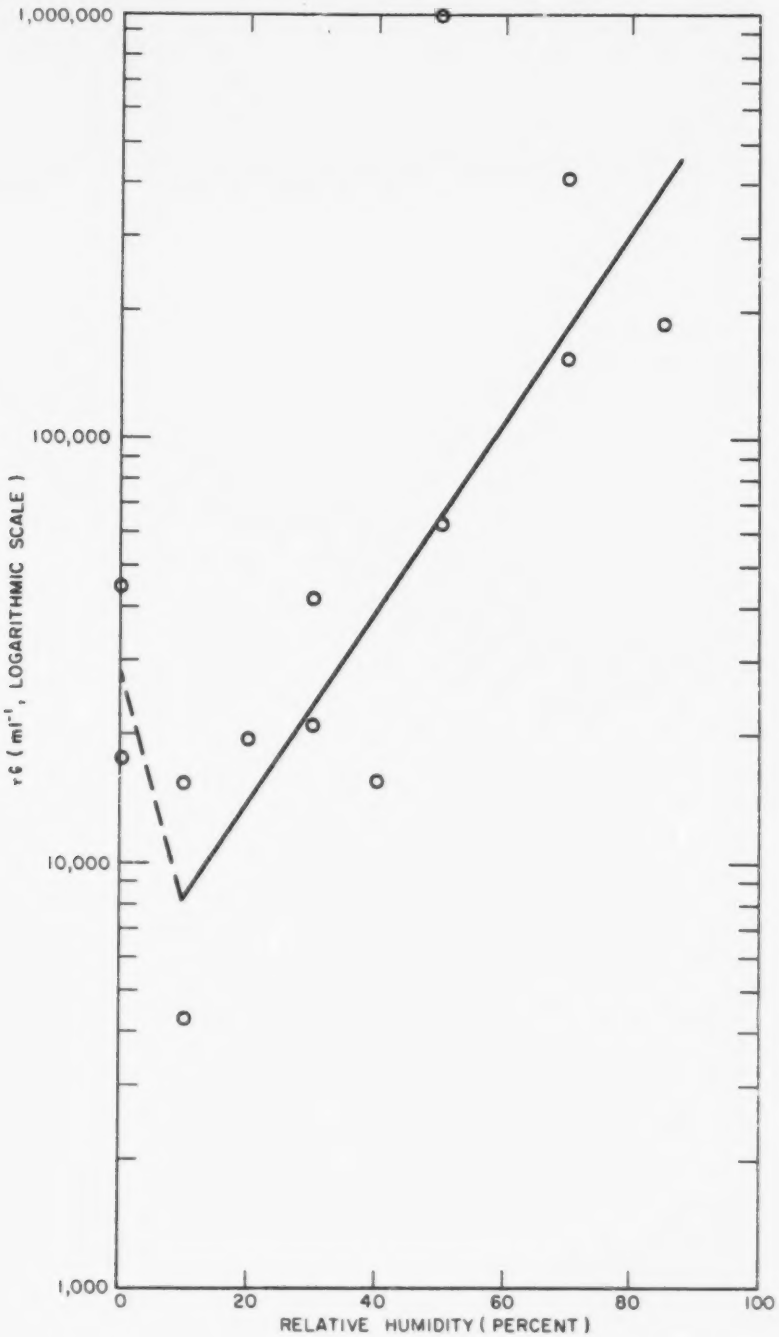

Fig. 27

INTERCEPTS OF THE CURVES OF FIGURE 24
PLOTTED AGAINST RELATIVE HUMIDITY

(2) a model for the behavior of atmospheric aerosols on change of humidity is obtained. Four experiments were therefore carried out to investigate briefly the effect of extreme changes in humidity on photochemical aerosols.

Aerosols were generated in the previously described manner, using a mixture of 3 ppm of 2-methyl-2-butene, 1 ppm of nitrogen dioxide, 0.1 ppm of sulfur dioxide, a residence time of 17 minutes, and humidified purified air. Two relative humidities were used, 10 percent and 85 percent. Samples of the effluents were conditioned by being passed over constant-humidity solutions of sulfuric acid (either 10 percent or 85 percent relative humidity). The conditioning apparatus consisted of a 150-mm crystallizing dish filled with the stirred sulfuric acid solution to within 2-5 mm of a sealed-on glass cover. The aerosol was fed into the center of the disk-shaped space above the solution and was collected from a toroidal plenum at the periphery and fed to the counter-photometer. The air circulating in the counter-photometer sampling and dilution system was also humidified by being continually repassed over a sulfuric acid solution of the same concentration as that in the crystallizing dish. Aerosol sampling rates were of the order of 100-300 ml/min, usually around 100 ml/min.

The light scattering observed in the conditioned effluent is shown in Figures 28 and 29. Each curve is identified by a pair of numbers indicating relative humidity, the first being that in the reactor and the second being that in the conditioning apparatus. The steady-state light scattering depends entirely on the conditioning humidity. Aerosols formed at 10 percent relative humidity showed a larger transient peak than those formed at 85 percent relative humidity.

That this apparently simple behavior conceals a relatively complex phenomenon is demonstrated by the count data given in Figures 30 through 32. In Figures 30 and 31 counts are compared after 110 minutes of irradiation for the pairs of experiments shown in Figures 28 and 29. Aerosols formed at 10 percent relative humidity tend to have maxima within the size range attainable by the counter-photometer. The temporal behavior of the particle count distribution for aerosols formed at 10 percent relative humidity and conditioned at 85 percent relative humidity is shown in Figure 32. The maxima observed at shorter times for aerosols formed at 10 percent relative humidity becomes a shoulder on the distribution curve at longer times.

These results reveal that changing humidity has a definite effect on light scattering which depends greatly on the final humidity and to a much lesser extent on the humidity prevailing at the time of formation and growth. The particle size data contradict this finding to some extent; apparently, countable (larger) particles formed at high humidity can undergo changes in size with humidity while those formed at low humidity show little

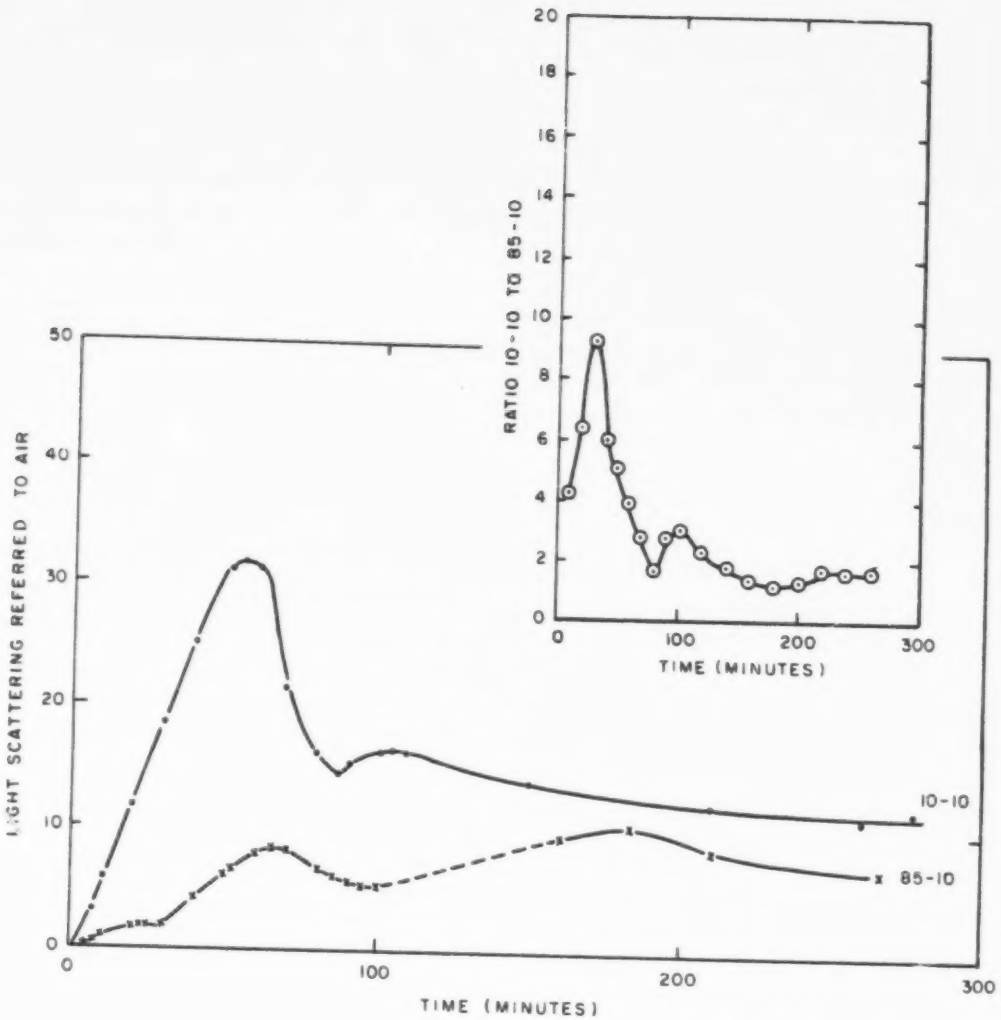

Fig. 28

LIGHT SCATTERING OF EFFLUENTS
CONDITIONED AT 10 PERCENT RELATIVE HUMIDITY

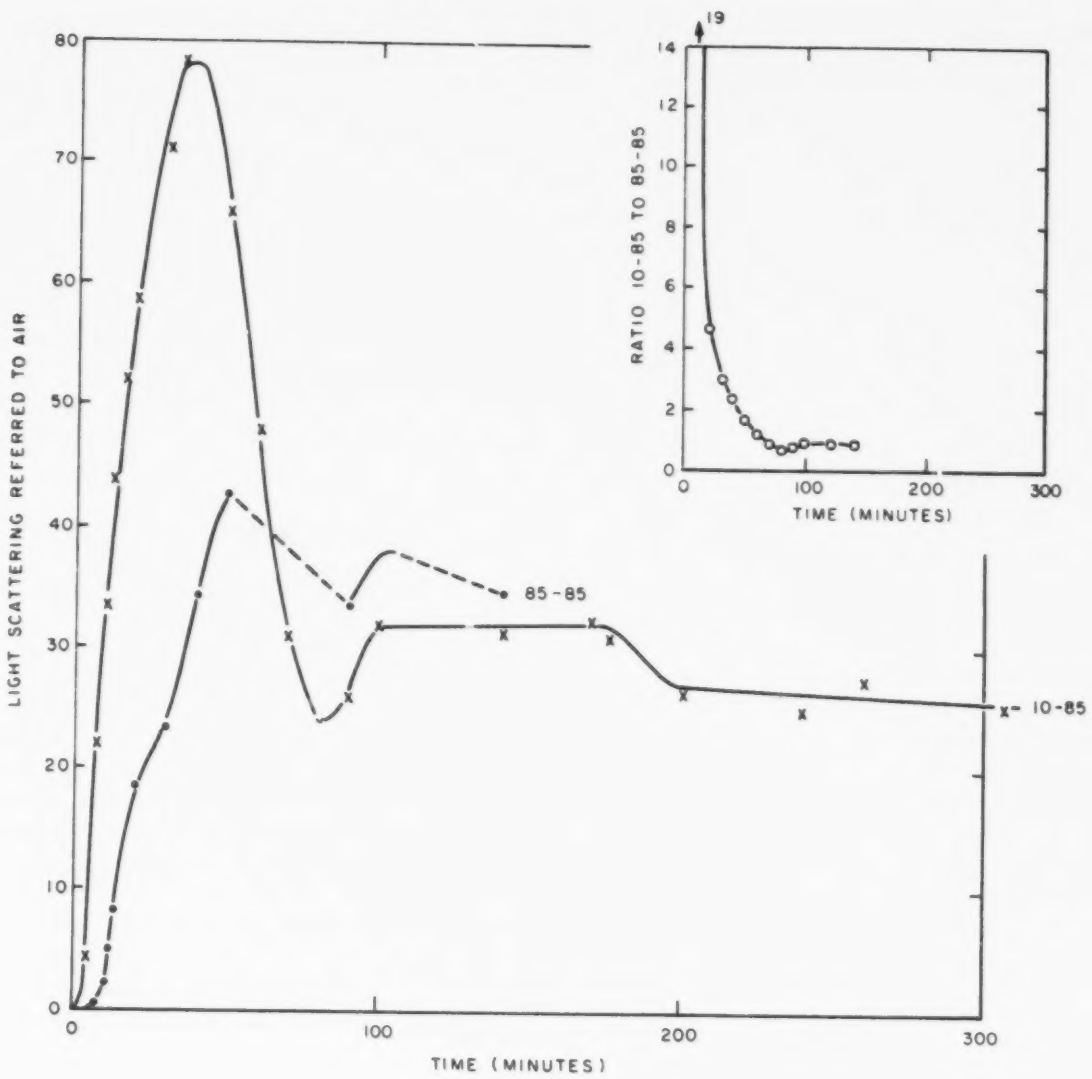

Fig. 29

LIGHT SCATTERING OF EFFLUENTS
CONDITIONED AT 85 PERCENT RELATIVE HUMIDITY

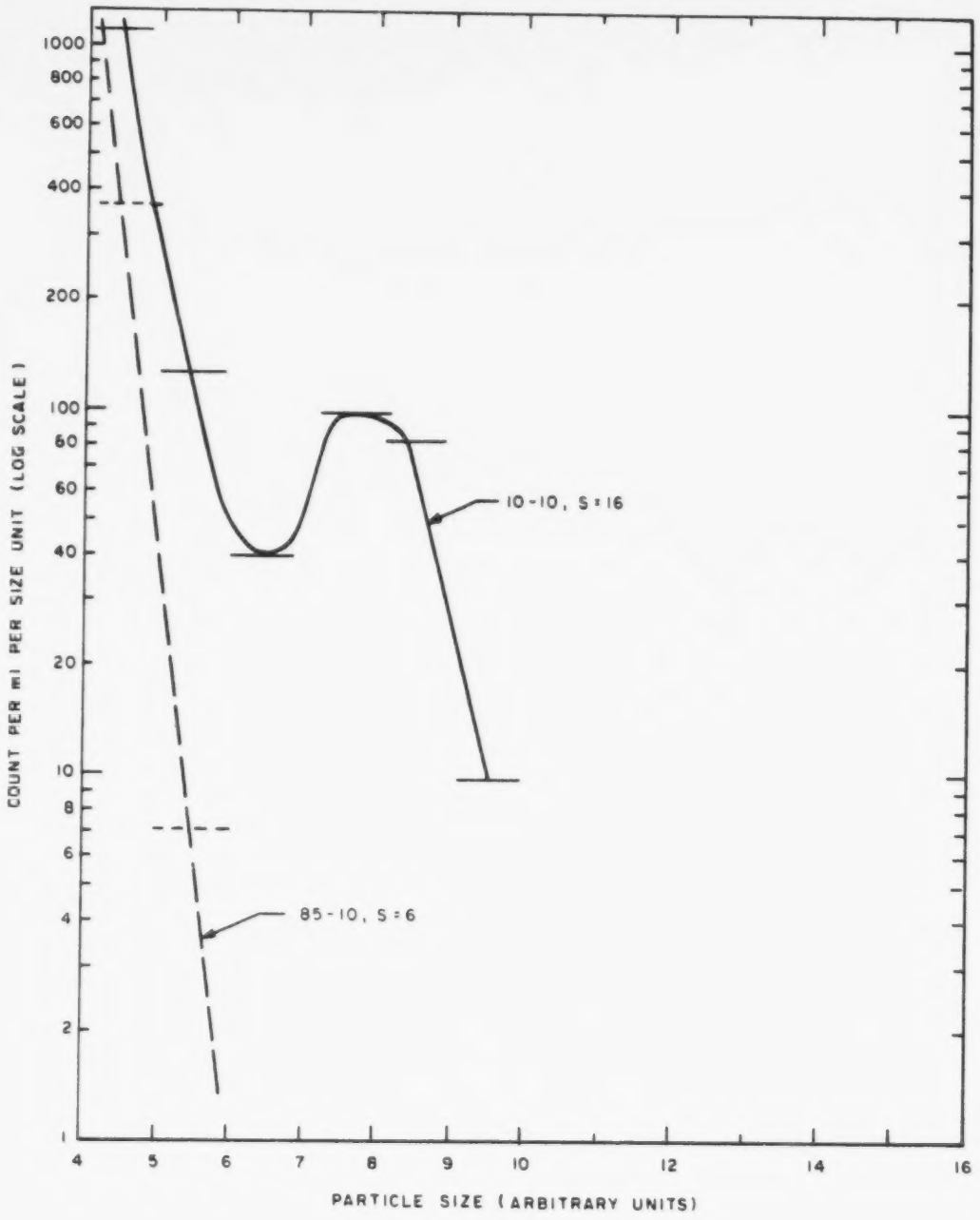

Fig. 30

PARTICLE COUNT DISTRIBUTION FOR EFFLUENTS CONDITIONED AT 10 PERCENT RELATIVE HUMIDITY AFTER 110 MINUTES OF IRRADIATION

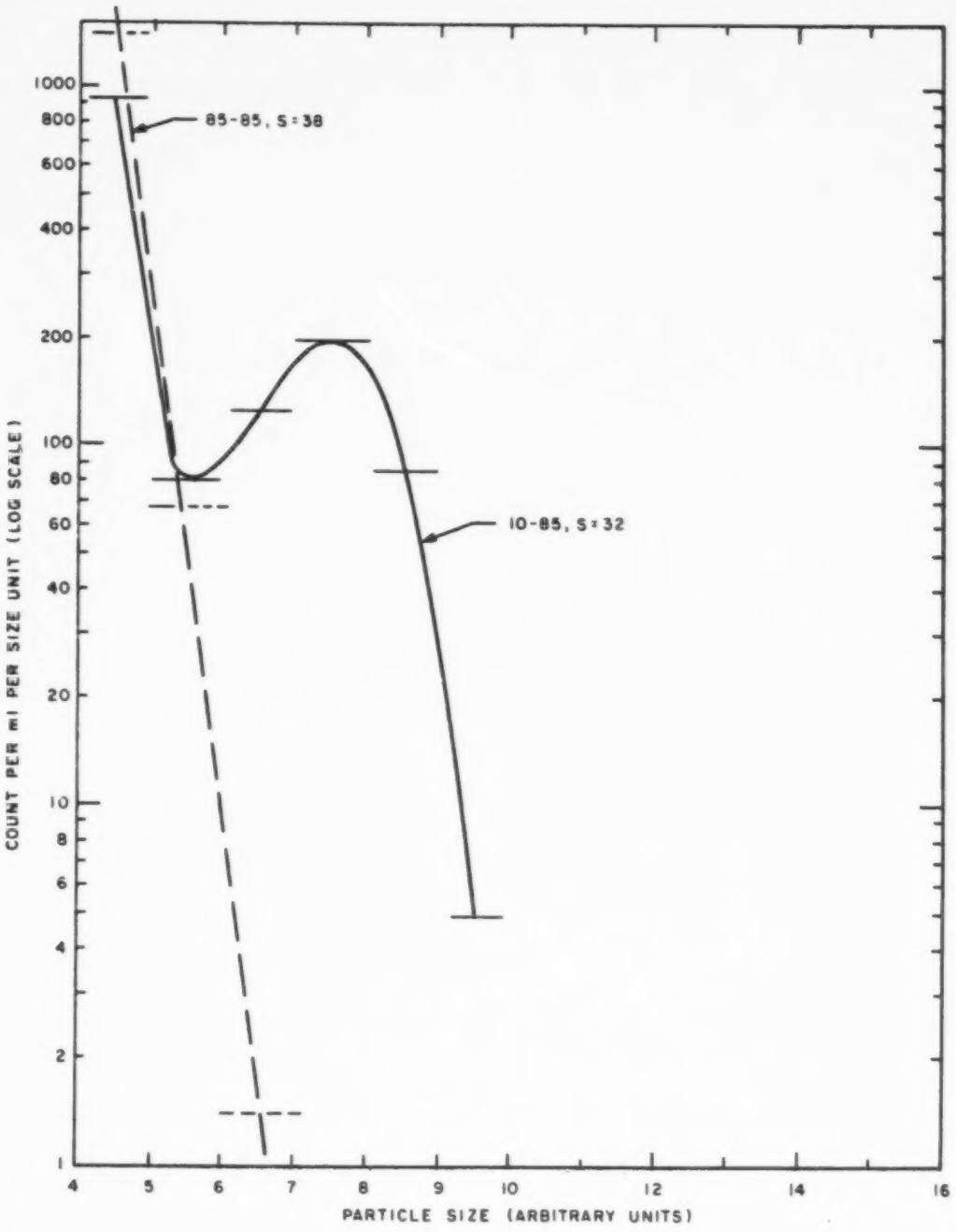

Fig. 31

PARTICLE COUNT DISTRIBUTION FOR EFFLUENTS CONDITIONED AT 85 PERCENT RELATIVE HUMIDITY AFTER 110 MINUTES OF IRRADIATION

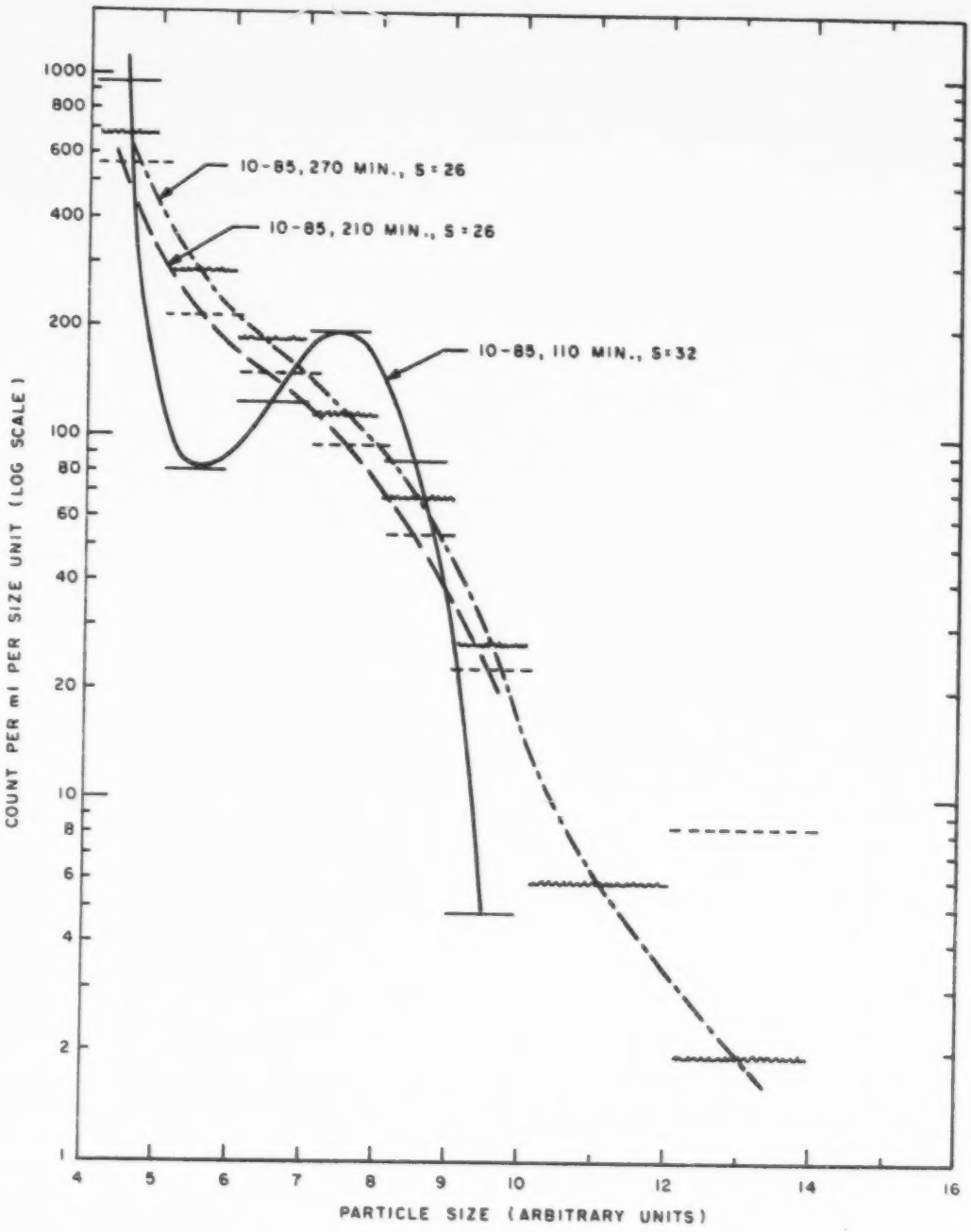

Fig. 32

TYPICAL TEMPORAL BEHAVIOR OF PARTICLE COUNT DISTRIBUTION OF AEROSOLS FORMED AT 10 PERCENT RELATIVE HUMIDITY AND CONDITIONED AT 85 PERCENT RELATIVE HUMIDITY

sensitivity to humidity change. That some complex time-dependent phenomenon is the cause of this contradiction is apparent from the transient behavior of the light scattering before reaching steady state and from the change of size distribution with time for particles formed at 10 percent relative humidity and conditioned at 85 percent relative humidity.

One partial explanation lies in the deductions from earlier work that (1) at low humidity particles grow faster but fewer particles are formed, (2) at low humidity the concentration of hygroscopic material in the particles is high, and (3) the countable particles are those with longer lifetimes in the reactor. These deductions, combined with the present results, suggest that countable particles are a different breed from the bulk of the particles in the aerosol, which are apparently hygroscopic, and that this difference might be accentuated with time, especially at low humidities. For example, as the average age of particles in the flask approaches the mean value (the residence time), the chemical nature of the large particles with lifetimes several times the residence times might change at low humidities by accumulation of organic material; this would tend to make them less sensitive to humidity changes, at least as far as light scattering is concerned. Such an interpretation would be at least partially consistent with the results of the pioneer investigations of the nature of smog aerosols(14, 15, 16).

3. Effect of Added Materials

In still other studies we investigated the effect of various pollutants and photooxidation products on the light-scattering properties of aerosols formed via sulfur dioxide. In some cases the material was added at parts per million concentrations to a mixture of 3 ppm of 2-methyl-2-butene, 1 ppm of nitrogen oxide, and 0.1 ppm of sulfur dioxide; the mixture was then photooxidized at a residence time of either 17 or 34 minutes. In other cases 2-methyl-2-butene was replaced by an olefin which is known to yield the material under investigation as a major photooxidation product.

The results with ethylene and acetylene added are shown in Tables VII and VIII, respectively; no significant effect on light scattering was found under these conditions.

The effect of acrolein was studied indirectly by re-examination of the light scattering from the standard mixture with 3 ppm of 1, 3-butadiene replacing the 2-methyl-2-butene. There was no significant difference from the results observed using standard mixture; the light scattering and particle count were somewhat less.

Table VII

EFFECT OF ETHYLENE ON LIGHT-SCATTERING PROPERTIES OF AEROSOLS(a)

Relative Humidity (Percent)	Residence Time (min)	Light Scattering Referred to Air		Particle Count (ml^{-1})(b)					
		In Presence(c) of Ethylene	In Absence(d) of Ethylene	Total	Counting Channel 1	2	3	4	5
10	34	35-58(46)	29	1962	1926	38	0.7	0.0	0.0
50	17	21-44(33)	31	1967	1926	42	0.3	0.0	0.0
80	34	44-21(33)	38	2578	2518	60	0.6	0.1	0.1

(a) Photooxidation of 10 ppm of ethylene, 3 ppm of 2-methyl-2-butene, 1 ppm of nitrogen oxides, and 0.1 ppm of sulfur dioxide.
(b) Calibrated with polystyrene spheres; channel (1) equivalent to 0.25-0.31μ; channel (2), 0.31-0.38μ; channel (3), 0.38-0.44μ; channel (4), 0.44-0.50μ; and channel (5), 0.50-0.56μ.
(c) Figures in parentheses are averages.
(d) These figures are all at 17 minutes' residence time.

Table VIII

EFFECT OF ACETYLENE ON LIGHT-SCATTERING PROPERTIES OF AEROSOLS(a)

Relative Humidity (Percent)	Residence Time (min)	Light Scattering Referred to Air		Particle Count (ml^{-1})(b)					
		In Presence(c) of Acetylene	In Absence of Acetylene	Total	Counting Channel 1	2	3	4	5
10	34	36	29	1705	1685	20	0.0	0.0	0.0
50	17	18-36(27)	31	1924	1675	248	10	0.5	0.0
50	34	23-43(33)	31	2333	2269	65	2	0.2	0.0

(a) Photooxidation of 10 ppm of acetylene, 3 ppm of 2-methyl-2-butene, 1 ppm of nitrogen oxides, and 0.1 ppm of sulfur dioxide.
(b) Calibrated with polystyrene spheres; channel (1) equivalent to 0.25-0.31μ; channel (2), 0.31-0.38μ; channel (3), 0.38-0.44μ; channel (4), 0.44-0.50μ; and channel (5), 0.50-0.56μ.
(c) Figures in parentheses are averages.

Adding 0.2 ppm or more of ammonia to the standard mixture did have a pronounced effect. The scattering was somewhat suppressed, and the population of countable particles was drastically reduced--by about 10-fold. This effect is consistent with the picture of chemically active acid droplets and with the idea that the older and countable particles have the greater amounts of organic material. Neutralization by ammonia probably would completely inhibit the chemical activity of the droplets.

The addition of 3 ppm of propylene oxide to the standard mixture before photooxidation apparently resulted in a slight enhancement of light scattering and countable particle concentration after photooxidation. The effect was marginal but does indicate that olefin oxides or some photo-oxidation product derived from the oxides may be incorporated into the aerosol. Olefin oxides themselves constitute one of the minor products of photooxidation of olefins.

The effect of formaldehyde was studied in two ways. One was by using isobutylene in place of 2-methyl-2-butene; the comparative results are shown in Table IX. The other was by adding dilute gaseous formaldehyde to the mixture; the results are shown in Table X. Isobutylene yielded about the same results as 2-methyl-2-butene. The addition of 3 ppm of formaldehyde (see Table X) had little effect on countable particles but did reduce the light scattering by a factor of two to three. This indicates a strong effect on particles below the counting range of the counter-photometer. This phenomenon is undoubtedly connected with an earlier observation that the addition of sulfur dioxide to photooxidizing isobutylene markedly reduces the yield of formaldehyde.

4. Nuclei Concentrations

During these experiments a partial study was made of nuclei concentration in the effluent. This portion of the study was made possible by the Navy's loan of an automatic nuclei counter, but work was incomplete because the Navy required the return of the instrument before the study was completed. The study was confined to the humidity region between 0 percent and 50 percent. The temporal behavior of nuclei concentration was followed at 0 percent, 30 percent, and 40 percent relative humidity. At other humidities, only steady-state nuclei concentration was measured.

A typical example of the temporal variation of nuclei in the effluent is shown in Figure 33, while pertinent data on nuclei concentration are shown in Table XI. The total count obtained by the counter-photometer is included for comparison with the steady-state nuclei count. Within the humidity range the peak nuclei concentration seems the same. The steady-state nuclei concentration presumably is a direct measure of the

Table IX

COMPARATIVE EFFECTS OF ISOBUTYLENE AND 2-METHYL-2-BUTENE ON THE LIGHT-SCATTERING PROPERTIES OF AEROSOLS[a]

Relative Humidity (Percent)	Residence Time (min)	Hydrocarbon Concentration (ppm)	Light Scattering[b] Referred to Air	Particle Count (ml^{-1})[c]					
				Total	Counting Channel 1	2	3	4	5
With isobutylene									
50	34	3.0	24-25	1508	1497	11	0.3	0.0	0.0
50	34	6.0	17	NI[d]	NI	NI	NI	NI	NI
50	34	6.0	20-36(28)	2180	1460	680	46	5	0.2
80	34	3.0	12-25(18)	839	836	7	0	0	0
With 2-methyl-2-butene									
50	17	3.0	31	1410	1380	33.8	0.6	0.0	0.0
80	17	3.0	38	1568[e]	1460	103	2.7	0.0	0.0

(a) Photooxidation of varying concentrations of isobutylene and 2-methyl-2-butene and 0.1 ppm of sulfur dioxide.

(b) Figures in parentheses are averages.

(c) Calibrated with polystyrene spheres; channel (1) equivalent to 0.25-0.31μ; channel (2), 0.31-0.38μ; channel (3), 0.38-0.44μ; channel (4), 0.44-0.50μ; and channel (5), 0.50-0.56μ.

(d) NI means no information.

(e) This count was taken at 85 percent relative humidity.

Table X

EFFECT OF FORMALDEHYDE ON THE LIGHT-SCATTERING PROPERTIES OF AEROSOLS[a]

Relative Humidity (Percent)	Residence Time (min)	Light Scattering Referred to Air	Particle Count (ml^{-1})[b]					
			Total	Counting Channel 1	2	3	4	5
With formaldehyde								
10	17	6-16	1099	1060	363	2	0.5	0
			1854	1578	272	10	0.7	0
50	17	8-16	908	886	5	0	0	0
			1530	1378	150	4	0	0
80	17	8-24	1529	1244	178	93	20	1
			1777	1419	232	89	32	7
Without formaldehyde								
10	17	37	2950	1780	740	200	93	82
		19	1195	615	153	277	131	21
50	17	31	1410	1380	33.8	0.6	0	0
85	17	38	1568	1460	103	2.7	0	0

(a) Photooxidation of 3 ppm of formaldehyde, 3 ppm of 2-methyl-2-butene, 1 ppm of nitric oxide, and 0.1 ppm of sulfur dioxide.

(b) Calibrated with polystyrene spheres, channel (1) equivalent to 0.25-0.31μ, channel (2), 0.31-0.38μ, channel (3), 0.38-0.44μ; channel (4), 0.44-0.50μ; and channel (5), 0.50-0.56μ.

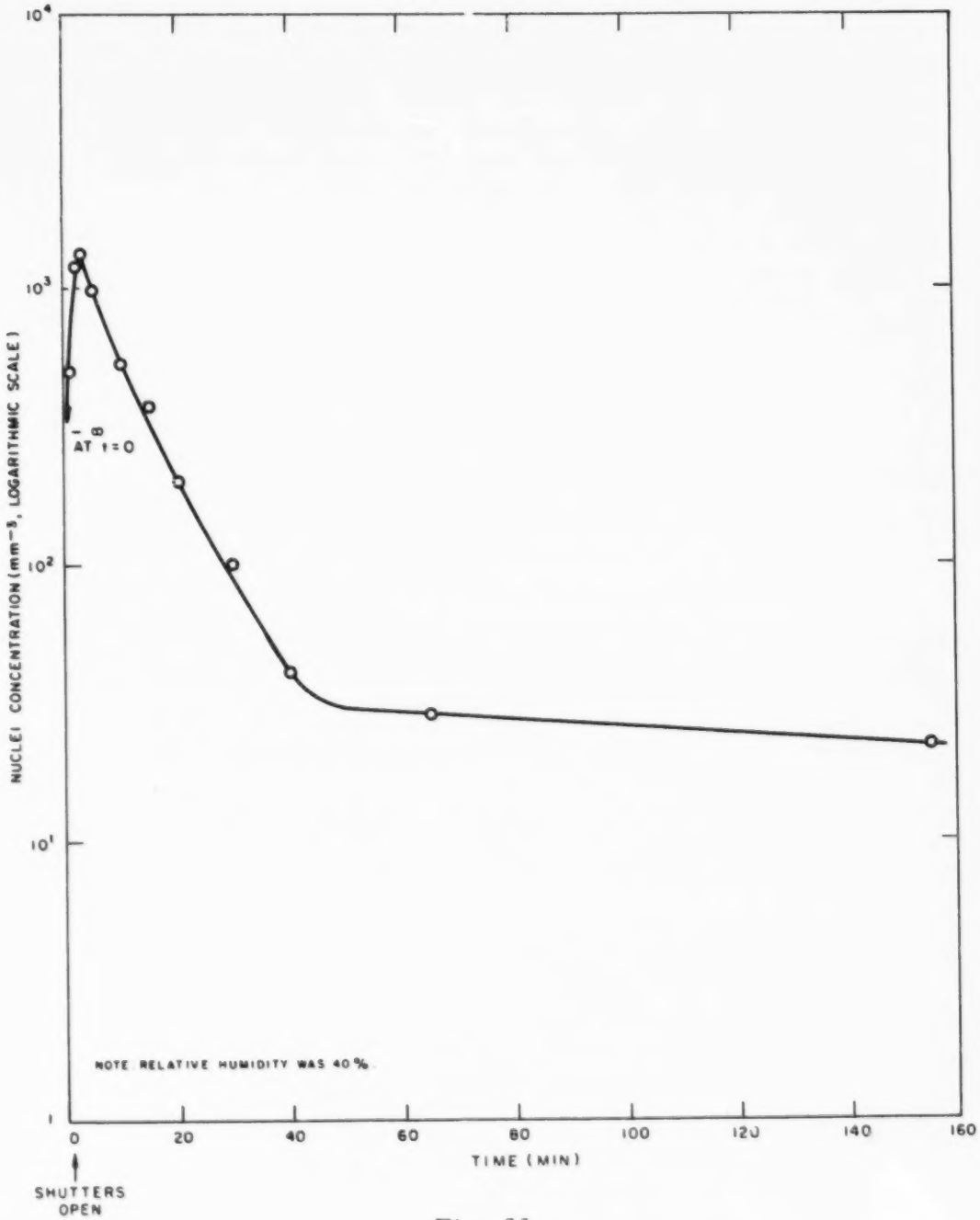

Fig. 33

TYPICAL TRANSIENT IN NUCLEI CONCENTRATION OBSERVED DURING EXPERIMENTS ON THE EFFECT OF RELATIVE HUMIDITY

values of τG used above in interpreting the particle count data. Values of τG taken from the curve shown in Figure 27 are given in column 3 of Table XI for comparison with the data in column 4 of Table XI. These are of the same order of magnitude and agree within the variance indicated by the experimental points of Figure 27. The values at 0 percent relative humidity are exceptional. A comparison of total count with nuclei count for 0 percent shows that all nuclei were counted. Contrary to the simple theory which predicts that the size distribution extends indefinitely to smaller sizes, we find that the steady-state aerosol particles at 0 percent relative humidity have mean diameters around 0.3 mμ and are essentially monodispersed.

Table XI

PERTINENT DATA ON NUCLEI CONCENTRATION

Relative Humidity (Percent)	Peak Nuclei Concentration (mm^{-3})	τG[a]	Steady-State Nuclei Concentration (mm^{-3})	Total Count (mm^{-3})	Initial Diameter (Micron)
0	1100	28.0	1.4	1.3	0.028
10	NI[b]	8.1	13.0	3.0	NI
20	NI	14.0	19.0	2.0	NI
30	1100	23.0	19.0	1.6	0.17
40	1400	39.0	26.0	2.0	0.14
50	NI	65.0	28.0	1.1	NI

(a) Taken from curve shown in Figure 27.
(b) NI means no information.

The decay of transients, shown in Figure 33, was interpreted by the equation

$$\frac{dn}{dt} = kn^2 - \alpha n + K$$

where k = coagulation constant, α = stirred reactor constant = $1/\tau$, and K = a function of time expressing the combined effects of generation rate, nonuniform coagulation, and loss to the reactor walls. The data treated

in this manner are shown in Figure 34. Not much meaning can be attributed to the value of K. However, the slopes were further interpreted in terms of the coagulation constant by the equation

$$k = \frac{4RT}{3\eta N}\left(1 + \frac{2A\lambda}{d}\right)$$

where R = gas constant per mole, T = absolute temperature, η = gas viscosity, N = Avogadro's number, A = Cummingham's constant, λ = mean free path of the gas molecules, and d = particle diameter. Since all of the values except d are known, we may calculate values of d from values of k. These values of d are given in column 6 of Table XI. Since $2A\lambda \simeq 0.18\mu$ under these conditions, it is obvious that rapid coagulation of the initially highly concentrated nuclei is at least one of the major processes occurring in the decay of transients.

5. Other Nuclei Sources

It is doubtful that the sulfur dioxide mode of aerosol formation is the only one operating in polluted atmospheres. An experimental program was therefore carried out to survey other nuclei for aerosol growth. These experiments consisted of adding nuclei known to be present in the atmosphere or to be similar in some respects to atmospheric nuclei to photooxidizing mixtures of olefin and nitrogen oxide in air and measuring the effect on the light scattering of the mixture.

Other nuclei were added to the photooxidizing mixture, with and without 0.1 ppm of sulfur dioxide. These nuclei were generated by placing a layer of solid material on an electrically heated coil of heavy Nichrome V wire in the pure air stream to the reactor at a point upstream from the mixer where the minor constituents were added. A preliminary rough calibration using a General Electric nuclei counter indicated that the coil power was sufficient to produce the desired nuclei concentration.

The effect of sodium chloride nuclei on the light scattering from the standard mixture is shown in Table XII. At medium and high humidities, sodium chloride is not effective in nucleating aerosol growth. No synergism with sulfur dioxide aerosols is observed at high humidities.

The nuclei from not sodium carbonate also were not effective as nucleating agents for aerosol. However, they did interact with the system containing sulfur dioxide, as shown in Table XIII. Their effect was to

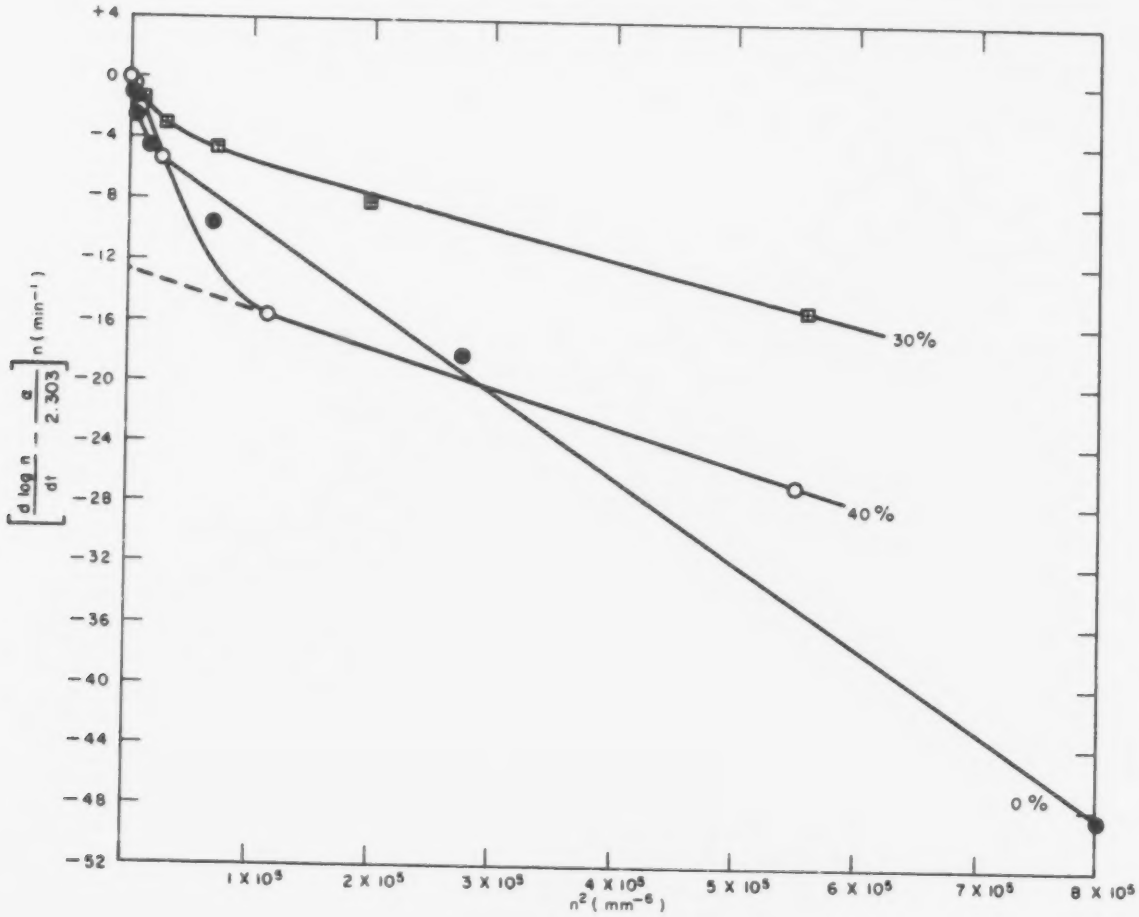

Fig. 34

SEMIQUANTITATIVE INTERPRETATION OF THE DECAY OF THE NUCLEI CONCENTRATION TRANSIENT AT THREE RELATIVE HUMIDITIES

Table XII

EFFECT OF SODIUM CHLORIDE NUCLEI ON THE LIGHT-SCATTERING PROPERTIES OF AEROSOLS

Relative Humidity (Percent)	Residence Time (min)	Sulfur Dioxide Concentration (ppm)	Sodium Chloride Nuclei Concentration (ml^{-1})	Light Scattering Referred to Air	Particle Count (ml^{-1})[a]					
						Counting Channel				
					Total	1	2	3	4	5
50	17	0	3×10^4	1.8	NI[b]	NI	NI	NI	NI	NI
80	17	0	3×10^4	2.0	NI	NI	NI	NI	NI	NI
80	17	0	3×10^3	3.0	NI	NI	NI	NI	NI	NI
85	17	0.10	$\sim 10^4$	46	1490	1470	20	0	0	0
85	17	0.10	0	39	1568	1460	103	2.7	0	0

(a) Calibrated with polystyrene spheres; channel (1) equivalent to 0.25-0.31μ, channel (2), 0.31-0.38μ; channel (3), 0.38-0.44μ; channel (4), 0.44-0.50μ; and channel (5), 0.50-0.56μ.
(b) NI means no information.

Table XIII

EFFECT OF ALKALINE NUCLEI ON THE LIGHT-SCATTERING PROPERTIES OF AEROSOLS (From Volatilization of Sodium Carbonate)

Relative Humidity (Percent)	Residence Time (min)	Sulfur Dioxide Concentration (ppm)	Alkaline Nuclei Concentration (ml^{-1})	Light Scattering[a] Referred to Air	Particle Count (ml^{-1})[b]					
						Counting Channel				
					Total	1	2	3	4	5
50	17	0.10	5×10^3	39-44(42)	1482	1476	8	0.0	0.0	0.0
50	17	0.10	0	29-46(38)	2293	2183	106	5	0.3	0.0
50	17	0.10	6×10^4	<16(decr.)	902	692	170	34	9	0.7
50	17	0.10	0	>24(incr.)	NI[c]	NI	NI	NI	NI	NI
80	17	0.10	0	40-60(50)	2433	2375	61	0.8	0.0	0.0
80	17	0.10	6×10^4	30-33(32)	1051	1051	2	0.0	0.0	0.0
80	17	0	6×10^4	0	NI	NI	NI	NI	NI	NI
80	17	0.10	5×10^4	34-35(34)	530	529	0.7	0.2	0.0	0.0
80	17	0.10	5×10^4	44-49(46)	1168	1162	5.6	0.2	0.0	0.0
80	17	0.10	5×10^5	23-30(26)	278	286	0.0	0.0	0.0	0.0

(a) Figures in parentheses are averages.
(b) Calibrated with polystyrene spheres; channel (1) equivalent to 0.25-0.31μ; channel (2), 0.31-0.38μ; channel (3), 0.38-0.44μ; channel (4), 0.44-0.50μ; and channel (5), 0.50-0.56μ.
(c) NI means no information.

suppress the light scattering somewhat and to act strongly to suppress the concentration of countable particles. The effect is similar to the effect of adding gaseous ammonia and probably may be explained in the same way. We may conclude that alkaline materials, either gaseous or particulate, will have a definite effect on aerosols formed through the presence of sulfur dioxide.

Lead-containing nuclei are prominent suspects in the nucleation of aerosols in atmospheres contaminated by motor vehicle exhaust. Nuclei resulting from the volatization of plumbous chloride into moist air were therefore tested for their effect. The results are shown in Table XIV. Lead-bearing nuclei have no effect in the absence of sulfur dioxide. In the presence of 0.1 ppm of sulfur dioxide, light scattering is suppressed and there is a tendency for the number of countable particles to be greater, especially at low humidities. It is evident that lead-containing nuclei can have an appreciable effect on aerosols formed in this manner.

6. Discussion

The sequence of events leading to the formation and growth of aerosols via the sulfur dioxide path in the stirred reactor seems fairly clear. As the chemical reaction proceeds, the system becomes supersaturated relative to some sulfur compound--possibly sulfuric acid--and multicomponent nucleation begins (the other major component being water). The supersaturation increases and the nucleation accelerates rapidly until loss of material through particle growth on the nuclei begins to use up the supply of gaseous aerosol material and to result in a rapid deceleration of nucleation. The large concentration of small particles so produced coagulates to form larger particles and the rate of nucleation is reduced to a relatively low value sufficient to maintain the steady-state population in the reactor. The particle population so formed seems to be inhomogeneous, not only in size but also in properties. The smaller and younger particles change size markedly with humidity changes, much as a mist of sulfuric acid would behave. The larger and older particles, particularly when formed at low humidities, seem much less sensitive to changes in humidity. Presumably, these are the particles that have picked up a great deal of organic matter from the reacting mixture via relatively slow processes. This interpretation of the phenomenon seems reasonable, although it is based on more or less indirect and ambiguous evidence. It is expected that an intensive study of particle composition will yield more direct evidence. Studies will also be made of a model system consisting of the usual photooxidizing mixture (no sulfur dioxide) plus a homogeneous small-particle ($\sim$0.1μ diameter) aerosol of sulfuric acid from a La Mer-Sinclair generator.

Table XIV

EFFECT OF LEAD-BEARING NUCLEI ON THE LIGHT-SCATTERING PROPERTIES OF AEROSOLS[a]
(From Volatilization of Plumbous Chloride)

Relative Humidity (Percent)	Residence Time (min)	Sulfur Dioxide Concentration (ppm)	Lead-Bearing Nuclei Concentration (ml^{-1})	Light Scattering Referred to Air	Particle Count (ml^{-1})[b]					
						Counting Channel				
					Total	1	2	3	4	5
10	34	0.00	10^6	0.2	3.16	3.14	0.02	0.00	0.00	0.00
10	34	0.10	10^6	24-28	3641	3474	170	0.5	0.2	0.3
					3536	3066	447	33	1.5	0.0
					3354	2319	736	290	32	3.4
50	34	0.10	10^6	24-29	2647	2382	98	2.0	0.0	0.0
					2349	2262	89	2.7	0.0	0.3
80	34	0.00	10^6	0.5	6 01	6.00	0.04	0.01	0.00	0.00
80	34	0.10	10^6	21-28	1270	1262	8.5	0.0	0.0	0.0
					1459	1433	28	0.0	0.2	0.0
50	17	0.00	10^6	0.0	NI[c]					
50	17	0.10	10^6	10-11	524	520	5.8	0.2	0.0	0.0

(a) Photooxidation of 3 ppm of 2-methyl-2-butene and 1 ppm of nitric oxide with and without sulfur dioxide.

(b) Calibrated with polystyrene spheres; channel (1) equivalent to 0.25-0.31μ; channel (2), 0.31-0.38μ; channel (3), 0.38-0.44μ; channel (4), 0.44-0.50μ; and channel (5), 0.50-0.56μ.

(c) NI means no information.

No effect was observed with the addition or presence of ethylene, acetylene, or formaldehyde. Acrolein and propylene oxide have a small effect, if any. With ammonia, and presumably other alkaline gases, the effect is dramatic and may be interpreted as an inhibition of the slow secondary processes principally affecting the growth of the older particles.

Nuclei of sodium chloride, sodium carbonate, and lead chloride do not produce an aerosol under the conditions employed. When sulfur dioxide is added to systems containing these nuclei, no synergism is observed with sodium chloride. Sodium carbonate apparently neutralizes the nuclei formed from sulfur dioxide and thus inhibits the secondary growth process. Lead chloride nuclei definitely enhance the formation of light-scattering aerosol via the sulfur dioxide mode, possibly by catalysis of secondary growth processes and probably with some small contribution via changes in the optical properties of the aerosol material. Future studies will be carried out on iron oxide and lead oxide and possibly on zinc oxide nuclei generated separately by photochemical means.

To date, the production of appreciable aerosol via photooxidation of light straight-chain or slightly branched olefins has required the presence of a relatively small amount of sulfur dioxide.

III Future Research

The over-all objective of this research is to broaden the understanding of the reactions involved in the formation of photochemical smog. In keeping with this objective, we have pointed out in this report several areas requiring further investigation.

In the area of kinetics we need to know a great deal more about ozone-olefin reactions so that we may delineate the mechanism of the reactions during photooxidation. To this end we have designed and constructed a glass reaction cell to replace one of the present aluminum cell coverings of the infrared spectrophotometer. With this apparatus it will be possible to study the rates of many reactions which cannot be studied in the 500-cu-ft chamber. Reactions dependent upon free-radical sources, variations in diluent gases, and variations in reaction times will become useful tools with use of this glass reaction cell.

The methods of measurement of eye irritation and photooxidation products must be improved so that results from the present synthetic system may be correlated with pollution in the atmosphere. In this interest we are considering acquiring new analytical equipment, such as

the Beckman IR-7 with 80-meter cells. Theoretically, this instrument will greatly increase our ability to examine complex mixtures at lower concentrations.

The mechanism of cophotooxidation of sulfur dioxide and subsequent aerosol formation also requires further investigation. Thus, techniques such as infrared analysis will be applied to the analysis of the aerosol particles to determine their constituents.

IV Acknowledgments

The authors wish to express their appreciation for the assistance and guidance provided by the following people: W. L. Faith, P. A. Leighton, and N. A. Renzetti of the Air Pollution Foundation; J. H. Easthagen, C. A. Jones, L. M. Richards, and D. A. Skinner of the American Petroleum Institute; A. J. Haagen-Smit of the California Institute of Technology; and Mr. G. C. Haas, Department of Public Health, State of California.

REFERENCES

1. Schuck, E.A. and G.J. Doyle. Photooxidation of Hydrocarbons in Mixtures Containing Oxides of Nitrogen and Sulfur Dioxide. Report No. 29, Air Pollution Foundation, San Marino, California, October 1959.

2. Hanst, P.L., E.R. Stephens, W.E. Scott, and R.L. Doerr. Atmospheric Ozone-Olefin Reactions. Report by the Franklin Institute to the American Petroleum Institute, August 1958.

3. Harding and Norrish. Proc. Roy Soc. A212, 291 (1952).

4. Badin, E.J. p. 382, Third Combustion Symposium, Baltimore, Maryland, 1943.

5. Schuck, E.A. Eye Irritation from Irradiated Auto Exhaust. Report No. 18, Air Pollution Foundation, San Marino, California, March 1957.

6. Schuck, E.A., H.W. Ford, and E.R. Stephens. Air Pollution Effects of Irradiated Automobile Exhaust As Related to Fuel Composition. Report No. 26, Air Pollution Foundation, San Marino, California, October 1958.

7. Schuck, E.A. and G.J. Doyle. A Study of Irradiated Auto Exhaust. Report No. 9, Technical Report No. II, Stanford Research Institute to Air Pollution Foundation, San Marino, California, February 1958.

8. Doyle, G.J. and N.A. Renzetti. Formation of Aerosols by Dilute Auto Exhaust. Paper presented at the American Chemical Society Meeting, September 9, 1957.

9. Fronla, H., A.F. Bush, and E.S.C. Bowler. Use of Thermal Precipitator and Electron Microscope for Evaluation of Air Born Particles. p. 102, Proc. 3rd National Air Pollution Symp., Pasadena, California, April 1955.

10. Calvert, Jack G. Photoactivated Surface Reactions. Report No. 15, Air Pollution Foundation, San Marino, California, November 1956.

11. Prager, M.J., E.R. Stephens, and W.E. Scott. Aerosol formation from gaseous air pollutants. Ind. and Eng. Chem. 52, 521-4 (1960).

12. Volmer, M. Der Kinetik der Phasenbildung. pp. 65-68, 76-89, 97-100, 121-145, 152-155, Leipzig, Steinkopff, 1933.

13. Reiss, H. Chem. Phys. 19, 482 (1951).

14. The Smog Problem in Los Angeles County. pp. 104-107, Report by Stanford Research Institute to the Western Oil and Gas Association, January 1954.

15. Steffins, Carsten and Sylvan Rubin. Visibility and Air Pollution. Proc. 1st National. Air Pollution Symp., Stanford Research Institute, Stanford, California, 1949.

16. Rubin, Sylvan. Liquid particles in atmospheric haze. J. Atm. and Terr. Phys. 2 (2), 130 (1952).

Appendix A

EXPERIMENTAL CONDITIONS

Appendix A

EXPERIMENTAL CONDITIONS

I Experimental Method

All of the photochemical experiments described in this report (except the aerosol experiments) were static experiments conducted in a 520-cubic-foot, glass-lined irradiation chamber (Figure A-1). Appropriate amounts of pure grade Phillips hydrocarbons (research grade in the case of isobutene) and Matheson nitrogen dioxide were introduced into the chamber, which contained purified air, and the photochemical reaction was started by turning on the ultraviolet lamps. The ethyl nitrite used in later photolysis experiments was a Mallinckrodt product.

The light intensity was the same in all of the experiments in which the mixtures were irradiated and, in the 3,000Å to 4,000Å region, was equivalent to that of full sunlight. The artificial sunlight was provided by twenty H400 E-1 medium pressure mercury arcs and 78 Blacklite fluorescent tubes. Analytical measurements were obtained with a Perkin-Elmer Model 21 long-path infrared spectrophotometer, a continuous-recording colorimetric nitrogen dioxide analyzer employing the Griess-Saltzman reagent, two Loenco Model 11 gas chromatographs with poly-ethylene glycol columns, and by wet chemical analysis.

The infrared spectrophotometer was able to follow the hydrocarbon levels and the concentrations of most of the major products. Liquid analyses were made for formaldehyde. For the minor products as well as some of the major products, gas chromatographic analyses of cold trap samples were employed. These samples were taken at liquid oxygen temperatures in stainless steel traps packed with glass beads. In the earlier experiments, 3-inch-long glycerol-firebrick filters (similar to a short gas chromatographic column) were used to remove water. In later experiments, no filters were used. Both Carbowax 600 and Carbowax 1500 were used in the analytical columns. Both 5-foot and 25-foot columns were used in analyzing the higher-boiling as well as low-boiling products. Several columns were used due to the poor recovery of some of the products after continued use of the columns.

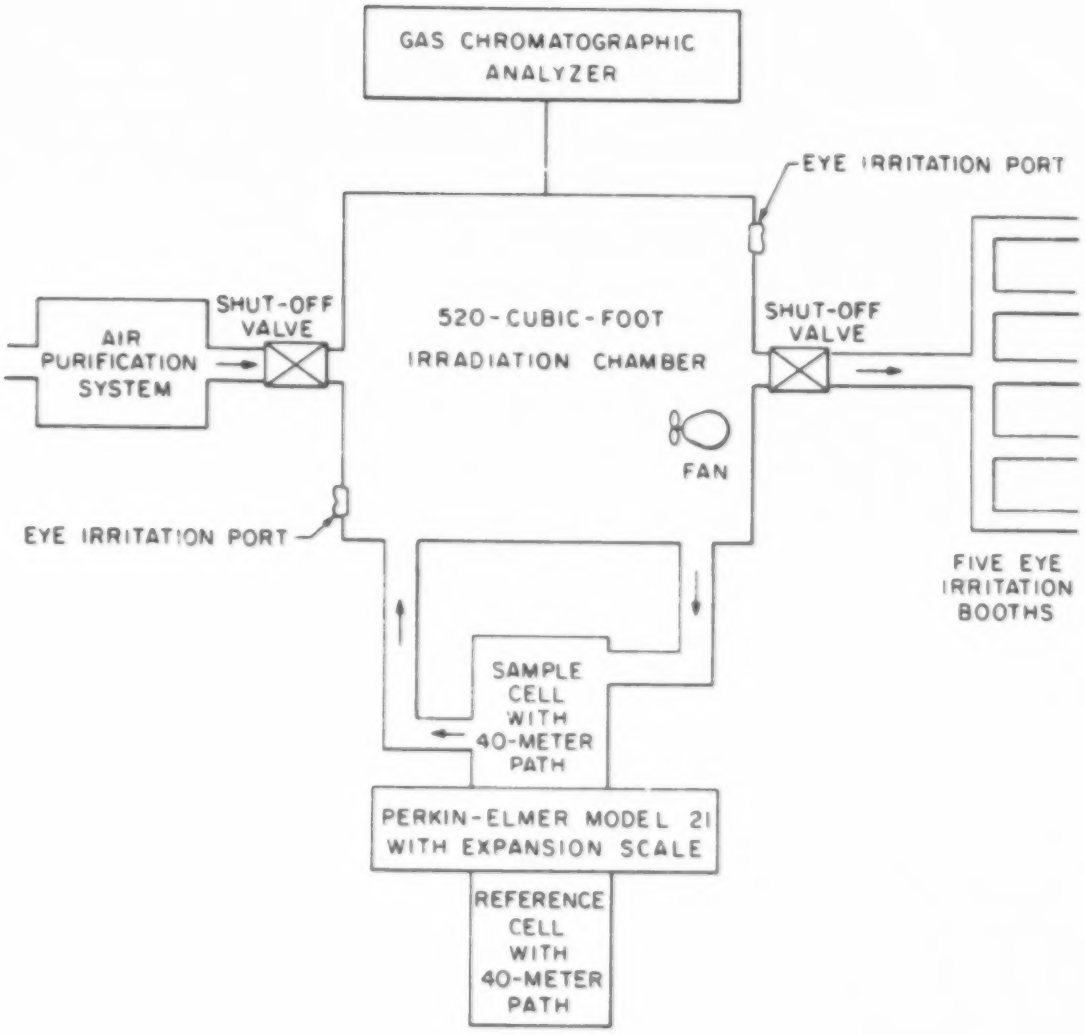

Fig. A-1

IRRADIATION FACILITY

II Analytical Procedures

A Colorimetric Microdetermination of Formaldehyde

A colorimetric determination of 0 μg to 20 μg of formaldehyde per milliliter is based on the formation of a violet color which develops on heating with 1,8-dihydroxynaphthalene-3,6-disulfonic acid (chromotropic acid) in the presence of strong sulfuric acid. This reagent is highly specific for formaldehyde.

To a solution of 0 6g of chromotropic acid (1,8-dihydroxynaphthalene-3,6-disulfonic acid, an Eastman Kodak Company product) in 20 ml of water are added 180 ml of concentrated sulfuric acid. The gas to be sampled is drawn through a suitable absorber (ASTM sulfur type containing a fritted glass disk, a bead-packed bulb, or other efficient type) containing 50 ml of 1 percent sodium bisulfite.

The volume of gas is measured by drawing it through a wet test meter by means of a vacuum pump and exhausting it to air At a concentration of 1 ppm of formaldehyde, a sample of 5 ft^3 of air is sufficient, and it may be drawn through the bisulfite scrubber at a rate of up to 20 ft^3 per hour.

After the sampling, 6 ml of chromotropic acid reagent are added to 4 ml of the scrubber solution. The mixture is heated in a test tube in a boiling water bath for 30 min, with precaution taken against absorption of water vapor and uneven illumination; the color which develops is determined photoelectrically, using a filter with peak transmission at 570 mμ.

The relationship between colorimeter reading and quantity of formaldehyde is established by measuring the color produced by a series of standards of 0 μg to 20 μg of formaldehyde in 1 percent sodium bisulfite (prepared by appropriate dilution of 40 percent formaldehyde) submitted for the procedure described above.

With the chromotropic acid reagent, negative results are obtained with acetaldehyde, isobutyraldehyde, isovaleraldehyde, crotonaldehyde, acrolein, benzaldehyde, salicylaldehyde, and many other aromatic aldehydes; glyceraldehyde gives a yellow color with a green fluorescence when present in quantity, and furfural gives a yellow-brown color. (One part formaldehyde can be determined in the presence of 380 parts furfural.)

B. Method for Determination of Formic Acid*

The sample is collected by drawing air through scrubbers containing dilute sodium hydroxide. The scrubber solution is acidified and stirred to remove carbon dioxide. The solution is brought to pH 8-9 and treated with an 0.2 percent solution of Voorlander's Reagent (dimethyl dihydroresorcinol) in a phosphate buffer to remove formaldehyde from further reaction. The formic acid present is then reduced with nascent hydrogen to formaldehyde, which is determined colorimetrically in strong sulfuric acid with chromotropic acid.

III Improvement of the Counter-Photometer

At present the lower size limit for countable particles lies in the region of 0.25μ to 0.30μ diameter. Indirect but fairly conclusive evidence obtained in these laboratories, along with direct evidence obtained by others, shows that most of the particles formed in synthetic and semi-synthetic systems lie below these limits. It is of great interest, therefore, to reduce the lower limit for counting.

One approach to this problem is to increase the brightness of the light source. The only practical approach at present is the use of incandescent sources; this means an appreciable increase in color temperature above the 2950°K of the present strip filament tungsten lamp. One commercially available lamp consists of a 5/16-in tantalum carbide disk heated to yield a color temperature of 3200°K to 3700°K by means of radio-frequency inductive heating. One such lamp and its auxiliary equipment were procured for use with the counter-photometer. Preliminary tests revealed that, at 3200°K, this lamp produced 2.2 times as much scattering from air as the original lamp, with a measured gain in signal-to-noise ratio of 1.6 using air scattering as the signal and noise count rate as a measure of noise. Operation at this or higher color temperatures should push the lower limit for counting down to or below 0.2μ diameter.

A second approach is to use the improved photomultipliers developed later than the present 1P21. Only a modest improvement can be expected, however, judging from published data on these tubes.

---

* APCD Method 9-53, Laboratory Methods, Los Angeles County Air Pollution Control District.

A third approach is to take full advantage of the increased color temperature of the radio-frequency heated source and shift the spectral response of the optical system and detector to somewhat shorter wave lengths--for example, to peak at 300 mμ instead of at the present 400 mμ to 500 mμ. This shift will produce an effective increase in light-scattering cross section for the smaller particles. A moderate improvement of less than 2-fold can be expected in the signal-to-noise ratio because of the rapid decrease of lamp spectral intensity with decreasing wave length. However, this approach will be exploited if future work shows it to be worthwhile.

Appendix B

ADDITIONAL DATA ON PRODUCTS OF PHOTOOXIDATION

Appendix B

ADDITIONAL DATA ON PRODUCTS OF PHOTOOXIDATION

In a number of experiments, gas chromatography was used to follow the variations in the concentrations of the minor products with variations in irradiation time. The purpose of these experiments was to obtain information on the course of the reaction which might provide a clue to the mechanism of the fast reaction. From a previous study of variations in the concentrations of isobutene and major products with variations in irradiation time, it was learned that the rates of disappearance of the reactants and the rates of appearance of the major carbonyl products reach maxima at approximately 25 min. It was thought that unstable intermediates might possibly be present before or during the fast rate period and that identification of these intermediates would clarify the route to the final products. It was also thought that following the variations in the rates of formation of the minor products might possibly provide information on the course of the reaction.

The sampling technique consisted of taking 5-min cold-trap samples corresponding to periods before, during, and following the fast rate period. Scrub samples were also taken during the course of the reaction, using 1 percent sodium bisulfite solution, and these samples were analyzed for formaldehyde by a wet chemical method. (The analytical procedure used for formaldehyde is described in Appendix A.) The cold-trap samples were analyzed on a 12-foot polyethylene glycol gas chromatograph column operated at 40°C.

In all of these experiments the light intensity was maintained at 1.15×10^{16} quanta cm^{-2} sec^{-1} in the near ultraviolet wave length region.

I Isobutene-Nitrogen Dioxide Reactions

Three reactant concentration ratios of isobutene to nitrogen dioxide were investigated with isobutene as the olefin: 1:6, 2:3, and 3:1; in these experiments the initial isobutene concentrations were 0.5 ppm, 2 ppm, and 3 ppm, respectively. Many compounds present during the early part of the reaction were not present after 70 min, the time interval at which most of the isobutene had reacted. Other compounds were present at much higher concentrations during the early part of the reaction than after 70 min. Still other compounds increased gradually in concentration with increased exposure of the mixture to irradiation.

In the experiment in which 0.5 ppm of isobutene and 3 ppm of nitrogen dioxide were irradiated, low concentrations (~0.02 ppm) of methyl nitrite, acetaldehyde, isobutene oxide, and isobutyraldehyde were observed, and moderate concentrations (0.1 ppm) of RVR* = 0.12 were observed. The methyl nitrite, acetaldehyde, and isobutene oxide appeared to peak before and during the fast rate period and to have disappeared in 70 min. Isobutyraldehyde and RVR = 0.12 were present in the final (70 min) product mixture.

In the experiment in which 2 ppm of isobutene and 3 ppm of nitrogen dioxide were irradiated, the above-named minor products were all observed but at higher concentrations (0.02-0.2 ppm). Of these products, however, only acetaldehyde and RVR = 0.12 were observed to peak during the fast rate period; and methyl nitrite, RVR = 0.16, isobutyraldehyde, and isobutene oxide all showed a gradual rise in concentration during the course of the experiment.

In the experiment in which 3 ppm of isobutene and 1 ppm of nitrogen dioxide were irradiated, concentrations of 0.2 ppm to 0.6 ppm of new species were observed in addition to those compounds described earlier; at present, these species are identified only by their retention volume ratios as RVR = 0.23 and RVR = 1.2. These new species were present only during the fast rate period; this was also the case with acetaldehyde. Methyl nitrite and isobutyraldehyde were also found to peak, but at later times. Of the minor products formed, only isobutene oxide appeared stable. The rates of formation of RVR = 0.23, RVR = 1.2, and acetaldehyde were considerably higher than the rates of the other minor products. On the bases of both peak concentration and rate of formation these compounds may be considered as major products during the fast rate period.

The identity of some of the products has been checked by microchemical tests (see Table B-1) described in Section B-III. By means of these tests it has been possible to confirm or reject some of the tentative identifications based on characteristic retention times. In this manner the tentative identification of RVR = 0.18 as ethyl nitrite was rejected and the identification of RVR = 0.08 as methyl nitrite was confirmed. Since RVR = 0.18 gives a positive test for aldehyde, it may be that this peak is due to formaldehyde, which normally is not passed by the polyethylene column.

---

* RVR = Retention volume ratio relative to acetone.

Table B-1

PRODUCTS OF THE ISOBUTENE-NITROGEN DIOXIDE REACTION

Compound	Retention Volume Ratio Relative to Acetone = 1.00	Functional Group Test
Methyl nitrite	0.08	Nitrite, positive
Unknown	0.18	Nitrite, negative; aldehyde, positive
Unknown	0.23	
Acetaldehyde	0.38	Aldehyde, positive
Isobutene oxide	0.62	
Isobutyraldehyde	0.86	
Unknown	1.15	
Unknown	1.3	

II Ethylene-Nitrogen Dioxide Reaction

One experiment was run to study the photochemical reaction between 3 ppm of ethylene and 1 ppm of nitrogen dioxide in purified air. Only the concentration of formaldehyde was followed during the course of the 4-hour period. The concentration-time curve, shown in Figure B-1, indicates that there was an increase in the rate of formation of formaldehyde with irradiation time just as in the photooxidation of the higher monoolefins.

A cold-trap sample taken after 3 hours of irradiation showed formaldehyde, acetaldehyde, propionaldehyde, methanol, methyl nitrate, ethyl nitrate, and some unidentified compounds to be present at very low concentrations. No ethylene oxide was found. If ethylene oxide had been present, its concentration would have been less than 0.002 ppm. Its absence is consistent with reports of other investigators which indicate that ethylene oxide is not a product of the atomic oxygen reaction with ethylene. The 3-hour product concentrations are given in Table B-II.

The presence of acetaldehyde and methyl nitrate might be explained on the basis of hydrogen transfer in the unstable intermediate and subsequent photolysis.

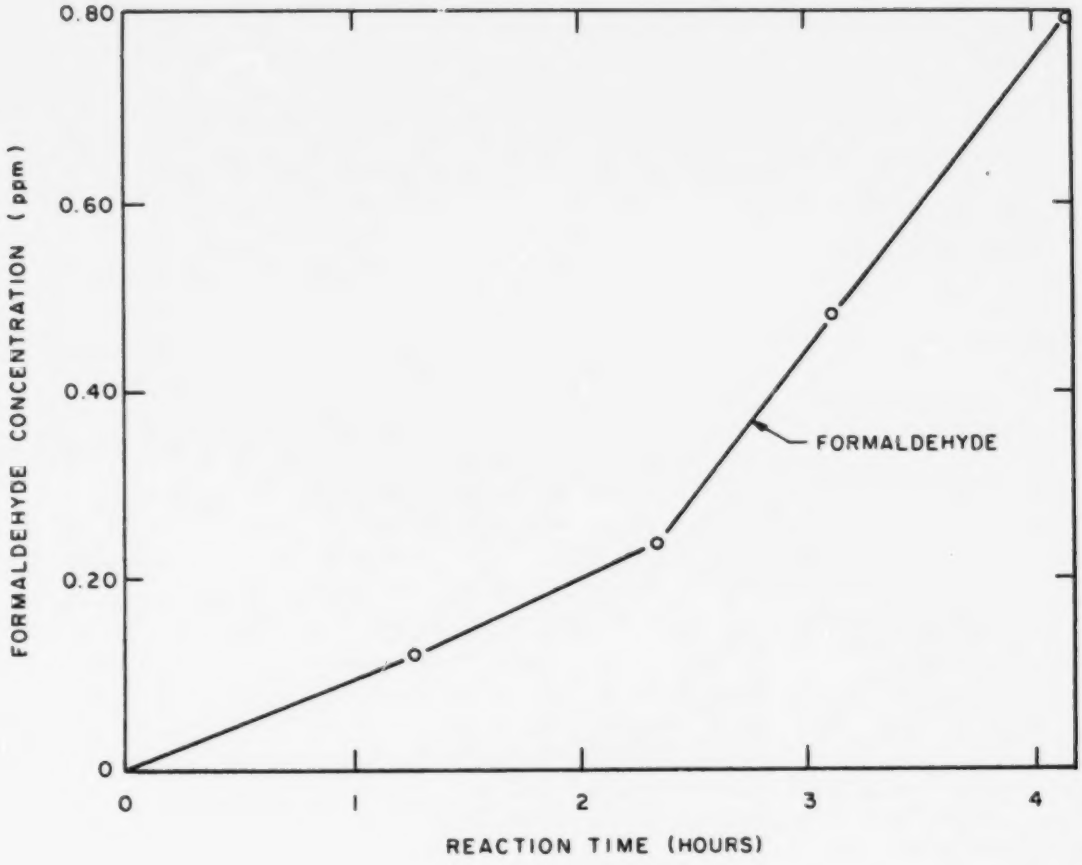

Fig. B-1

FORMALDEHYDE FORMED IN THE
ETHYLENE-NITROGEN DIOXIDE REACTION

Table B-II

PRODUCTS OF THE ETHYLENE-NITROGEN DIOXIDE REACTION[a]

Compound	Retention Volume Ratio Relative to Acetone = 1.00	Concentration (ppm)
Unknown	0.26	0.04
Unknown (possibly formaldehyde)	0.29	0.08
Acetaldehyde	0.38	0.01
Propionaldehyde	0.77	0.002
Methyl nitrate	1.76	0.01
Methanol	2.4	0.05
Ethyl nitrate	2.8	0.007
Formaldehyde	--[b]	0.48

(a) 3 ppm of ethylene, 1 ppm of nitrogen dioxide, and 3 hours of irradiation.
(b) Not detected on the chromatograph.

III Propylene-Nitrogen Dioxide Reaction

The reaction between propylene and nitrogen dioxide in purified air was studied in two experiments. Both were conducted with 3 ppm of propylene and 1 ppm of nitrogen dioxide. The minor products observed include methyl nitrite and propylene oxide and possibly ethyl nitrate and some unidentified compounds. Of these products, propylene oxide and compounds with RVR = 0.1 and 3.3 were observed to peak during the fast rate period. After 40 min of reaction, the propylene oxide concentration reached 0.2 ppm, a concentration which was approximately one-half to one-third that of the major carbonyl product concentrations at that time. By the time that samples were taken toward the end of the experiment, the epoxide concentration had dropped to less than 0.005 ppm. One postulate is that compounds which peak during the excess rate period are precursors of the major products. An interesting point to consider here is that propylene oxide is one of the few compounds which was found to accelerate the rate of the isobutene photooxidation. The nature of the oxide that makes it unique in accelerating the reaction has not yet been determined.

The tentative identification of some of the reaction products by gas chromatograph retention volumes was checked by wet microchemical tests (see Table B-III). Chromatographed fractions were collected in cold traps, then thawed and bubbled through solutions of Griess-Saltzman reagent and of Schiffs' reagent to check for nitrites and aldehydes, respectively.

Table B-III

PRODUCTS OF THE PROPYLENE-NITROGEN DIOXIDE REACTION

Compound	Retention Volume Ratio Relative to Acetone = 1.00	Functional Group Test
Unknown	0.1	
Acetaldehyde	0.38	Aldehyde, positive; nitrite, negative
Unknown	0.44	
Propylene oxide	0.54	Aldehyde, positive; nitrite, negative
Propionaldehyde	0.77	
Methyl nitrate	1.8	
Unknown	2.2	Aldehyde, positive; nitrite, negative
Unknown	3.3	

None of the peaks tested (those beyond RVR = 0.14) gave a positive test for nitrite. Three of the peaks (RVR = 0.38, 0.54, and 2.2) gave positive tests for aldehyde.

Appendix C

ADDITIONAL INFORMATION ON SULFURIC ACID MISTS

Appendix C

ADDITIONAL INFORMATION ON SULFURIC ACID MISTS

Previous work in this[1] and other laboratories has demonstrated that sulfur dioxide can play an important role in aerosol formation during the photooxidation reaction between hydrocarbons and oxides of nitrogen. The possibility that these aerosols might be closely related to sulfuric acid mists, both in composition and in behavior, has stimulated some continuing work based on published data on calculated equilibria and rates of formation of droplets of sulfuric acid in humid atmospheres. Since the last publication[1] of the results of our work on this subject, experimental work has been concerned with the effects of matrix humidity on the light-scattering properties of aerosols produced by cophotooxidation of sulfur dioxide (0.1 ppm) in the presence of 2-methyl-2-butene (3 ppm) and nitric oxide (1 ppm) in humidified pure air. Some incidental and incomplete studies of nuclei formation in these same systems were also carried out.

I Equilibria and Formation of Sulfuric Acid Mists

Experimental work has been done on equilibrium sizes of sulfuric acid smoke particles as a function of humidity.[2] The basic theory which has been developed[3,4] for the phenomena involves adapting Kelvin's equation for vapor pressure over curved surfaces to two-component systems. However, to our knowledge, these equations have not been applied to the sulfuric acid-water system.

The basic equation is

$$\left(\frac{\partial \ln p_1}{\partial P}\right)_{T,x} = \frac{V_1}{RT} \qquad (1)$$

where fugacity of the volatile component (for example, water) has been approximated by p_1 = its partial pressure, P = total pressure, T = absolute temperature, x determines composition and is taken as the mole fraction of the nonvolatile component sulfuric acid, V_1 = partial molar volume of the first component, and R = gas constant.[5] With

no change in V_1 over the range of total pressures P_0 to P, integration of equation (1) along a contour of constant composition and temperature yields

$$\ln \frac{p_1(P)}{p_1(P_0)} = \frac{(P-P_0)V_1}{RT} \qquad (2).$$

The effect of surface free energy of a droplet can be represented as an effective excess pressure on the droplet,

$$P-P_0 = \frac{2\gamma}{r} \qquad (3),$$

over that prevailing over a flat surface of a phase of the same composition, P_0. Here, γ = surface tension of the solution of composition x and temperature T and r = radius of the droplet under consideration.[6] Combination of (3) with (2) yields equation (4), or Kelvin's equation for a two-component system:

$$\ln \frac{p_1(P)}{p_1(P_0)} = \frac{2V_1\gamma}{RTr} \qquad (4).$$

In the case of the sulfuric acid-water system, the simplifying assumptions made by LaMer and Gruen[3] for dioctyl phthalate-toluene systems are not applicable because these systems, being concentrated solutions of electrolytes, do not follow Raoult's law and do not allow the assumptions of additivity of volumes. It might also be pointed out that the treatment of hygroscopic nuclei often seen in the literature can be in error for these as well as other reasons.[7]

The method of calculation was, first, to assume a radius at 0 percent relative humidity, thereby fixing the sulfuric acid content of the droplet; the next step was to compute, for various assumed larger radii, the composition and, from equation (4), the increase in the partial pressure of water above that prevailing over a flat surface of that composition. From these results it is easy to calculate the corresponding relative humidity.

Composition of the droplet is determined by volume ratio $(r_0/r)^3$, which is equal to $\rho P/\rho_0$ where ρ = density of the droplet solution, ρ_0 = density of pure sulfuric acid, and P = weight fraction of sulfuric acid in the droplet. This quantity is calculable using published data as a function of P[8]. Surface tensions of sulfuric acid solutions at 25°C were interpolated from data given in the International Critical Tables for 18°C and

30°C.[9] These two sets of data are shown in Figures C-1 and C-2. Partial molal volumes were calculated from density versus composition data,[8] using Lewis and Randall's Method III from the apparent molal volumes,[10] and are shown in Figure C-3 as a function of the weight fraction of sulfuric acid. It is apparent from Figure C-3 that inaccuracies of calculation are playing a role. These quantities were calculated because no explicit calculations could be found in the literature. The accuracy attained is sufficient for the present purpose.

One interesting consequence of equation (4) and the data shown in Figures C-1 through C-3 is a finite limiting size of droplet at 100 percent relative humidity. If we take $p_1(1)$ to be equal to the saturation pressure of water, then equation (4) becomes

$$r_{100\%} = \frac{2V_1\gamma}{RT\ln a_{H_2O}} \qquad (5)$$

where a_{H_2O} = activity of water in a sulfuric acid solution of the composition of the droplet of radius $r_{100\%}$. Specifying a_{H_2O} (<1) gives the composition V_1 and γ, which in turn gives $r_{100\%}$ from equation (5). From $r_{100\%}$ and the composition, one can then calculate $r_{0\%}$, the initial droplet size. Figure C-4 shows the consequences of equation (5) for sulfuric acid contents from 0.2 percent to 2.4 percent. Water activity data for these calculations were calculated by Harned and Owen from electromotive force data.[11]

Work was continued on the calculation of variation of radius with relative humidity which connects the two extremes depicted in Figure C-4. In Figure C-5 the results for droplets of three different diameters at 0 percent relative humidity are compared with the result for the bulk phase (infinite diameter). Water activity data were obtained from Harned and Owen,[11] from vapor pressure data given in the Chemical Engineer's Handbook,[12] and from publications by Abel.[13] These data are unreliable at low water activities which affect the trend of the curves from 0 percent to about 1 percent relative humidity. The data in a recent paper by Giauque et al.[14] will allow more accurate calculations in the very low humidity region.

II Nucleation of Sulfuric Acid Aerosols

A preliminary attack was made on the question of rate of nucleation and critical supersaturation in gaseous systems containing gaseous water and sulfuric acid. The first objective was to discover the order of magnitude of sulfuric acid vapor concentrations necessary to initiate aerosol formation.

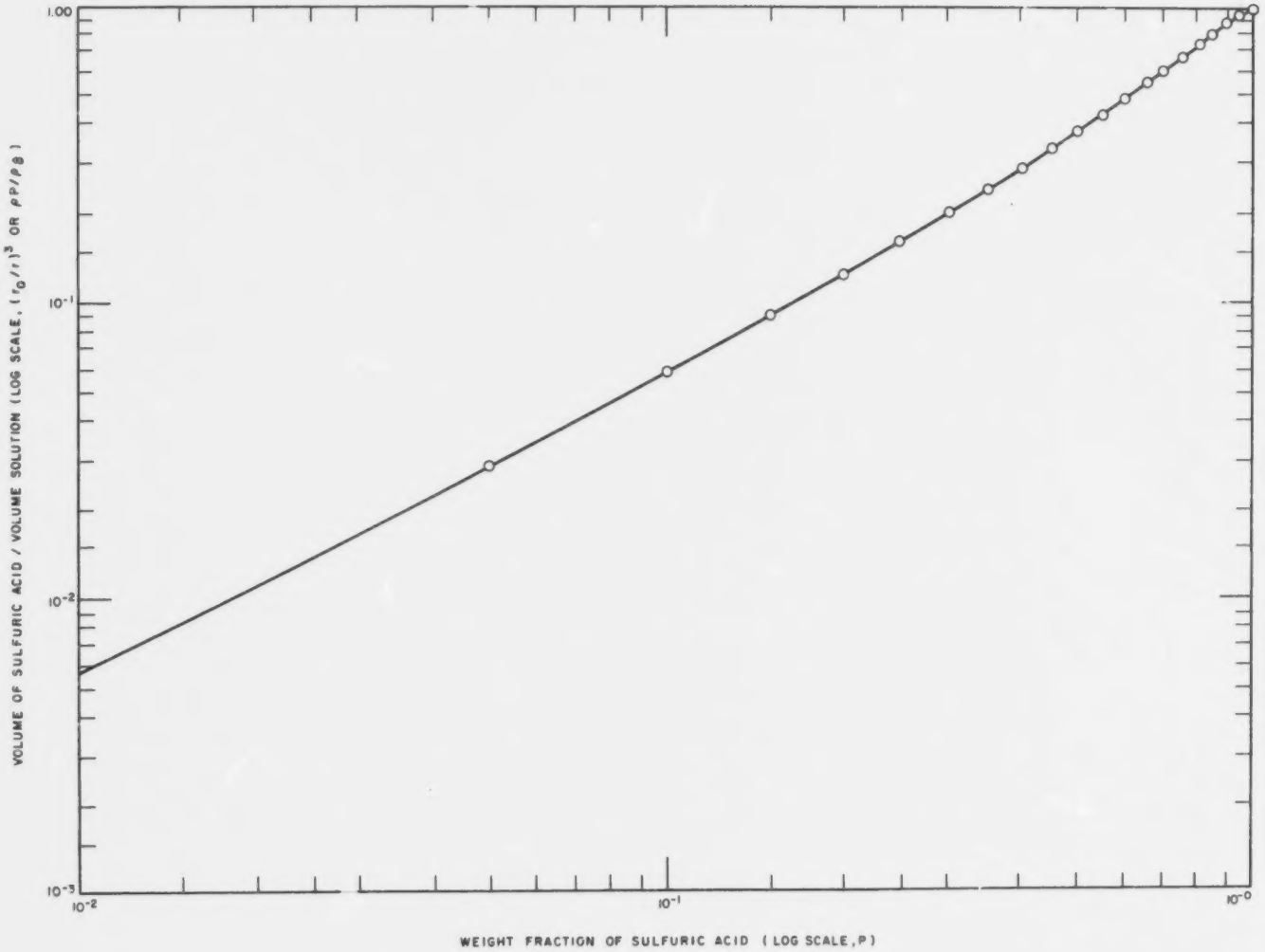

Fig. C-1

VOLUME OF PURE SULFURIC ACID PER VOLUME OF SOLUTION IN WATER AS A FUNCTION OF WEIGHT FRACTION OF SULFURIC ACID IN THE SOLUTION AT 25°C

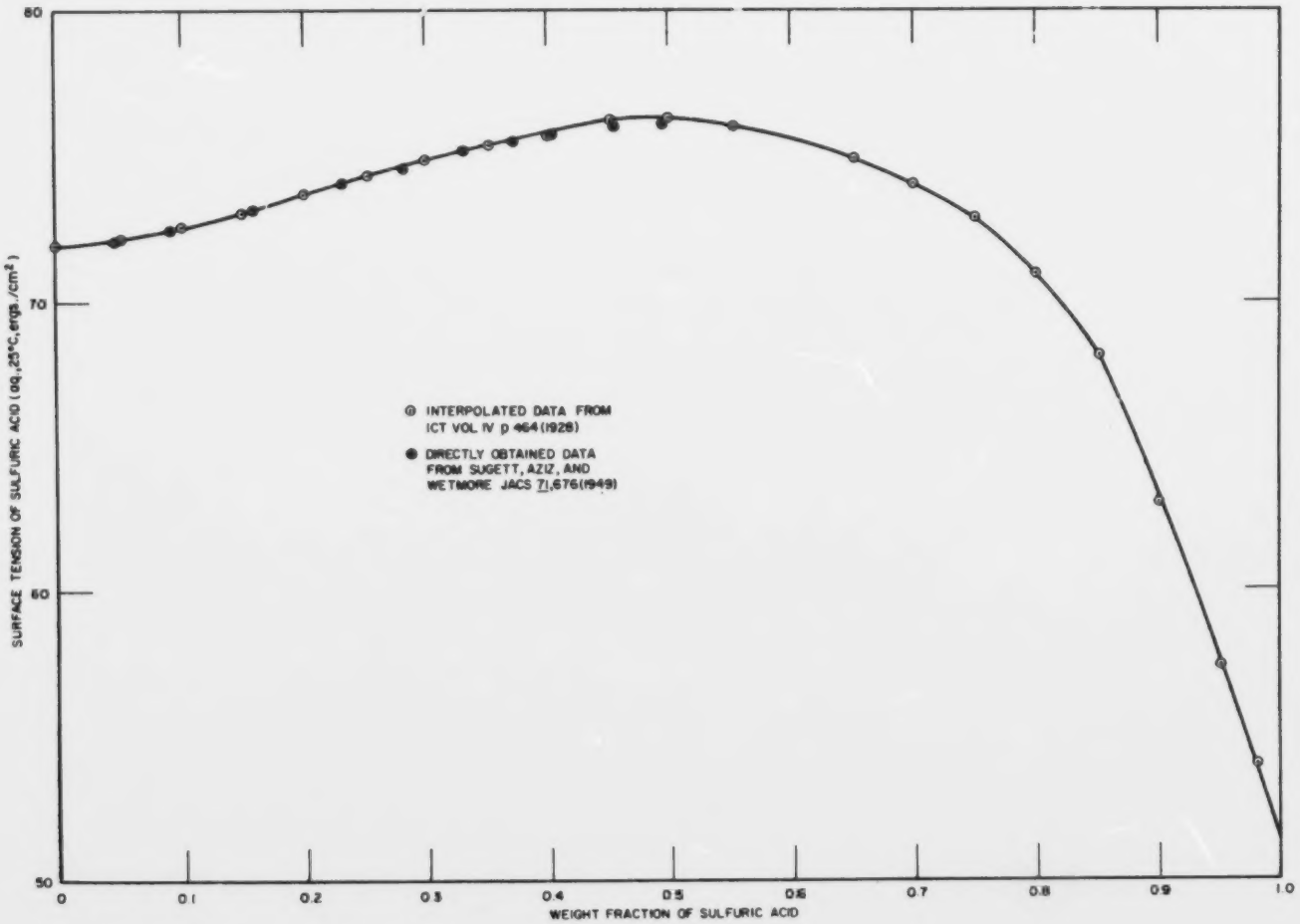

Fig. C-2

INTERPOLATED VALUES OF THE SURFACE TENSION OF SULFURIC ACID SOLUTIONS IN WATER AT 25°C AS A FUNCTION OF WEIGHT FRACTION OF SULFURIC ACID

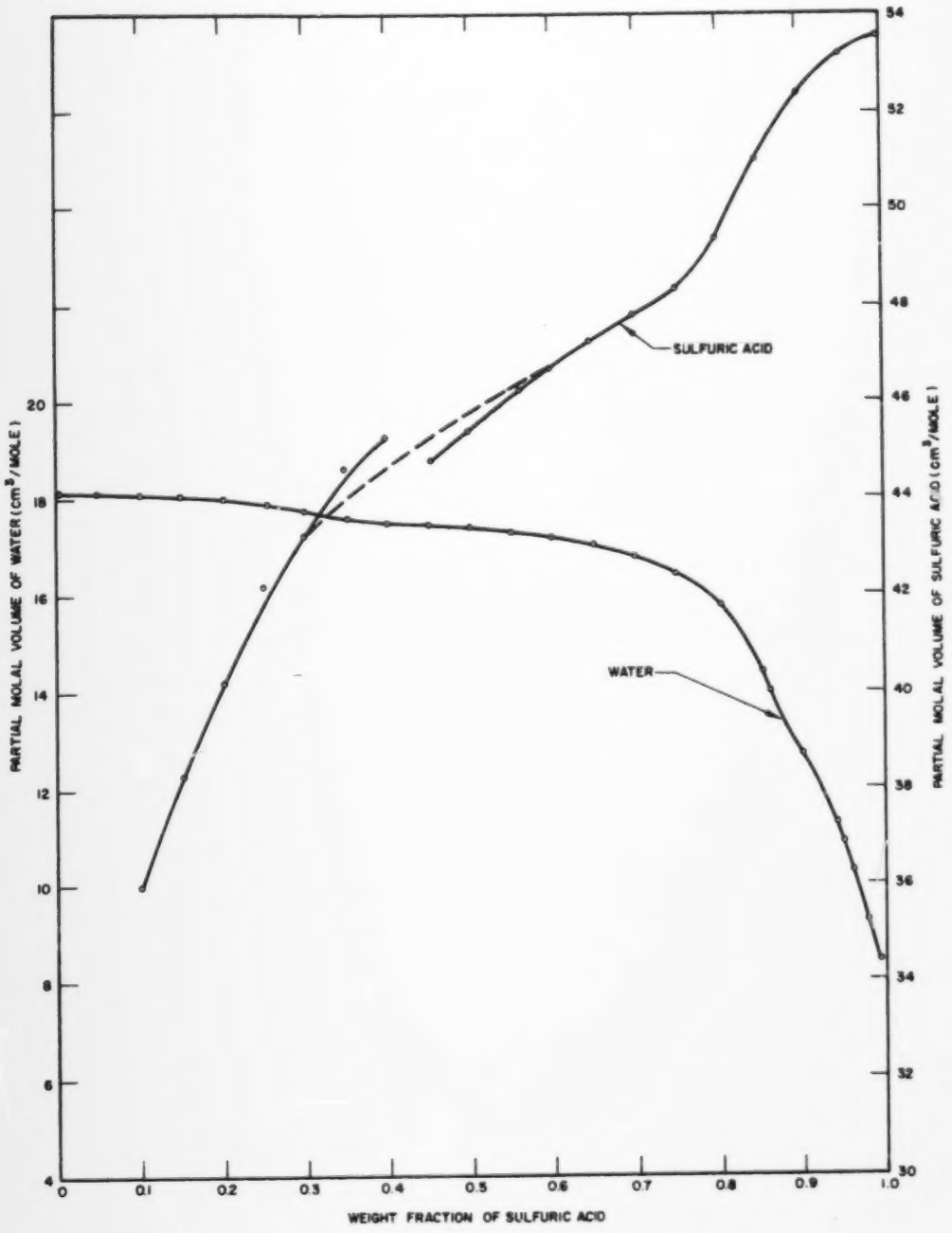

Fig. C-3

PARTIAL MOLAL VOLUMES OF WATER AND SULFURIC ACID IN AQUEOUS SOLUTIONS OF SULFURIC ACID AT 25°C

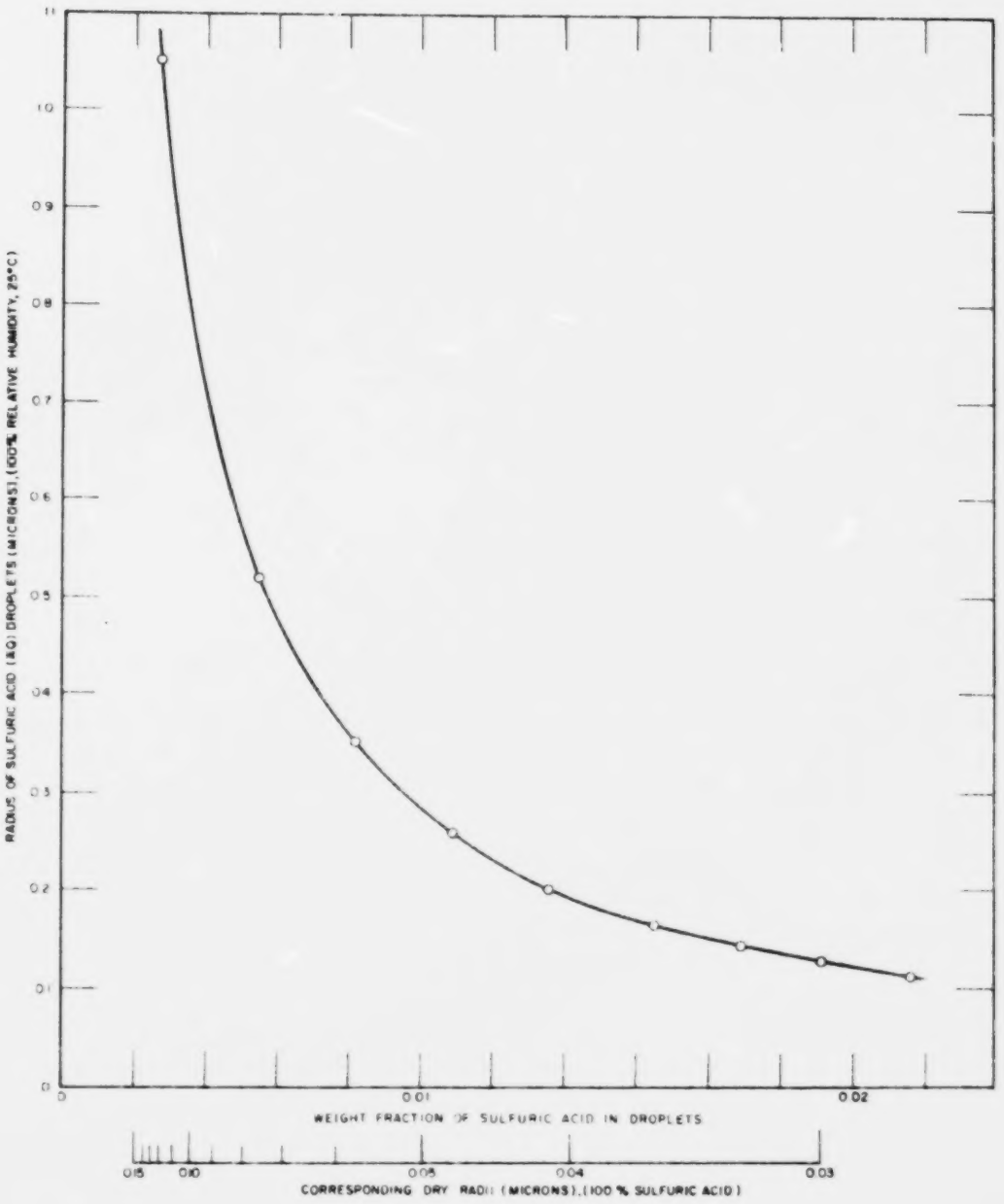

Fig. C-4

LIMITING SIZE OF SULFURIC ACID DROPLETS AT 100 PERCENT RELATIVE HUMIDITY AND 25°C AS A FUNCTION OF SULFURIC ACID CONTENT AND OF DROPLET SIZE AT 0 PERCENT RELATIVE HUMIDITY

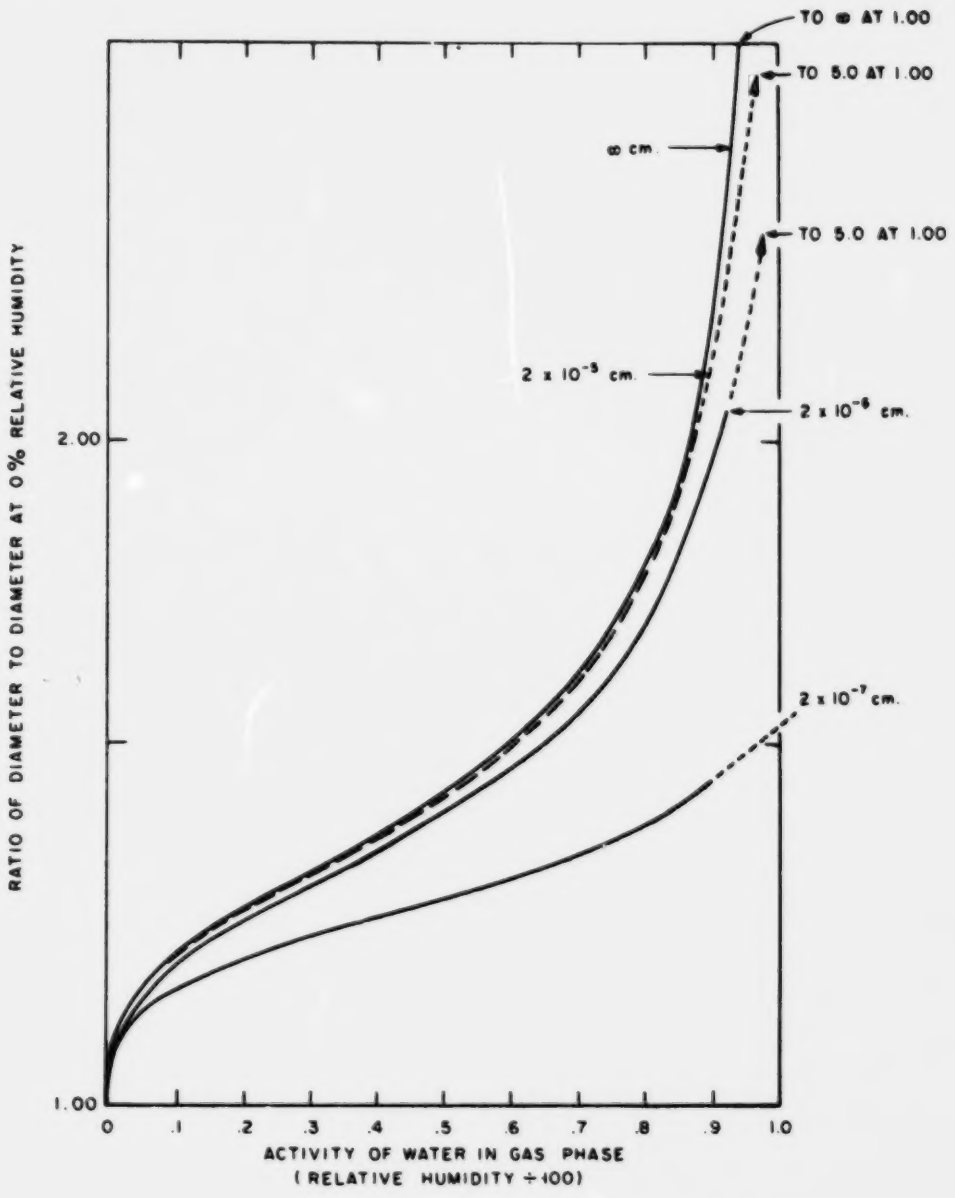

Fig. C-5

GROWTH OF SULFURIC ACID DROPLETS OF VARIOUS SIZES DUE TO ACQUISITION OF WATER AT VARIOUS HUMIDITIES AT 25°C

An idealized system was considered, consisting of an enclosure having walls of perfect reflectivity for water and sulfuric acid molecules. The gases were taken as perfect, and the approach used was the quasi-thermodynamic approach used by Volmer and given by Frenkel for single component systems.[15] The enclosure was taken to contain n_1 moles of component 1 and n_2 moles of component 2. Superscript α denotes the gas phase and β the liquid (droplet) phase. The droplet was assumed to be small enough that it would not appreciably disturb the chemical potentials in the gaseous phase. In the absence of a droplet,

$$G_0 = n_1\mu_1^{\alpha} + n_2\mu_2^{\alpha} \tag{6},$$

where G_0 = Gibbs free energy of the system and μ = chemical potential. In the presence of a droplet of radius r and surface tension γ,

$$G = n_1^{\alpha}\mu_1^{\alpha} + n_2^{\alpha}\mu_2^{\alpha} + n_1^{\beta}\mu_1^{\beta} + n_2^{\beta}\mu_2^{\beta} + 4\pi r^2\gamma \tag{7}$$

where

$$n_1 = n_1^{\alpha} + n_1^{\beta} \text{ and } n_2 = n_2^{\alpha} + n_2^{\beta}.$$

Therefore, the free energy change due to droplet formation is

$$\Delta G = n_1^{\beta}\left(\mu_1^{\beta} - \mu_1^{\alpha}\right) + n_2^{\beta}\left(\mu_2^{\beta} - \mu_2^{\alpha}\right) + 4\pi r^2\gamma \tag{8}.$$

Equation (7) may be used to find the conditions for an extremum of G at constant temperature and constant molar content of the components--that is,

$$\delta G = 0 \qquad \delta n_1 = 0 \qquad \delta n_2 = 0 \tag{9}.$$

The first of these variational equations becomes

$$\delta G = \mu_1^{\alpha}\delta n_1^{\alpha} + \mu_1^{\beta}\delta n_1^{\beta} + \mu_2^{\alpha}\delta n_2^{\alpha} + \mu_2^{\beta}\delta n_2^{\beta} + 4\pi\gamma\delta(r^2) + 4\pi r^2\left(\frac{\partial\gamma}{\partial n_1^{\beta}}\delta n_1^{\beta} + \frac{\partial\gamma}{\partial n_2^{\beta}}\delta n_2^{\beta}\right) \tag{10}.$$

Negelecting the contribution of the surface phase to the volume of the droplet gives

$$\frac{4\pi}{3}r^3 = n_1^{\beta}V_1^{\beta} + n_2^{\beta}V_2^{\beta} \tag{11}$$

where V_1^β and V_2^β are partial molal volumes of the components in the liquid phase. Equation (11) implies that

$$V_1^\beta \delta n_1^\beta + V_2^\beta \delta n_2^\beta = 4\pi r^2 \delta r = 2\pi r \delta(r^2)$$

or

$$\delta(r^2) = \frac{V_1^\beta}{2\pi r}\delta n_1^\beta + \frac{V_2^\beta}{2\pi r}\delta n_2^\beta \qquad (12).$$

In addition, conservation of the components requires

$$\delta n_1^\alpha = -\delta n_1^\beta \qquad \delta n_2^\alpha = -\delta n_2^\beta \qquad (13).$$

Substitution into (10) of (12) and (13) yields

$$\delta G = \left(\mu_1^\beta - \mu_1^\alpha + \frac{2\gamma}{r}V_1^\beta + 4\pi r^2 \frac{\partial \gamma}{\partial n_1^\beta}\right)\delta n_1^\beta + \left(\mu_2^\beta - \mu_2^\alpha + \frac{2\gamma}{r}V_2^\beta + 4\pi r^2 \frac{\partial \gamma}{\partial n_2^\beta}\right)\delta n_2^\beta \qquad (14).$$

The condition for an extremum of G, $\delta G = 0$, with δn_1^β and δn_2^β arbitrary, yields two simultaneous equations for the extremum:

$$\left.\begin{aligned} \mu_1^\beta - \mu_1^\alpha + \frac{2\gamma}{r}V_1^\beta + 4\pi r^2 \frac{\partial \gamma}{\partial n_1^\beta} = 0 \\ \mu_2^\alpha - \mu_2^\alpha + \frac{2\gamma}{r}V_2^\beta + 4\pi r^2 \frac{\partial \gamma}{\partial n_2^\beta} = 0 \end{aligned}\right\} \qquad (15).$$

It remains to resolve the partials of the surface tension into products of specific properties and functions of droplet size. We write

$$\left.\begin{aligned} \frac{\partial \gamma}{\partial n_2^\beta} = \frac{d\gamma}{dx}\left(\frac{\partial x}{\partial n_2^\beta}\right)_{n_1^\beta} \\ \frac{\partial \gamma}{\partial n_1^\beta} = \frac{d\gamma}{dx}\left(\frac{\partial x}{\partial n_1^\beta}\right)_{n_2^\beta} \end{aligned}\right\} \qquad (16),$$

where x = mole fraction of component 2. We can also write

$$\left.\begin{aligned} \left(\frac{\partial x}{\partial n_2^\beta}\right)_{n_1^\beta} = \frac{1}{n_1^\beta + n_2^\beta}(1-x) \\ \left(\frac{\partial x}{\partial n_1^\beta}\right)_{n_2^\beta} = \frac{x}{n_1^\beta + n_2^\beta} \end{aligned}\right\} \qquad (17).$$

From equation (11)

$$\frac{4}{3}\pi r^3 = \left(n_1^\beta + n_2^\beta\right)\left[(1-x)\,V_1^\beta + xV_2^\beta\right]$$

or

$$n_1^\beta + n_2^\beta = \frac{4\pi r^3}{3\left[(1-x)V_1^\beta + x\,V_2^\beta\right]} \qquad (18).$$

Substituting (18) into (17) and the result into (16) yields

$$\left.\begin{aligned}\frac{\partial\gamma}{\partial n_2^\beta} &= 3(1-x)\frac{\left[(1-x)V_1^\beta + xV_2^\beta\right]}{4\pi r^3}\frac{d\gamma}{dx}\\ \frac{\partial\gamma}{\partial n_1^\beta} &= -3x\frac{\left[(1-x)V_1^\beta + xV_2^\beta\right]}{4\pi r^3}\frac{d\gamma}{dx}\end{aligned}\right\} \qquad (19).$$

Equations (19) and (15) yield working equations for determing the composition and size of the critical nuclei of a two-component system,

$$\left.\begin{aligned}\mu_1^\beta - \mu_1^\alpha + \frac{2\gamma}{r}V_1^\beta - \frac{3x}{r}V\frac{d\gamma}{dx} &= 0\\ \mu_2^\beta - \mu_2^\alpha + \frac{2\gamma}{r}V_2^\beta + \frac{3(1-x)}{r}V\frac{d\gamma}{dx} &= 0\end{aligned}\right\} \qquad (20),$$

where $\tilde{V}$ = the volume of one mole of solution having x mole fraction of component 2, $\tilde{V} = (1-x)\,V_1^\beta + xV_2^\beta$.

A method of solving (20) is to plot two curves of $1/r$ versus x from the equations, given values of μ_1^α and μ_2^α corresponding to gaseous concentrations to be investigated. The result is two families of single parameter curves whose intersections yield values of critical radius r* and critical composition x* for given pairs of values of gaseous concentrations or chemical potential μ_1^α and μ_2^α.

A few interesting and useful general relationships may be derived from the above equations. One such relationship is derived by finding the dependence of the free energy of formation of nuclei on nuclei size

along a contour of constant composition equal to that of the critical nucleus. This is done by setting

$$\mu_1^{\beta} - \mu_1^{\alpha} = -\frac{2\gamma^*}{r^*}\tilde{V}_1^{\beta *} + \frac{3x^*}{r^*}V^*\left(\frac{d\gamma}{dx}\right)^*$$

$$\mu_2^{\beta} - \mu_2^{\alpha} = -\frac{2\gamma^*}{r^*}\tilde{V}_2^{\beta *} - \frac{3(1-x^*)}{r^*}V^*\left(\frac{d\gamma}{dx}\right)^*$$

from (20) and substituting into (8), taking all other specific quantities in those equations to be equal to the values at the critical composition. The result is

$$\Delta G = 4\pi\gamma^*\left(r^2 - \frac{2}{3}\frac{r^3}{r^*}\right) \qquad (21)$$

or

$$\frac{3\Delta G}{4\pi\gamma^* r^{*2}} = 3\left(\frac{r}{r^*}\right)^2 - 2\left(\frac{r}{r^*}\right)^3$$

This relationship is depicted in Figure C-6 and is of the same form as that determining the barrier to nucleation of a single component system.[15]

Since the critical size and composition of the particles are uniquely determined by the chemical potentials in the gas phase of equation (20), we may substitute their values in terms of these parameters into equation (8) and obtain, after algebraic manipulation involving the identity (equation (11)),

$$\frac{3\Delta G}{4\pi\gamma^* r^{*2}} = 3\left(\frac{r}{r^*}\right)^2\frac{\gamma}{\gamma^*} - 2\left(\frac{r}{r^*}\right)^3\left\{\frac{\tilde{V}^*}{\tilde{V}}\left[1 + (x - x^*)\frac{V_2^{\beta *} - V_1^{\beta *}}{V^*}\right]\right. \qquad (22)$$

$$\left. + \frac{3}{2}\left(\frac{d\ln\gamma}{dx}\right)^*\frac{\tilde{V}^*}{\tilde{V}}(2x^* - 1)(x - x^*) + \frac{r^*}{2\gamma^*}\frac{(1-x)\left(\mu_1^{\beta *} - \mu_1^{\beta}\right) + x\left(\mu_2^{\beta *} - \mu_2^{\beta}\right)}{\tilde{V}}\right\}$$

or the analog of equation (21) for arbitrary nucleus composition in dimensionless form. This can be written

$$\phi(\rho, x) = 3\,\alpha(x)\rho^2 - 2\beta(x)\rho^3$$

where $\rho = r/r^*$ and $\alpha(x)$ and $\beta(x)$ are functions of nucleus and gas phase composition. For fixed compositions this function has extrema at $\rho = 0$ and $\rho = \alpha(x)/\beta(x)$. The first extremum is a minimum, and the second a maximum, provided that $\alpha(x) = \gamma/\gamma^*$ and r are positive, which is a physical necessity for this situation. These results, combined with the

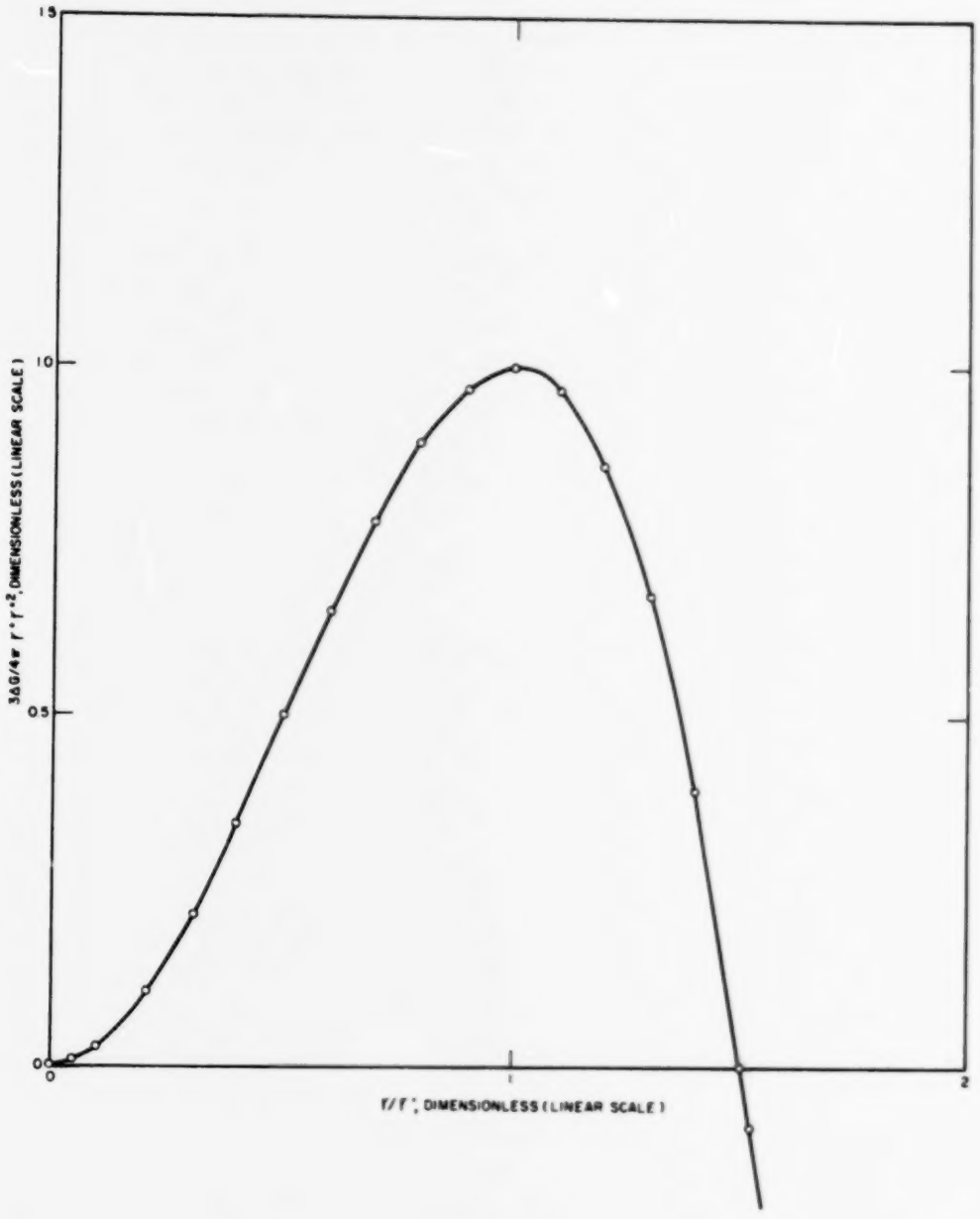

Fig. C-6

INTERCEPT OF PLANE OF CRITICAL COMPOSITION WITH FREE ENERGY BARRIER SURFACE FOR NUCLEATION OF A TWO-COMPONENT SYSTEM
(Surface Plotted Against x and r)

contour at $x = x^*$ shown in Figure C-6 give a qualitative picture of the shape of the free energy barrier surface as a peaked ridge having a sharp drop-off and with the peak at (x^*, r^*). Constant composition contours have a shape similar to Figure C-6. Thus, no composition or size is really critical. There is a continuous range of critical size and corresponding critical compositions.

A preliminary set of calculations has been carried out applying these equations to the sulfuric acid-water system. However, the results suffer from the apparent lack of accurate data connecting activity of sulfuric acid in the aqueous phase with activity in the vapor phase at 25°C. The estimates by Abel[12] of the partial pressure of sulfuric acid, which depend on an indirect method, seem much too high, as has been discovered experimentally by LaMer et al.[1] and confirmed by experience in Stanford Research Institute laboratories. Extrapolations of partial pressures observed at higher temperatures[16] also indicate tenfold overestimates by Abel, but are not sufficiently accurate to be reliable values for calculation.

Although these errors preclude our presenting the results of these calculations here, qualitatively these calculations indicate that extremely small concentrations of sulfuric acid vapor are sufficient to achieve supersaturation at the relative humidities usually encountered in the lower atmosphere. Calculations indicate that the absolute maximum on the free energy barrier surface corresponds to the largest nucleus radius

Further work on this system awaits the obtaining of an accurate value of the partial pressure of sulfuric acid over concentrated sulfuric acid of known composition at 25°C. We can then pursue the objective of estimating the minimum sulfuric acid generation rate required to yield mists at an appreciable rate in humid air.

APPENDIX REFERENCES

1. Schuck, E. A. and G. J. Doyle. Photooxidation of Hydrocarbons in Mixtures Containing Oxides of Nitrogen and Sulfur Dioxide. Report No. 29, Air Pollution Foundation, San Marino, California, October 1959.

2. LaMer, V. K., E. C. Y. Inn, and I. B. Wilson. The methods of forming, detecting, and measuring the size and concentration of liquid aerosols in the size range of 0.01 to 0.25 microns diameter. J. Coll. Sc. 5, 471 (1950).

3. LaMer, V. K. and R. Gruen. A direct test of Kelvin's equation connecting vapour pressure and radius of curvature. Transactions of the Faraday Society 48, 410 (1952).

4. Volmer, O. Kinetik der Phasenbildung. p. 80, Edwards Brothers, Ann Arbor, Mich., 1945.

5. Guggenheim, E. A. Thermodynamics. p. 187, Interscience Publishers, Inc., New York, 1949.

6. Guggenheim, E. A. op. cit. p. 41.

7. See Green, H. L. and W. R. Lane. Particulate Clouds: Dusts, Smokes and Mists. pp. 14-15, London, D. Van Nostrand Co., Inc., 1957.

8. Chemical Engineer's Handbook, John H. Perry, ed. pp. 184-5, New York, McGraw-Hill Book Co., Inc., 1950. These data are taken from the International Critical Tables.

9. International Critical Tables. Volume IV. p. 464, New York, McGraw-Hill Book Co., Inc., 1928.

10. Lewis, G. N. and M. Randall. Thermodynamics. pp. 37-38, New York, McGraw-Hill Book Co., Inc., 1923.

11. Harned, H. S. and B. B. Owen. The Physical Chemistry of Electrolytic Solutions. pp. 435-8, New York, Reinhold Publishing Co., 1943.

12. Chemical Engineer's Handbook. op. cit. p. 168.

13. Abel, E. The vapor phase above the system sulfuric acid-water. J. Phys. and Coll. Chem. 52, 908 (1948).

14. Giauque, W. F., E. W. Hornung, J. E. Kunzler, and G. R. Rubin. The thermodynamic properties of aqueous sulfuric acid solutions and hydrates from 15 to 300°K. J. Am. Chem. Soc. 82, 62 (1960).

15. Frenkel, J. Kinetic Theory of Liquids. Chapter VII. London, Oxford University Press, 1946.

16. Chemical Engineer's Handbook. op. cit. p. 169.